Réponses des perches de hêtre (Fagus sylvatica L.) à l'ouverture de la canopée : approche multidisciplinaire et multi-échelle.

Estelle Noyer

N°: 2017 AGPT 0008

Doctorat AgroParisTech

T H È S E

pour obtenir le grade de docteur délivré par

L'Institut des Sciences et Industries du Vivant et de l'Environnement

(AgroParisTech)

Spécialité : Biologie Végétale et Forestière

présentée et soutenue publiquement par

Estelle NOYER

le 12 mai 2017

Réponses des perches de hêtre (*Fagus sylvatica* L.) à l'ouverture de la canopée : approche multidisciplinaire et multi-échelle.

Directrice de thèse : **Catherine COLLET**

Co-encadrante de thèse : **Jana DLOUHA**

Jury

M. Bruno CLAIR, DR, ECOFOG, CNRS, Campus Agronomique, Kourou	Rapporteur
M. Philippe BALANDIER, DR, EFNO, IRSTEA, Nogent-sur-Vernisson	Rapporteur
M. Eric BADEL, CR, PIAF, INRA, U. Clermont 2, Clermont-Ferrand	Examinateur
Mme Mériem FOURNIER, Pr., LERFoB, INRA, AgroParisTech, Nancy	Présidente du jury
Mme Jana DLOUHA, CR, LERFoB, INRA, AgroParisTech, Nancy	Co-encadrante de thèse
Mme Catherine COLLET, CR, LERFoB, INRA, AgroParisTech, Nancy	Directrice de thèse

AgroParisTech
UMR INRA-AGROPARISTECH LERFoB 1092
54280 CHAMPENOUX

Réponses des perches de hêtre (*Fagus sylvatica* L.) à l'ouverture de la canopée : approche multidisciplinaire et multi-échelle.

Beech (*Fagus sylvatica* L.) poles responses to canopy opening: multi-disciplinary and multi-scale approaches.

arbre

agreenium
l'institut agronomique, vétérinaire & forestier de France

LERFoB

INRA
SCIENCE & IMPACT

Remerciements

Ces remerciements s'adressent en premier lieu à **Catherine Collet** et **Jana Dlouhá** pour m'avoir donnée ma chance dans cette aventure qui est la thèse. Merci pour vos conseils, pour les discussions scientifiques et celles moins scientifiques, votre écoute dans les moments de doutes. Merci aussi pour la confiance et la liberté d'action que vous m'avez accordées durant ces années.

Merci aux membres du jury de thèse, Messieurs **Bruno Clair** et **Philippe Balandier**, rapporteurs de cette thèse, et Monsieur **Éric Badel**, examinateur, qui ont accepté d'évaluer ce travail et ont contribué, grâce à leurs judicieuses remarques, à améliorer ce manuscrit.
Merci à **Mériem Fournier** et **Thiéry Constant** de m'avoir accueilli au LERFoB et les discussions enrichissantes malgré les emplois du temps chargés. **Mériem**, merci de m'avoir encouragé à postuler au LERFoB et d'avoir partagé les potins au détour d'un couloir ou d'un café. **Thiéry**, merci pour toute ton aide niveau technique et scientifique et ta disponibilité pour améliorer et personnaliser les outils.
Je remercie également **François Ningre** pour la mise à disposition des perches et d'avoir fait une place à la thèse dans son projet.
Merci à **Stéphane Ponton**, **Oliver Brendel** et **Patrick Heuret** d'avoir accepté de participer aux comités de thèse et dont les avis et conseils ont été avisés et ont permis de faire avancer cette thèse.
Je tiens aussi à remercier le LabEx ARBRE qui a financé ce travail pendant ces trois années.

Cette thèse n'aura pu être menée à bien sans les deux équipes techniques du LERFoB qui n'a pas que contribué techniquement à ce travail mais aussi humainement. Merci à tous de votre convivialité et votre disponibilité mais surtout de votre motivation malgré les imprévus à réaliser toutes ces mesures. Cela a été un réel plaisir de travailler avec vous !
Tout d'abord, merci au plateau Xyloscience pour votre bonne humeur, les pauses café et les rires. **Maryline Harroué**, un énorme merci pour ta détermination, ta gentillesse et ta grande aide de tous les instants pour les coupes anatomiques. Merci aussi pour toutes ses discussions et tes conseils. Sans toi, la réalisation des coupes aurait été bien monotone.
Merci à **Pierre Gelhaye** pour ton aide pour la densito, les préparations d'échantillons, ton humour plus ou moins douteux de toutes circonstances et surtout pour le phénomène tee-shirt / rouge à lèvre rouges.
Un grand merci à **Julien Ruelle** qui a toujours la banane, est toujours présent, et est toujours prêt à dégainer une solution, un plugin magique ou une blague. Je remercie aussi **Alain Mercanti**, pour tes anecdotes et tes conseils techniques. **Etienne Farré** pour tes dépannages informatiques, **Emmanuel Cornu**, la force tranquille de ce groupe d'exception,

et **Charline Freyburger** dont les cartes et les montages photos sont toujours un plaisir à admirer.
Un grand merci à l'équipe IEC. Je tiens à remercier **Daniel Rittié,** pour toutes ces mesures de croissance qui sont devenus avec le temps un défi personnel, ainsi que **Guy Maréchal**. Merci à **Florian Vast** pour mes premières mesures terrain et la musculation version LiDAR. Merci à **Loïc Dailly** (chatounet ! oui je grave ça dans le marbre de ce manuscrit) et **Frédéric Bordat** pour les phases de terrain et les rires qui en ont découlés.

Cette thèse ne serait pas aussi déroulée sans l'assistance administrative permanente. **Nathalie Morel**, merci pour ta bonne humeur, tes histoires incroyables avec certains appareillages motorisés et les poteaux électriques, et tes conseils avisés. **Elodie Taillefumier** (a.k.a. chaton), merci pour ta rapidité d'action, ton efficacité qui n'est plus à démontrer, les discussions sur la vie et toutes ces petites choses qui ont l'air de rien mais qui sont beaucoup. **Corinne Martin**, merci tout d'abord pour tes gâteaux et aussi pour tes conseils com' et ton volontariat en toutes circonstances. Merci aussi aux anciens membres, **Hélène Hurpeau** et **Patrick Rodrigues** qui ont toujours répondu présent pour répondre à toutes mes questions.

Un immense merci à mes colloques de bureau **Zineb Kebbi-Benkeder** et **Jialin Song**. Ah, que vous dire sans tomber dans le sentimental ? Je n'aurais pu rêver mieux comme compagnie : vous avez dit oui à ~~ma tyrannie~~ toutes mes lubies de décoration de bureau, accepté et écouté mes moments de râlage contre R entre autres… Il est difficile de poser par écrit à quel point je vous suis reconnaissante pour ces années à vos côtés. J'ai hâte de voir quelles routes nous allons suivre et espère qu'elles se recroiseront dans le futur.
Merci aux anciens doctorants du labo : **Nicolas Bilot** pour ton optimisme permanent, **Félix Hartmann** pour ton humour décapant, **Vivien Bonnesoeur** pour ton capital sympathie et surtout d'avoir remis les rouflaquettes à l'ordre du jour. Merci à **Raphaël Trouvé**, graphiste officiel des tee-shirts des doctorants. Merci à **Emilien Kuhn** pour tes séances de psychanalyse, les pic-nics du midi et ta bière. Je remercie aussi **Mathieu Dassot** et **Henri Cuny**, dont les conseils et les échanges ont été précieux.
Je remercie également la nouvelle génération de doctorants pour les potées et leur compagnie. Merci à **Anjy-Nandrianina Andrianantenaina**, **Masoumeh Saderi**, **Citra-Yanto-Ciki Purba**, **Van-Tho Nguyen** et **Jean-Charles Miquel** mais aussi à **Lise Maciejewski**, **Jonathan Lenglet**, **Adrien Taccoen** et **Lara Climaco De Melo** pour votre accueil chaleureux à AgroParisTech lors de la rédaction. Je vous souhaite de réussir haut la main vos projets ! Un remerciement un peu spécial pour **Lara**, sans toi, la vie de fin de thèse n'aurait pas eu la même couleur. Merci pour ton dynamisme contagieux et pour tout !

Je ne peux décidément pas faire l'impasse sur la succursale espagnole qui a ajouté une touche de soleil dans ce labo lorrain. Merci à **Ignacio Barbeito** pour son sourire digne de Julio Iglesias. Un grand merci à **Rubèn Manso** dont ton soutien inébranlable, les discussions et ton vocabulaire espagnol comme français qui ont colorés les échanges verbaux.

Pour votre accueil dans les locaux d'AgroParisTech et les pauses café, merci à **Bruno Ferry**, **Vincent Pérez**, **Christian Piédallu**, **Ingrid Seynave**, **Lide van Couwenberghe**, **Paulina Pito**, **François Lebourgeois** et l'ensemble du LERFoB côté APT. J'ajouterais un grand merci au couloir Croissance et au couloir QB côté Champenoux pour m'avoir intégré si facilement dans la dynamique d'équipe et surtout pour avoir toléré mon rire « plein de vie » et mes bruits de talons par toutes saisons.

Lors de cette thèse, j'ai été amené à réaliser 3 mois en Oregon. Je tiens à remercier chaleureusement **Barbara Lachenbruch** et son mari **Everett M. Hansen** dont les échanges ont autant été riches scientifiquement qu'humainement. Merci également à **Nathalie Gitt**, assistance du doyen, française expatriée qui a su me conseiller judicieusement à propos l'administration américaine et le mode de vie local. Un immense merci à **Marie Dury**, post-doc à l'époque, expatriée belge, avec qui j'ai pu découvrir le grand ouest américain et la Belgique.

Je remercie aussi les doctorants des autres unités de Nancy avec qui je n'ai pas que partagé les formations mais aussi tous les moments phares de la thèse. Merci à **Emeline Hily**, **Alexandre Fruleux** et **Yoran Bornot**, connus grâce au LabEx, **Cécilia Gana**, **Maxime Burst**, **Nicolas Dusart-Marquet** et **Pierre-Antoine Chuste** et bien sûr, **Laura Heid**, pour les séances piscine et les papotages.

Pour m'avoir supporté bien avant la thèse mais aussi pendant, un grand merci aux auvergnats : **Sébastien Ribeiro** (flûte, tête de linotte va !), **Robin Michard** (Inspecteur), **Clémence Bouvart** (Miss BE) et **Aurélien Chauvigné** (Doudou), **Titouan Bonnot** (El machina !!) et **Thomas Mazet** (Papy)**.** Que la Grand Vicieuse vous accompagne !
Merci aussi à **Doc Martin** (Ludo) pour ton humour des plus subtils (Salut toiiii !!! ça va bien se passer…) et tes photos d'arbres ~~creusois,~~ mais surtout pour avoir relu une partie de ce manuscrit.
Un énorme merci à toi **Emilie Froussart** (Mammiiieee). Toujours présente même quand on ne le sait pas (Ninjaaa), reine de l'ombre et dame de compagnie indispensable à toute survie psychologique. Merci pour ces appels au fin fond de la nuit et à ces partages de fous rires.

Parce que c'est magique entre nous depuis toutes ces années entre nous et que votre soutien est sans faille, merci à **Claire Fernandez** et **Marion Rouzaire** pour votre amitié inestimable, les chansons Disney que j'ai appris à apprécier avec le temps et vos voix de cristal et surtout longue vie au cigare cubain, au rosé et au Vogalib !

Je finirais ces remerciements par ma famille. Merci à mes parents de n'avoir jamais douté de moi et m'avoir toujours soutenu dans cette aventure. Merci à mon frère dont les avis sont toujours aussi avisés et pertinents, merci pour tout ce soutien même à plusieurs centaines de kilomètres.

Beaucoup de gens ont participé au cours de ces presque 4 années de thèse. Comme tous remerciements, certains sont trop succincts et la liste est non exhaustive. Sachez seulement, pour ceux qui ont participé de près ou de loin à cette thèse, je vous remercie de tout cœur pour avoir rendu ces années bien remplies d'expériences fortes en tous genres !

Table des matières

Liste des figures

Chapitre 1

Chapitre 2

Chapitre 3

Chapitre 4

Chapitre 5

Liste des tableaux

Chapitre 2

Chapitre 3

Chapitre 4

Chapitre 5

Chapitre 6

Abréviations et acronymes

Chapitre 1

AMF : angle des microfibrilles

MOE : module d'élasticité

MOR : module de rupture

Chapitre 3

BAI : surface de cerne

DR : nombre d'années après ouverture

H : hauteur

LGU : longueur d'unité de croissance

MResid : moyenne des résidus

PGC : pourcentage de changement de croissance radiale

R : rayon de la tige

RW : largeur de cerne

Chapitre 4

D : diamètre de la tige

dC_g : courbure gravitationnelle

dC_{mat} : courbure gravitropique

F_b : facteur de forme

H/D : facteur d'élancement

H_{CG} : hauteur du centre de gravité de la partie distale ou de l'arbre entier

ICC / GSI : indicateurs de contraintes de croissance

m : distribution de la biomasse

MV : potentiel de redressement de la section

n : défilement du tronc

SB : sécurité face au flambement

SW : sécurité vis-à-vis du vent

TLS : scans LIDAR terrestre

TW : bois de tension

ρ_T : facteur de chargement

Chapitre 5

D_{HP} : diamètre hydrauliquement efficace

K_S : conductivité hydraulique spécifique potentielle

K_{ring} : conductivité hydraulique potentielle du cerne

VD : diamètre des vaisseaux

VF : fréquence des vaisseaux

Chapitre 1 : Introduction

1.1. Contexte de l'étude

Le bois est un matériau à structure complexe et ingénieuse optimisée pour remplir de nombreuses fonctions au sein de l'arbre : il assure la sécurité mécanique et le maintien de la posture des axes, la conduction de la sève ou encore la mise en réserves des composés carbonés (Hacke & Sperry, 2001; Myburg *et al.*, 2013; Hacke, 2015). Sa production et sa qualité sont dépendantes des conditions de croissance des arbres, lesquelles sont fluctuantes au cours de la vie d'un arbre surtout dans le milieu forestier (Wright *et al.*, 2000). Par exemple, en forêt, les ouvertures de la canopée peuvent survenir ponctuellement suite à une tempête ou à la mort d'un arbre voisin. Par ailleurs, les itinéraires sylvicoles se basent sur la réalisation d'ouverture dans la canopée, c'est-à-dire éclaircies, pour favoriser la croissance des arbres cibles, dits arbres libérés (Pretzsch, 2010).

Le régime d'application de ces ouvertures de la canopée est régi par le type de structure verticale du peuplement forestier, c'est-à-dire l'organisation spatiale des tiges. Pour une gestion proche de la dynamique naturelle des peuplements, la gestion en système irrégulier est la plus pertinente. Ce système est défini par un continuum de tailles (hauteur et diamètre) des individus répartis entre l'étage dominant qui composent la canopée, et dominé où les arbres se développent à l'ombre des arbres dominants. Ce type de sylviculture se distingue par la persistance du couvert végétal de l'étage dominant *via* le renouvellement du peuplement par les individus dominés. La phase de transition entre l'étage dominé et l'établissement à l'étage dominant est amorcée par la création d'ouverture dans la canopée (Canham, 1990; Rentch *et al.*, 2003; Hart *et al.*, 2012). Dans le cas d'espèces tolérantes à l'ombrage, la période au sein de l'étage dominé peut durer plusieurs dizaines d'années.

Après ouverture de la canopée, les nouvelles conditions de croissance changent très fortement pour les individus libérés de la compétition inter-arbre. Parallèlement à un meilleur accès aux ressources telles que la lumière ou l'eau, l'augmentation des mouvements d'air, de température de l'air et du sol résulte en une demande de transpiration ainsi qu'un niveau de contrainte mécanique plus élevés (Aussenac, 2000). La survie des arbres libérés dépend alors de la mise en place de réponses en fonction de l'ensemble des contraintes rencontrées telles que l'augmentation du poids de l'arbre, les stimulations mécaniques répétées du vent, l'orientation des rayons lumineux, les températures extrêmes ou encore les déficits hydriques. La mise en place des réponses d'acclimatation aux nouvelles conditions de croissance et leurs dynamiques sont encore

mal connues. Les réponses observées comprennent des modifications de la morphologie et de l'architecture des arbres en complément à une amélioration de la croissance radiale (Diaci & Kozjek, 2005). Des ajustements des propriétés du bois liées aux fonctions biomécaniques (Medhurst *et al.*, 2012) et hydrauliques (Caquet *et al.*, 2009) du bois dans l'arbre ont aussi été rapportés.

Cette thèse vise à appréhender les processus d'acclimatation d'arbres dominés libérés après de longues périodes dans l'étage dominé. Le **chapitre 1** présentera une synthèse des connaissances actuelles de l'écosystème forestier et les réponses des arbres à l'ouverture de la canopée. Un court **chapitre 2** exposera la démarche globale mise en œuvre. Les **chapitres 3**, **4** et **5** sont composés des résultats sous forme de projets d'articles et sont organisés par discipline. Nous commencerons par l'étude de l'allocation de la biomasse, suivie par la biomécanique et terminerons par l'hydraulique. Enfin le **chapitre 6** est une discussion de l'ensemble des résultats dans un contexte plus général et conclura sur des perspectives ouvertes par les travaux réalisés.

1.2. L'écosystème forestier

Comme tout écosystème, la forêt est définie par la dynamique des individus la composant, les interactions entre les individus, et entre les individus et le climat.

1.2.1. Structure et dynamique forestières

Les peuplements forestiers irréguliers sont composés de plusieurs étages suivant un gradient vertical. Les statuts sociaux des arbres sont définis en fonction de la position de leur houppier le long du gradient vertical (Nicholas *et al.*, 1991; Pretzsch, 2010). L'étage dominant est formé par les arbres dominants et co-dominants, qui accèdent à la canopée. Les arbres dominants présentent des houppiers plus hauts que ceux des arbres co-dominants. L'étage dominé est constitué des arbres dont les houppiers sont situés en dessous de l'étage dominant et n'ont donc pas accès au haut de la canopée. Dans cet étage, plusieurs stades de développement sont identifiables en se basant sur les dimensions des individus. Les semis, dont la hauteur est par convention, définie comme inférieure à 3 m, constituent ce qu'on appelle la régénération du peuplement. Les arbres dominés d'une hauteur supérieure à 3 m et d'un diamètre du tronc à 1.30 m inférieur à 7.5 cm sont dénommés gaulis. Lorsque le diamètre du tronc à 1.30 m est supérieur à 7.5 cm on parlera alors de perches. Jusqu'à ce stade, les individus constituent le potentiel de recrutement du peuplement forestier.

Le taux de mortalité des individus dans l'étage dominé est plus fort que dans l'étage dominant et la mortalité est principalement causée par la forte compétition inter-arbre pour les ressources, notamment la lumière. Le passage de l'étage dominé à l'étage dominant, soit le recrutement, est donc une étape cruciale pour la survie des individus, notamment pour les espèces non tolérantes à l'ombre (Ward & Stephens, 1993). L'importance de la régénération naturelle a été étudiée (Clark *et al.*, 1999; Wagner *et al.*, 2010) mais peu d'informations sont disponibles quant à la phase de transition entre le stade perche et l'étage dominant.

Plusieurs stratégies d'accession à la canopée ont été identifiées à partir d'études dendroécologiques analysant la croissance en diamètre passée d'arbres dominants (Rentch *et al.*, 2003). Ces stratégies peuvent différer entre les espèces tolérantes ou non à l'ombrage (Canham, 1988; Hart *et al.*, 2010) mais, dans les peuplements irréguliers, toutes impliquent des épisodes de libération de la compétition inter-arbre via la formation de trouées dans la canopée. Ces ouvertures au sein de la canopée offrent de l'espace disponible dans l'étage dominant pour l'établissement d'un ou plusieurs arbres dominés. Elles peuvent être causées par la mort ou la chute d'un arbre dominant, e.g. suite à une

tempête. La dynamique de ces forêts est donc une succession d'ouvertures et de fermetures de la canopée (Emborg, 2007). De plus, pour favoriser le renouvellement du peuplement et contrôler la structure de l'étage dominant (Webster & Lorimer, 2005), la réalisation d'ouvertures de la canopée est partie intégrante des itinéraires sylvicoles. Ces phases d'ouvertures et de fermetures de la canopée impactent directement les conditions de croissance des arbres dominés.

1.2.2. Microclimat forestier et conditions de croissance

Les interactions entre les individus et le climat couplées aux interactions entre les individus résultent, au niveau local, en un microclimat particulier (Parker *et al.*, 1995; De Frenne *et al.*, 2013). Les conditions de croissance sont spécifiques au climat local (montagne, plaine, méditerranéen..), du site (type de sol, présence de rivière…) ou encore de la structure du peuplement (Chen *et al.*, 1999; Aussenac, 2000; Pretzsch, 2010).

Lors d'une ouverture de la canopée, les conditions de croissance changent soudainement. La libération de la compétition inter-arbre permet un meilleur accès à la lumière en termes de quantité et de qualité (rayonnements photosynthétiquement actifs, Brasseur and De Sloover, 1976; Ritter *et al.*, 2005). La teneur en eau du sol augmente mais l'air est plus sec (Bréda *et al.*, 1995; Latif & Blackburn, 2010; Von Arx *et al.*, 2013). De plus, les températures du sol et de l'air ainsi que les mouvements d'air sont plus importants (Ritter *et al.*, 2005; Ma *et al.*, 2010) résultant en une demande évaporatoire plus élevée (Von Arx *et al.*, 2013). La principale ressource limitant la croissance de l'arbre libéré n'est donc plus la lumière mais l'eau et les nutriments qu'il peut capter.

L'arbre libéré fait également face à des conditions moins avantageuses à son développement. Par exemple, les écarts de températures et le risque de gel ou d'épisodes de chaleur sont plus élevés (Rambo & North, 2009; Pinheiro *et al.*, 2013). L'augmentation des mouvements d'air ainsi que la perte du soutien des arbres voisins illustrent l'augmentation des contraintes mécaniques à laquelle l'arbre libéré doit faire face augmentant ainsi le risque de mortalité due au vent (Cremer *et al.*, 1982).

Les conditions de croissance en forêt sont très variables de par la succession d'ouvertures et de fermetures de la canopée. Les arbres dominés sont en attente d'une ouverture pour pouvoir accéder à la canopée. La vitesse de la mise en place des réponses d'acclimatation sera déterminante dans leur capacité à s'établir avant les arbres voisins au niveau de l'étage dominant.

1.3. Comment pousse un arbre ?

La croissance de l'arbre est l'une des caractéristiques indiquant la vitalité d'un individu (Dobbertin, 2005). Une courte synthèse est proposée sur les processus de croissance. Pour un arbre cela comprend, entre autre, la croissance axiale et radiale.

1.3.1. Croissance primaire : longueur d'unités de croissance

La croissance axiale est définie par la croissance en longueur des tiges, des branches et des racines. Elle est générée aux extrémités des organes dans les bourgeons terminaux par les méristèmes primaires, consortium de cellules génératrices. Les divisions anticlines des cellules nouvellement formées suivies d'une phase d'allongement cellulaire permettent l'élongation de la tige dans le sens longitudinal (Fontaine *et al.*, 1999; Grattapaglia *et al.*, 2009). D'un point de vue extérieur, la longueur de tige formée annuellement est appelé unité de croissance.

1.3.2. Croissance secondaire : formation du bois

Chez les ligneux un deuxième type de croissance est identifiable. Il s'agit de la croissance radiale, soit la croissance en diamètre, qui se traduit notamment par la formation du bois et est appelée communément la croissance secondaire.

Le bois est un tissu produit par le méristème secondaire, aussi appelé le cambium vasculaire. Il est localisé entre le phloème (écorce) et le xylème (bois) et est bifacial, c'est-à-dire qu'il produit des cellules vers l'extérieur (écorce) et aussi vers l'intérieur (bois) (Fig. 1.1). En régions tempérées où les saisons sont marquées, la formation du bois n'est pas continue et est arrêtée lors de l'hiver. Le bois annuellement produit forme alors une couche discernable en périphérie du tronc : le cerne.

Le cambium est composé de deux types de cellules : (i) les initiales radiales et (ii) les initiales fusiformes. Chez les angiospermes, les cellules initiales radiales sont les précurseurs des rayons ligneux qui traverseront radialement la section du cerne tandis que les initiales fusiformes se divisent dans le sens axial pour former les fibres, les vaisseaux et les parenchymes axiaux (Fig. 1.2). La formation du bois comprend une succession d'étapes développementales comprenant : (i) la division des cellules à partir des cellules initiales, (ii) l'élongation et l'élargissement radial des cellules, (iii) le dépôt de la paroi secondaire et le commencement de la lignification des parois, (iv) la mort programmée des cellules et (v) la fin de la lignification des parois cellulaires (Plomion *et al.*, 2001; Samuels *et al.*, 2006; Déjardin *et al.*, 2010).

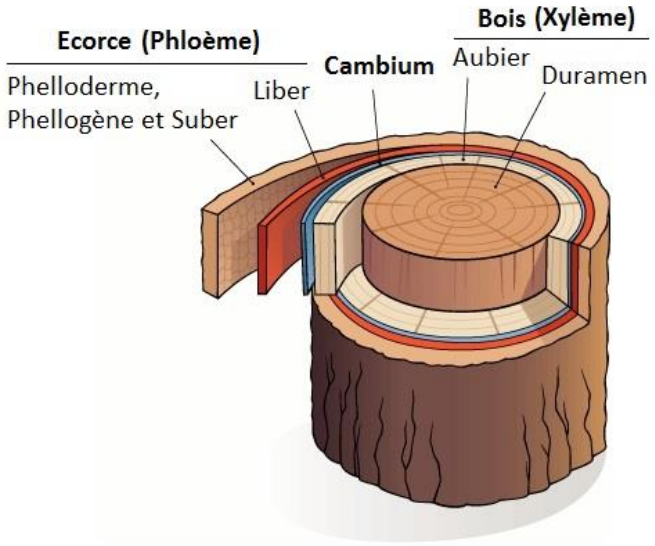

Figure 1.1 : Organisation tissulaire de la tige d'un arbre.
(Source : https://www.biologievegetale.be)

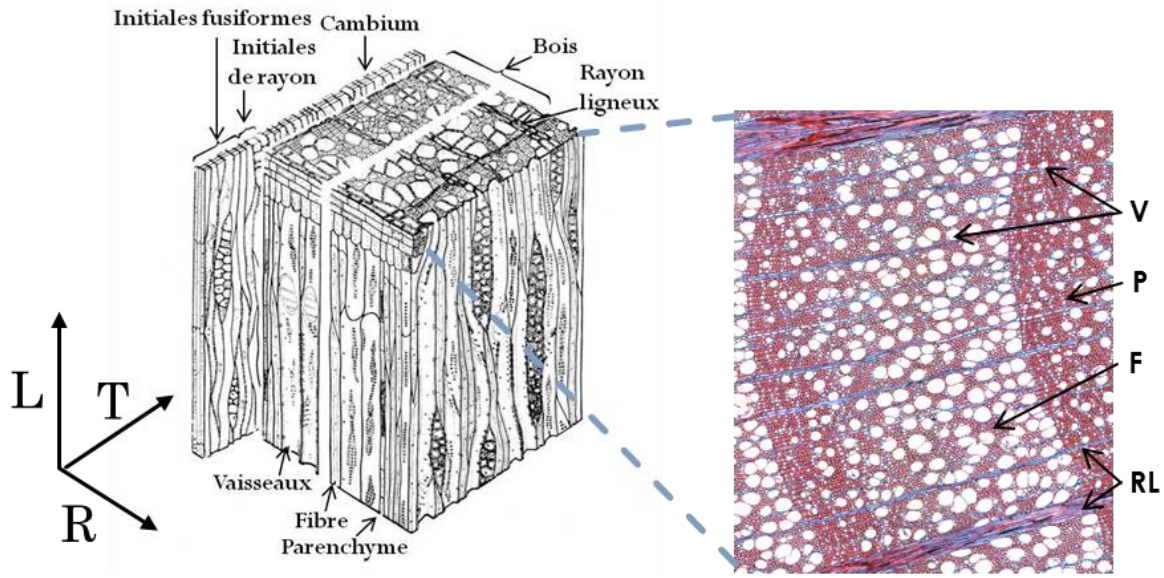

Figure 1.2 : Organisation des éléments ligneux du bois.
Gauche : Plan ligneux de bois d'angiosperme (L : sens longitudinal, T : sens transversal, R : sens radial).
Droite : Coupe transversale de bois de hêtre (*Fagus sylvatica* L.) colorée au Safranine-Bleu Astra obtenue par microscopie optique (grossissement x 10). (Source : INRA)
V : vaisseaux, P : parenchyme, F : fibre, RL : rayons ligneux.

Pendant le processus de maturation, des contraintes dites contraintes de maturation, sont générées dans les cellules fraîchement formées. Le processus exact de la genèse de ces contraintes n'est pas encore bien élucidé et ferait intervenir plusieurs processus entre les différentes composantes de la paroi cellulaire (Alméras & Clair, 2016). La paroi d'une cellule de bois est formée par trois couches successives (S1, S2, S3) dont la couche secondaire (S2, Fig. 1.3) est la plus épaisse et la plus importante pour les propriétés physiques et mécaniques du bois (Bergander & Salmén, 2000). Cette couche est composée de microfibrilles de cellulose logées dans une matrice de lignine et d'hémicellulose (Schindler, 1998). Les microfibrilles de cellulose sont composées à 70% de cellulose cristalline et confèrent à la paroi sa rigidité. L'orientation de ces microfibrilles par rapport à l'axe longitudinal (angle de microfibrilles, AMF) est très importante pour les propriétés telles que le retrait au séchage, le module élastique ou encore les contraintes de maturation (Booker & Sell, 1998; Thibaut *et al.*, 2001). L'organisation de la paroi résulte en une forte anisotropie des propriétés, c'est-à-dire que les propriétés diffèrent en fonction de la direction observée. La direction longitudinale est fortement privilégiée pour la mécanique devant les directions radiale et tangentielle, même si le retrait est le plus important dans le sens tangentiel (Salmén, 2004; Clair *et al.*, 2013).

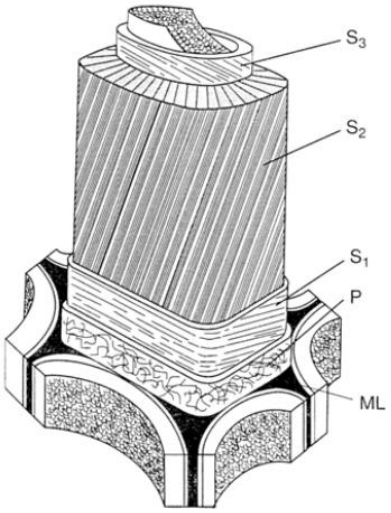

Figure 1.3 : Schéma de la structure de la paroi cellulaire secondaire avec agencement de l'angle des microfibrilles des différentes couches S (S1, S2 et S3). (Booker and Sell, 1998)
P : Paroi primaire, ML : Lamelle moyenne.

La croissance radiale est régie par l'influence de plusieurs facteurs de différentes natures : (i) des facteurs ontogéniques, qui comprennent le développement architectural, l'âge, la taille (Domec & Gartner, 2002; Meinzer *et al.*, 2011; Collet *et al.*, 2011) ; (ii) des facteurs environnementaux, i.e. la lumière, les mouvements d'air, les températures, la disponibilité en eau (Wimmer, 2002; Fonti *et al.*, 2010) ; et (iii) la stratégie de croissance comme la tolérance à l'ombrage (Canham, 1989). Ces facteurs impactent directement les traits du bois formé chaque année (Sass & Eckstein, 1995; Wimmer, 2002; Hacke *et al.*, 2017)

1.3.3. Allocation de la croissance

L'allocation de la croissance entre la hauteur et le diamètre d'un individu est utilisée pour étudier l'impact du climat (Franceschini *et al.*, 2016; Motallebi & Kangur, 2016) ou la stratégie d'acclimatation des arbres à divers facteurs (Poorter *et al.*, 2011). Cette relation reflète, tout d'abord, l'allocation du carbone assimilé par la plante et est variable dans le temps mais aussi suivant les espèces (Pretzsch *et al.*, 2013).

La répartition de la biomasse entre la hauteur et le diamètre des tiges est sensée régir la capacité de la plante à capter les ressources (Bloom *et al.*, 1985; Enquist, 2002; Poorter *et al.*, 2011). Par exemple, une forte densité de peuplement engendre une forte compétition inter-arbre pour les ressources. De ce fait, les arbres dominés présentent des tiges plus élancées que les arbres dominants pour optimiser l'acquisition de la lumière et mieux exploiter l'espace entre les houppiers des arbres dominants (Seki *et al.*, 2013; Sumida *et al.*, 2013; Dassot *et al.*, 2015). Un épisode de stress hydrique (Lines *et al.*, 2012) ou de sollicitations mécaniques, par exemple le vent (Pruyn *et al.*, 2000; Telewski, 2006), impactent aussi cette relation en favorisant l'augmentation en diamètre par rapport à la hauteur des tiges de l'individu.

Ces études ont analysé la relation entre la hauteur totale l'arbre et le diamètre total de la tige. En se basant sur les dimensions totales des individus, les résultats observés ne reflètent pas seulement la réponse d'un individu aux changements de conditions de croissance mais intègrent aussi l'impact des conditions de croissance passées et donc un biais dans l'interprétation des réponses observées. Pour estimer proprement les ajustements mis en place par l'individu, l'analyse de la croissance annuelle (largeur de cernes et longueur d'unités de croissance) sont les paramètres pertinents. Peu d'études proposent ce genre de résultats et concernent l'effet du statut social, d'un épisode de sécheresse ou de la densité du peuplement sur la relation entre croissances annuelles en hauteur et en diamètre (Sumida, 2015; Trouvé *et al.*, 2015).

La coordination entre croissance axiale et croissance radiale permet aux arbres de définir la forme de leur tige en fonction des besoins de l'arbre. Le changement d'allocation de la biomasse à un type de croissance par rapport à un autre peut augmenter les chances de survie d'un arbre après un changement brusque des conditions de croissance.

1.3.4. Impact de l'ouverture de la canopée sur la croissance

La largeur de cerne est un indicateur très utilisé dans les disciplines telles que la dendroécologie (Fritts & Swetnam, 1989; Rubino & McCarthy, 2004; Nagel *et al.*, 2007) ou la dendrochronologie (Lebourgeois *et al.*, 2005) qui sont capables de discerner ainsi les changements de conditions de croissance des individus. Ces études ont principalement été conduites chez des individus dominants qui ont réussi à accéder à la canopée.

De par sa facilité de mesure, l'immédiate augmentation de la croissance radiale est la modification la plus communément observée en réponse à une ouverture et est très documentée. Les effets d'une ouverture peuvent être visible sur plusieurs années en ce qui concerne la croissance radiale (Keyser & Brown, 2014). Suivant le site d'étude et l'espèce, l'amplitude de la réponse en croissance radiale peut aussi varier (Wright *et al.*, 2000) et des délais de réponse sont observés suivant l'espèce étudiée (Hart *et al.*, 2010) : les espèces intolérantes à l'ombrage peuvent réagir plus vite que les espèces tolérantes à l'ombrage.

Peu d'études ont été menées directement sur la croissance axiale après ouverture de par la complexité de mise en place des mesures en suivi, surtout chez les grands arbres où l'erreur liée à la mesure peut être forte. Chez les semis, la croissance axiale est stoppée la première année et reprend la deuxième après ouverture (Collet *et al.*, 2001). Une étude sur du Pin sylvestre a cependant démontré que la croissance axiale diminue après une ouverture (Valinger *et al.*, 2000). Le décalage entre la reprise de croissance radiale et axiale suggère que les dynamiques de réponse de la croissance radiale et axiale diffèrent pour les semis.

De plus, le ratio entre la surface de cerne et la surface du houppier augmente chez les semis libérés de hêtre illustrant une meilleure activité cambiale des semis libérés comparée aux semis dominés (Caquet *et al.*, 2009). Les auteurs suggèrent que l'augmentation de la saison de croissance est coordonnée avec des modifications structurelles et physiologiques à plus petite échelle.

1.4. Fonctions du bois

Chez les angiospermes, chaque élément ligneux remplit une fonction dans l'arbre. Les fibres assurent la fonction mécanique, les vaisseaux la fonction hydraulique et les parenchymes la fonction de réserve (Evert, 2006; Myburg *et al.*, 2013). La modification des traits des différents types cellulaires (proportions, taille, épaisseur de la paroi, agencement…) du bois permet de modifier les propriétés du tissu (élasticité, conductivité hydraulique…).

1.4.1. Fonction de soutien mécanique

L'épaisseur des parois secondaires des fibres est le déterminant principal de la densité du bois. L'organisation de la paroi (AMF, § 1.3.2) et la densité du bois permettent d'expliquer la plupart de la variabilité inter- et intra- spécifique des propriétés mécaniques du bois telles que le module d'élasticité ou le module de rupture. Cependant, certaines propriétés mécaniques comme la déformation à la rupture sont peu étudiées et difficiles à prédire à partir de la densité et de l'AMF.

Les propriétés mécaniques du bois les plus importantes pour l'estimation des traits de sécurité biomécaniques à l'échelle de l'arbre entier sont le module de Young, i.e. le module d'élasticité (MOE), et le module de rupture du bois (MOR) (Fournier *et al.*, 2013). Le diagramme de contrainte-déformation (Fig. 1.4) permet de visualiser le MOE en tant que la pente entre les deux variables dans le domaine des déformations élastiques. Le MOR correspond à la contrainte atteinte par le matériau au moment de la rupture.

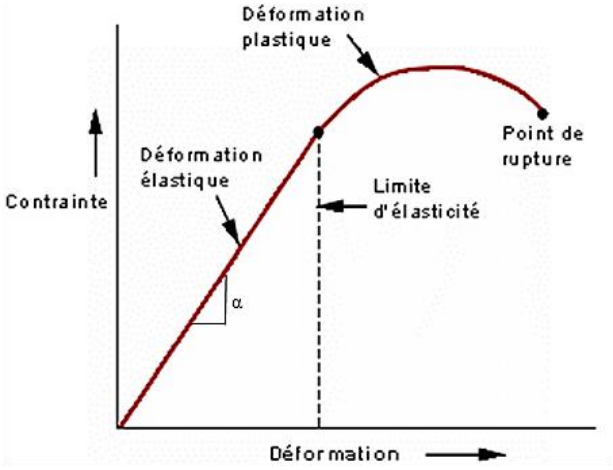

Figure 1.4 : Diagramme de contrainte-déformation.
La pente α correspond au MOE et le point de rupture au MOR.

Le MOE est dépendant des conditions de croissance d'un arbre. Par exemple, les arbres tropicaux qui poussent dans une plantation présentent un MOE plus faible et un bois plus dense que des arbres provenant d'une forêt naturelle (McLean *et al.*, 2011). Cette différence serait due à une réaction à la sollicitation mécanique des tiges liée au vent. Il a aussi été montré chez l'épicéa que le statut social d'un arbre influence le MOE (Brüchert *et al.*, 2000). Les arbres dominés sont plus élancés et, d'après les auteurs, auraient besoin d'une tige plus rigide pour supporter le poids de l'arbre et ne pas fléchir. Chez l'eucalyptus, une ouverture de la canopée induit des modifications des angles des microfibrilles mais pas de la densité du bois ou du MOE (Medhurst *et al.*, 2012). Les auteurs ont aussi montré que l'angle des microfibrilles est sensible à l'élancement des tiges (ratio hauteur/diamètre). L'élancement des tiges est souvent utilisé comme un indicateur simplifié de la résistance de l'arbre au vent (Cremer *et al.*, 1982; Mitchell, 2000).

1.4.2. Fonction de muscle

La fonction de muscle du bois se traduit par la capacité de l'arbre à maintenir et corriger l'orientation spatiale de ses axes. Le moteur principal de ce contrôle ou du processus de redressement est l'asymétrie des contraintes de maturation de part et d'autre de la section de la tige. Cette asymétrie permet de générer un moment de flexion et donc un mouvement de redressement. Les axes en redressement produisent un bois particulier dénommé le bois de réaction. Chez les angiospermes, ce bois est appelé bois de tension (BT) et se forme sur la partie supérieure des tiges.

Ses propriétés anatomiques et biomécaniques particulières permettent de le distinguer du bois normal (BN) (Jourez, 1996; Moulia & Fournier, 2009). Sa principale caractéristique est son état de tension supérieur à celui du bois normal (Trenard & Guéneau, 1975; Fang *et al.*, 2008). Selon les espèces considérées, il présente certains caractères comme la modification de la forme des vaisseaux, du diamètre des fibres, de l'épaisseur des parois ou la présence de fibres gélatineuses, appelées fibres G (Fig. 1.5) (Gardiner *et al.*, 2014). La couche de fibres G présente des microfibrilles parallèles entre elles et orientées selon l'axe longitudinal de la cellule. L'angle des microfibrilles dans la couche G est alors plus petit que celui du bois normal, voire même nul (Déjardin *et al.*, 2010).

Les conditions de croissance, les traitements sylvicoles ainsi que l'espèce affectent la quantité de bois de tension produit par l'arbre. Kubler (1988) avançait déjà que la sylviculture affectait de manière non négligeable la quantité de bois de tension et que des ouvertures fréquentes et graduelles limitaient la formation de bois de tension dans le

peuplement final. La même conclusion a été faite par Polge (1981) en étudiant les peuplements de hêtre soumis à différents régimes d'ouverture de la canopée. Néanmoins, prédire la quantité de bois de tension dans un arbre à partir de sa morphologie à un moment donné sans connaître son historique n'est pas évident : Jullien *et al.* (2013) a montré que pour le hêtre, le meilleur prédicteur des contraintes de maturation élevées est l'élancement de l'arbre qui n'explique pourtant que 10 % de la variabilité observée. Concernant la réaction immédiate à une ouverture de la canopée, moins d'information sont disponibles. L'angle d'incidence des rayonnements lumineux interceptés influence grandement la formation du bois de tension (Matsuzaki *et al.*, 2007). Chez de jeunes chênes libérés, l'ouverture de la canopée induit immédiatement la formation de bois de tension et un redressement des tiges (Hamilton *et al.*, 1985).

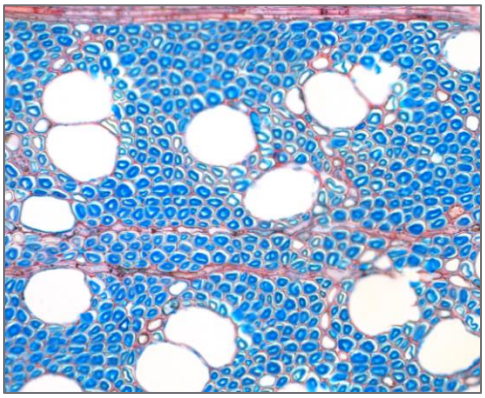

Figure 1.5 : Coupe transversale de bois de tension chez du hêtre (*Fagus sylvatica* L.) colorée au Safranine-Bleu Astra (grossissement x 20). (Source : INRA)
La couche G des fibres G apparait en bleu.

1.4.3. Fonction de conduction de la sève

La dernière fonction du bois développée dans cette synthèse bibliographique est la fonction de l'efficacité du transport de la sève brute. Chez les Angiospermes, le transport axial est assuré par les vaisseaux, des cellules larges et à paroi fine (Miyashima *et al.*, 2013) tandis que le transport radial des assimilas et de l'eau entre l'écorce et le bois est réalisé par les rayons ligneux. La montée de la sève des racines jusqu'aux feuilles *via* les vaisseaux est amorcée par la tension générée par les forces au sein de la sève couplée à la cohésion des molécules d'eau entre elles, c'est la théorie de la tension-cohésion (Dixon & Joly, 1894). Les vaisseaux formés à une hauteur donnée dans l'arbre doivent subvenir à la demande évaporative de la biomasse foliaire de la partie avale (pipe-model, Shinozaki *et al.*, 1964). La colonne d'eau formée par l'empilement des vaisseaux le long de la tige explique que la taille des vaisseaux est un trait clé du bois pour évaluer la capacité du tissu à conduire la sève brute (Hacke *et al.*, 2017). A partir des dimensions et de la

distribution des vaisseaux, il est possible d'estimer la performance du tissu en calculant la conductivité hydraulique spécifique potentielle (Steppe & Lemeur, 2007). Une meilleure capacité de conduction résulte en un meilleur potentiel de croissance (Fan *et al.*, 2012).

Plusieurs études ont montré que la taille des vaisseaux est un trait très sensible aux conditions de croissance notamment aux régimes de précipitations ou encore le taux de lumière interceptée (Sass & Eckstein, 1995; Barigah *et al.*, 2006; Hacke, 2014). La forte variation intraspécifique de la taille des vaisseaux peut donc être expliquée par des acclimatations locales à l'aridité du site ou encore aux températures auxquelles l'arbre fait face. Chez les semis, l'ouverture de la canopée peut induire des ajustements anatomiques et d'efficacité de la conduction de la sève (Hoffmann & Schweingruber, 2002; Caquet *et al.*, 2009) ou non (Maherali *et al.*, 1997).

1.4.4. Lien entre les propriétés du bois et la taille et la forme de l'arbre

Quelques études ont prospecté les traits du bois en fonction de la taille ou de la forme des individus. Le diamètre des tiges impacte le potentiel de croissance d'un arbre (Mencuccini *et al.*, 2005; Caquet *et al.*, 2010). Read et Stokes (2006) ont suggéré que la taille (hauteur et diamètre) peut influencer la survie des individus en altérant les propriétés biomécaniques du bois. En effet, la fonction de support du bois peut être plus sollicitée si l'arbre présente une plus grande surface de houppier (Kuprevicius *et al.*, 2013). La surface de houppier impacte aussi les contraintes de croissance tout comme l'élancement des tiges (Saurat & Guéneau, 1976; Jullien *et al.*, 2013) ou encore l'inclinaison des tiges (Polge, 1981). Brüchert *et al.* (2000) suggèrent que la stabilité de l'individu à la flexion de la tige dépend de ses caractéristiques morphologiques telles que la forme de la tige, du houppier et des propriétés matérielles de l'axe. La capacité du bois à soutenir l'individu dans son ensemble comprend donc la rigidité et la résistance du matériau, mais aussi la géométrie et le chargement (Fournier *et al.*, 2013).

En ce qui concerne le redressement des tiges, la vitesse et l'amplitude du redressement dépendent de l'épaisseur de la tige (Kubler, 1988). Un arbre présentant une large section engendre un moment d'inertie plus important rendant la section plus difficile à courber. Par ailleurs, la formation de bois de tension n'est pas le seul moyen dont les arbres disposent pour redresser leurs axes. Une forte excentricité de la croissance radiale peut aussi promouvoir le mouvement des tiges (Alméras *et al.*, 2005b; Fisher & Marler, 2006). Pour augmenter l'efficacité du processus, la croissance peut être couplée à la formation de bois de réaction (Alméras *et al.*, 2005b; Dassot *et al.*, 2012). De plus, il a été observé chez

des semis de hêtre et d'érable suite à une ouverture de la canopée que le redressement est promu par soit la réorientation des axes relais ou par le redressement de l'axe principal suivant l'espèce étudiée (Fig. 1.6) (Collet *et al.*, 2011). Cette étude ne comprend pas de quantification de la production de bois de tension et n'informe pas quant à la répartition de la contribution des ajustements opérés aux différentes échelles.

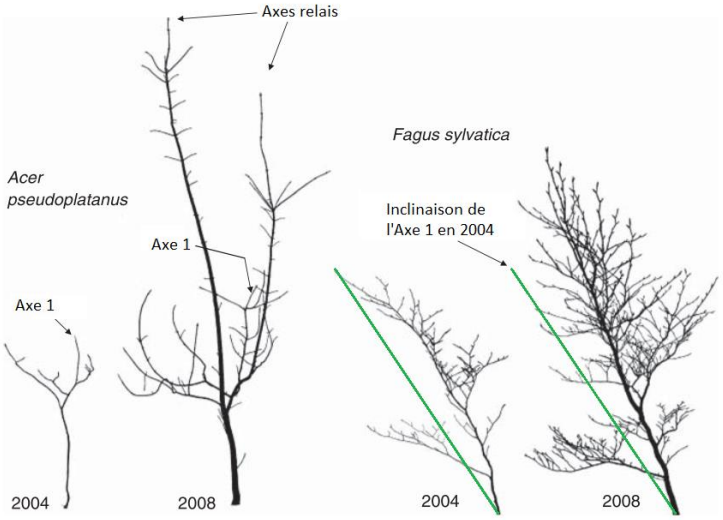

Figure 1.6 : Redressement des axes principaux et relais chez *Acer pseudoplatanus* et *Fagus sylvatica* L. avant (2004) et après (2008) ouverture. (Collet *et al.*, 2011)
Les photographies sont à la même échelle.

L'influence de la taille a aussi été prospectée pour les traits liés aux performances hydrauliques du bois. Le diamètre des vaisseaux mesuré à une même hauteur dans la tige augmente avec la hauteur totale de l'arbre (Preston *et al.*, 2006; Fan *et al.*, 2012). Ce fait illustrerait l'effilement de la taille de vaisseaux avec la longueur de la tige, c'est-à-dire que les vaisseaux à la base d'un arbre sont plus larges qu'à l'extrémité de sa cime (modèle WBE, Mencuccini, 2002). De plus, le diamètre des vaisseaux et surtout la conductivité hydraulique spécifique sont dépendants du diamètre de la tige (McCulloh *et al.*, 2010, 2015). Les arbres peuvent ajuster les performances de leurs tissus grâce à la croissance radiale : des arbres avec des conductivités hydrauliques spécifiques différentes peuvent supporter la demande évaporatoire d'une même surface foliaire en ajustant leur surface de bois conducteur (Becker *et al.*, 1999).

Les modifications des propriétés du bois suite à un changement de conditions de croissance reflètent des processus d'acclimatation mis en œuvre par l'individu. Néanmoins, pour bien comprendre l'effet de ces changements sur la performance de l'arbre entier il faut intégrer ces propriétés aux ajustements de la forme et de la taille (Violle *et al.*, 2007; Lachenbruch & Mcculloh, 2014)**.**

L'approche intégrative prend en compte les traits structuraux mesurés à différentes échelles pour comprendre leur impact sur la réponse à l'échelle de l'individu. Ces traits comprennent les dimensions et la forme des arbres, les propriétés matérielles du bois et le chargement.

1.4.5. Importance de la taille et de la stratégie de croissance des arbres dans la réponse à l'ouverture

Comme statué dans le paragraphe précédent, la taille et la forme d'un arbre sont des composantes à part entière à prendre en compte dans les mécanismes de réponse. Au fur et à mesure de sa vie, l'arbre augmente sa taille et les contraintes qu'il rencontre changent de nature et impactent les dynamiques mais aussi l'amplitude de ces réponses.

L'augmentation de la taille des arbres engendrerait moins de plasticité en termes d'allocation de biomasse et de morphologie du houppier en réponse à des changements de régimes lumineux (Messier & Nikinmaa, 2000). Pour les espèces tolérantes à l'ombrage, l'augmentation de la taille s'accompagnerait d'une sensibilité croissante aux régimes de températures et de disponibilité en eau (Mérian & Lebourgeois, 2011).

Il est aussi statué qu'un arbre plus jeune sera plus réactif aux changements de ses conditions de croissance (Meinzer *et al.*, 2011). Dans le cas d'une ouverture de la canopée, cela serait dû au fait que les jeunes arbres montrent une augmentation plus élevée des performances photosynthétiques les premières années (Skov *et al.*, 2004). Pour les espèces tolérantes à l'ombrage, l'âge a un impact non négligeable sur les relations allométriques entre hauteur et diamètre des tiges (Bohlman & O'Brien, 2006; Franceschini & Schneider, 2014) et sur l'architecture (Yagi, 2009).

Le statut social d'un arbre est très important pour sa croissance. La longueur de la saison de croissance des arbres dominés est plus courte en comparaison des arbres dominants (van der Maaten, 2013). Couplée à la forte compétition pour les ressources, les arbres dominés sont plus petits en termes de diamètre et de hauteur que les arbres dominants (Brüchert *et al.*, 2000; Nicolini *et al.*, 2001; Löf *et al.*, 2005; Petritan *et al.*, 2009). Ces petites dimensions peuvent être un atout pour la mise en place des réponses biomécaniques telles que le redressement suite à l'ouverture de la canopée. Par contre, le fort élancement des tiges peut s'avérer être un inconvénient pour la stabilité face au vent et au flambement.

1.5. Questionnement et objectif

La synthèse des connaissances actuelles nous apprend que les processus d'acclimatation des arbres résulteraient d'un compromis entre une acquisition maximale des nouvelles ressources disponibles pour une croissance rapide de l'arbre et la mise en place de structures spécifiques pour contrer les diverses contraintes rencontrées après l'ouverture de la canopée telles le vent ou encore le plus large intervalle de variations des températures. La réponse en croissance résulte d'une succession de processus sous-jacents. L'objectif principal de la thèse est de définir les principales composantes de réponse à l'ouverture de la canopée ainsi que les cinétiques mises en place.

1.6. Hypothèses de travail

Nous supposons que l'acclimatation s'accompagnera par des ajustements structurels et fonctionnels à plusieurs niveaux d'organisation :

- Afin d'augmenter sa résistance vis-à-vis du vent à l'échelle de l'individu, l'arbre libéré devra stabiliser sa structure élancée grâce à une allocation préférentielle de la croissance vers la croissance radiale (**Hypothèse 1**).
- L'arbre va produire plus de bois de tension et accessoirement allouer la biomasse de façon asymétrique autour de sa périphérie dans le but de générer un moment de flexion suffisant pour contrebalancer l'apport de biomasse sur un axe non vertical et permettre le redressement de sa tige (**Hypothèse 2**).
- L'augmentation de la demande évaporatoire et le meilleur accès à l'eau vont induire une augmentation de la conductivité hydraulique à l'échelle du cerne. En plus de la croissance radiale augmentée, les arbres libérés montreront des ajustements des traits des vaisseaux (taille, fréquence) du bois des tiges (**Hypothèse 3**).

Chapitre 2 : Démarche expérimentale

2.1. Choix effectués

2.1.1. Etude expérimentale et observationnelle

Dans cette étude, nous avons combiné une approche expérimentale à une approche observationnelle. L'étude expérimentale a consisté en la création d'ouverture du couvert forestier, pratique sylvicole fréquente. Plus précisément, les ouvertures appliquées sont d'une taille supérieure à celles réalisées communément par les forestiers (§ 2.2.2). De plus, le matériel végétal étudié peu fréquent. Il s'agit alors d'une étude de cas extrême visant à comprendre si de vieux arbres dominés sont encore en capacité de répondre à une ouverture et comment ils s'y adaptent. Les réponses observées à l'ouverture de la canopée expérimentale sont interprétées d'un point de vue fonctionnel. Nous tenterons de caractériser l'évolution des traits biomécaniques et hydrauliques après ouverture à partir des ajustements de la géométrie des tiges et de propriétés du bois observées à posteriori.

L'approche observationnelle se focalisera sur les traits du bois des arbres avant l'ouverture créée expérimentalement jusqu'à remonter à leur naissance. D'une part, le dispositif expérimental a été mis en place en 2006 pour répondre à des questions de gestion sylvicole et non dans le but d'une analyse fonctionnelle. Les données concernant les conditions de croissance passées n'ont alors pas été suivies. Le jeu de données ne permet donc pas explorer les relations entre les variables pertinentes caractérisant les conditions de croissance (précipitations, angle d'incidence et taux de lumière) et les réponses observées. L'ouverture de la canopée étant une modification de l'ensemble des variables de l'environnement immédiat de l'arbre libéré et dépendant de la taille de l'ouverture mais aussi de la localisation de celle-ci (présence d'une pente, orientation cardinale), les réponses observées seront interprétées comme des ajustements à l'ensemble des modifications des variables microclimatiques limitrophes de l'arbre libéré. D'autre part, les mesures réalisables en suivi sur des grands arbres en contexte sylvicole pour caractériser les changements de conductions hydriques (vulnérabilité à la cavitation, conductance stomatique) ou mécaniques (régime de déformation) ne sont possibles qu'au prix de protocoles expérimentaux lourds dans le cas où ils ont été développés et validés. Cela implique donc des limites en termes d'interprétation fonctionnelle.

2.1.2. Mesures en rétrospectif

Le bois enregistre l'histoire de l'arbre et reflète les changements de conditions de croissance (Wimmer, 2002; Fonti *et al.*, 2010). La lecture des largeurs de cernes et des longueurs d'unités de croissance renseignent sur l'ajustement de la forme de l'arbre et de sa taille au cours de sa vie. Toutes ces informations permettent une vision assez complète de la réaction de l'arbre à un traitement tel que l'ouverture de la canopée. Par contre, cette approche rétrospective présente aussi des limites. Entre autre, les informations sur les performances hydrauliques sont indirectes et limitées à une interprétation fonctionnelle de l'anatomie du bois. Une approche physiologique serait nécessaire pour être précis dans la caractérisation de l'acclimatation hydraulique. Ce type d'étude a déjà fait l'objet de certaines études auparavant et l'anatomie du bois a été étudié en parallèle des mesures physiologiques (Caquet, 2008; Gebauer *et al.*, 2014). Nous espérons que les modifications de l'anatomie du bois permettront d'identifier les processus clés de l'acclimatation hydraulique et dégageront des pistes pour de futures investigations plus précises.

2.1.3. Approche multidisciplinaire et intégrative

Une approche multidisciplinaire a été adoptée pour cette étude. Les modifications des performances hydrauliques induites par le changement de conditions de croissance sont beaucoup plus documentées que les performances biomécaniques. De ce fait, nous avons choisi de conduire la majorité des travaux sur les performances biomécaniques où la bibliographie est rare sur les grands arbres et, plus particulièrement, sur les grands arbres en cours d'acclimatation.

Comme soulevé dans le **chapitre 1**, l'échelle la plus pertinente pour évaluer les performances biomécaniques est l'échelle individuelle (Violle *et al.*, 2007; Fournier *et al.*, 2013). Néanmoins, chaque paramètre mesuré à une échelle différente peut contribuer de façon plus ou moins importante à la performance observée à l'échelle individuelle. Pour déterminer l'influence des différents paramètres tels que les dimensions et la forme des arbres, les propriétés matérielles du bois et le chargement, nous avons utilisé les traits intégratifs biomécaniques proposés par Fournier *et al.* (2013). Les traits calculés se focaliseront sur deux différentes composantes de la fonction de support du bois : (i) le squelette, qui fait intervenir l'épaisseur et le défilement de la tige avec la rigidité du bois ; (ii) la motricité, qui est impliquée dans les mouvements actifs générés par les auto-stress mécaniques.

Deux jeux de données originaux ont été obtenus pendant cette étude et ont aussi conditionné le choix des disciplines mises en avant : les accroissements axiaux (longueur d'unités de croissance) et l'évolution de l'inclinaison des arbres après ouverture (scans T-LIDAR). Les accroissements axiaux permettent d'analyser la relation entre la réponse en croissances radiale et axiale après ouverture, ce qui est très peu étudié expérimentalement chez les grands arbres (Article 1). Les scans T-LIDAR permettent pour la première fois de confronter le redressement modélisé des tiges après une ouverture avec des données expérimentales (Article 2).

2.1.4. Le hêtre

L'espèce modèle choisie pour cette étude est le hêtre européen (*Fagus sylvatica* L.). Son aire naturelle est vaste et s'étend sur une grande partie de l'Europe pour atteindre une superficie de 14 millions d'hectares. En France, cette espèce occupe 1 422 000 ha pour un volume de 312 Mm^3 (source : IFN), ce qui en fait la troisième essence feuillue sur le territoire français. Il s'agit donc d'une espèce d'intérêt sylvicole important.

Espèce opportuniste, elle est tolérante à l'ombrage. Il est donc possible d'observer des individus âgés resté dans l'étage dominé (Emborg, 2007). Dans ce cas, les hêtres dominés peuvent présenter des cernes manquants rendant l'estimation de l'âge des individus ardus (Grundmann *et al.*, 2008). Le hêtre est capable de répondre rapidement aux changements de ses conditions de croissance (Collet *et al.*, 2001; Caquet *et al.*, 2010). Même des individus restés durant de longues périodes dans l'étage dominé sont capables d'augmenter leur croissance radiale après l'ouverture de la canopée (Emborg, 2007; Trotsiuk *et al.*, 2012) ce qui augmente les probabilités d'obtenir des réponses mesurables.

Cette espèce est dite « nerveuse », elle est encline à produire une grande quantité de bois de tension. Ce qui est probablement lié à son caractère opportuniste qui nécessite une grande réactivité aux changements de conditions externes. C'est donc une bonne espèce modèle pour étudier le redressement des tiges.

Par ailleurs, le hêtre présente un bois à pores diffus et plusieurs de ses précédents cernes annuels sont fonctionnels en termes de conduction de la sève (Gasson, 1985; Dalsgaard *et al.*, 2011). La stratégie d'acclimatation des performances hydrauliques sera donc spécifique à cette espèce et non généralisable à des espèces telles que le chêne où le bois présente une structure à zone initiale poreuse et où le dernier cerne assure la majorité de la conduction de la sève (Granier *et al.*, 1994).

2.2. Dispositif expérimental

2.2.1. Descriptif du site

Le site étudié fait partie d'une étude expérimentale de plus grande ampleur sur la réactivité des perches en forêt hétérogène (Ningre *et al.*, 2011). Le site est situé dans la parcelle n°15 (47.9507°N, 6.3857°E), en forêt syndicale du massif du Grand Poiremont en Haute-Saône (70). La parcelle d'étude s'étend sur 13 ha à une altitude de 470 m. Un ruisseau borde le côté ouest de la parcelle qui a une pente de 12% (Fig. 2.1).

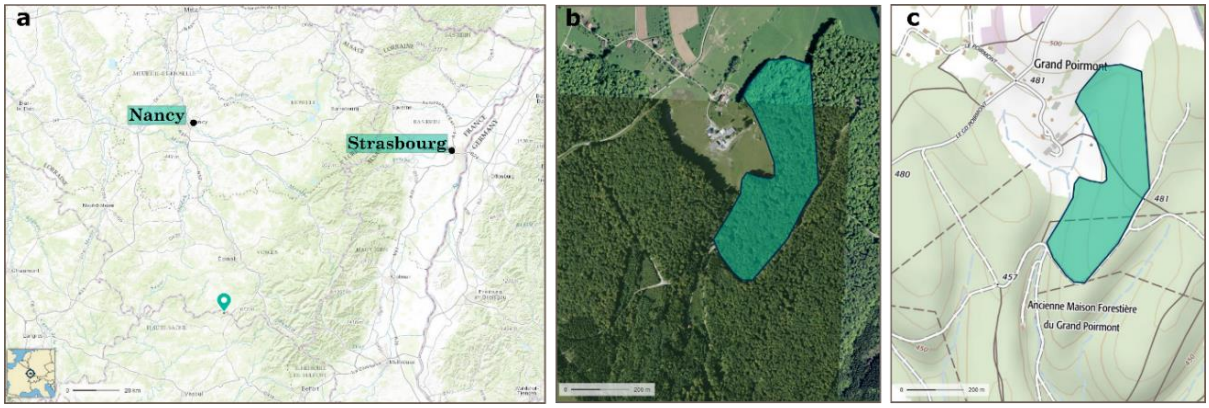

Figure 2.1 : Emplacement du dispositif expérimental (en bleu).
a : carte géographique de la forêt syndicale du Grand Poiremont au sud de Nancy (marqueur bleu). b : photographie aérienne de la parcelle. c : carte IGN (courbe de niveaux tous les 10 m). (© IGN 2016 – *www.geoportail.gouv.fr/mentions-legales*)

La forêt a été acquise en 1970 et depuis, elle est gérée en tant que futaie irrégulière avec des coupes jardinatoires à rotation de 10 ans. En 1955-56 tous les diamètres 35 et plus ont été prélevés. La dernière date d'exploitation connue est en 1995. En 2006, la parcelle est dominée par *Fagus sylvatica* L. en mélange avec *Quercus spp.*, *Fraxinus excelsior* L., *Acer pseudoplatanus* L., *Carpinus betulus* L., *Betula spp., Abies alba* Mill, et *Picea abies* L. (H) Karst. La surface terrière était de 28.3 m^2 ha^{-1} hors perches et la hauteur des arbres dominants était de 31.6 m.

Figure 2.2 : Photos des traitements appliqués.
a : couvert au-dessus d'une perche témoin. b : couvert au-dessus d'une perche éclaircie après 6 ans de traitement. c : perche éclaircie après 6 ans de traitement en période hors feuille. (Source : INRA)

2.2.2. Traitement

Un échantillon de 42 perches de hêtres distribuées sur toute la parcelle et éloignées de 18 m ont été sélectionnées suivant des critères morphologiques (Ningre *et al.*, 2011). Pendant l'hiver 2007-08, la moitié des perches ont été libérées de toute compétition dans un rayon de 12 m autour de l'arbre d'intérêt (perches « libérées »), tandis que l'autre moitié de l'échantillonnage demeure sous couvert (perches « dominées ») (Fig. 2.2), les caractéristiques morphologiques sont résumées dans le Tableau 2.1.

Tableau 2.1 : Récapitulatif des caractéristiques morphologiques mesurées 6 ans après ouverture de la canopée (2013) des perches dominées et libérées.

H : hauteur de l'arbre, D_b : diamètre basal, DBH : diamètre à 1.30 m, H/D_b : ratio d'élancement, A_w : surface projeté du houppier.

	Age	H (m)	D_b (m)	DBH (m)	H/D_b	A_W (m²)
Dominées	86	18.3 ± 3.3	0.16 ± 0.04	0.12 ± 0.05	113.8 ± 11.9	30.7 ± 14.0
Libérées	84.8	18.4 ± 3.32	0.19 ± 0.03	0.15 ± 0.05	96.9 ± 17.6	35.5 ± 13.4

2.2.3. Mesures

Les mesures ont été réalisées en trois temps (Fig. 2.3). En hiver 2013-14, la totalité des perches étudiées est abattue et ramenée au laboratoire. Pour les mesures faites sur le terrain, un suivi annuel tous les 3 ans a été réalisé pour les projections de houppier et les mesures morphologiques (encadré vert). Les mesures de distribution de la biomasse, de défilement du tronc et les indicateurs de contraintes de croissance ont été réalisées l'année de la récolte. Toutes les mesures au laboratoire ont permis l'acquisition des données en rétrospectif. Le détail des méthodes utilisées est précisé dans la partie matériel et méthode des articles.

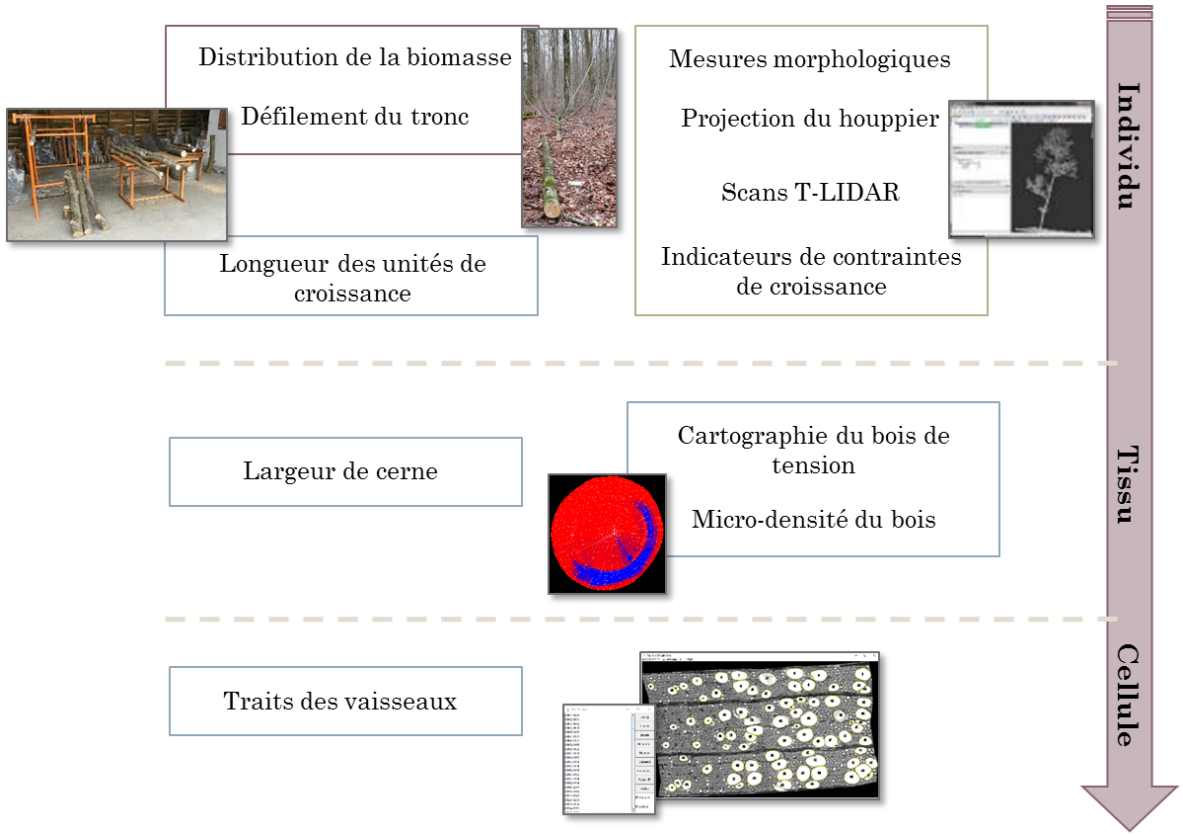

Figure 2.3 : Schéma récapitulatif des mesures effectuées par échelle.
Encadré vert : arbre sur pied. Encadré violet : pendant l'abattage. Encadré bleu : au laboratoire.

2.3. Démarche globale

Les chapitres suivants présenteront les résultats d'une étude multidisciplinaire. Pour couvrir l'analyse de l'acclimatation, une approche intégrative est développée. Des mesures rétrospectives permettent la réalisation de cinétiques.

Nous commencerons par une étude de la réponse en croissance du hêtre à l'ouverture de la canopée. Pour cela, le **chapitre 3** se concentrera sur une étude de la stratégie de l'allocation de la croissance des perches sous couvert. La relation statique et temporelle entre la croissance en hauteur et la croissance en diamètre sera analysée ainsi que l'impact des ouvertures passées de la canopée.

Le **chapitre 4** est divisé en trois parties. La première est une estimation rétrospective des contraintes de maturation. La seconde et la troisième se focaliseront sur les performances biomécaniques des perches dominées et libérées ainsi que sur l'évolution des performances des perches après l'ouverture de la canopée de 2007-08.

Le **chapitre 5** sera axé sur les caractéristiques anatomiques du bois de hêtre par une analyse à l'échelle cellulaire mais aussi tissulaire. Les traits du bois liés aux performances hydrauliques des perches, tels que les caractéristiques des vaisseaux, seront comparés à ceux de hêtres dominants de la même parcelle. La réponse à l'ouverture de la canopée des perches sera, quant à elle, confrontée à celle de semis de hêtres d'une précédente étude pour apprécier l'impact de la taille initiale des individus sur la stratégie de réponse du hêtre à cette échelle.

Chapitre 3 : Caractérisation de la stratégie de croissance du hêtre sous couvert

3.1. Avant-propos

Cette première partie de résultats concerne l'allocation de la croissance entre la hauteur et le diamètre des tiges et est présentée sous forme d'avant-projet d'article (Article 1). Seules les parties « matériel et méthodes » et « résultats » sont complètes. Les parties « introduction » et « discussion » sont des premières ébauches et seront sujet à des remaniements avant soumission. La contribution de chaque co-auteur à cet article est précisée dans le Tableau 3.1.

L'objectif de ce chapitre est d'estimer la relation entre la croissance axiale et radiale en statique et en temporelle. L'effet des ouvertures passées de la canopée sur cette relation est analysé et discuté.

Tableau 3.1 : Contribution des co-auteurs à l'Article 1.

Auteurs	**Contribution à l'Article 1**
Estelle NOYER	Acquisition des données, analyse des résultats, principale rédactrice de l'article
Catherine COLLET	Traitement statistique (modèle asymptotique et corrélation temporelle), contribution à la discussion et à la rédaction
Jana DLOUHA Mériem FOURNIER	Contribution à la discussion et à la rédaction
François NINGRE	Mise en place du site d'expérimentation du Grand Poiremont

3.2. Article 1 : Canopy release influences allocation in height and diameter growth in understory beech trees. (In progress)

Estelle NOYER, Jana DLOUHA, François NINGRE, Mériem FOURNIER and Catherine COLLET

LERFoB, INRA, AgroParisTech, F-54000, Nancy, France

3.2.1. Introduction

Forest is composed by several layers which correspond to a gradient of growth conditions (Rambo & North, 2009). Overstory trees, i.e. trees established at the canopy layer, form the forest cover. They have a better access to light, water (soil and rainfall) and nutrients resources (Bréda *et al.*, 1995; Aussenac, 2000) that favour an improved height and diameter growth rates than trees under the canopy (Nicolini *et al.*, 2001; Löf *et al.*, 2005; Petritan *et al.*, 2009). To maximise resource acquisition under the canopy, trees may adjust their growth allocation (Bloom *et al.*, 1985; Poorter *et al.*, 2011). It was reported that understory trees could favour the height growth and show slender stem to improve light interception in a high tree-competition context (King, 1990; Seki *et al.*, 2013; Sumida *et al.*, 2013; Trouvé *et al.*, 2015).

An improve height growth at the expense of the diameter growth might be an advantage in this context but the ratio between height and diameter growth could be limited to avoid hydraulic risks such as the disruption of the water transport (Ryan & Yoder, 1997; Becker *et al.*, 2000), and avoid mechanical damage as stem buckling (Niklas, 2002, 2007). Moreover, height and diameter growth rates are also related to water availability (Delagrange *et al.*, 2004; Trouvé *et al.*, 2015), leaf area and lateral growth (Coomes & Grubb, 1998; Sumida *et al.*, 2013). Though the ratio between the tree height and the stem diameter growth evaluate with the age or the tree size increasing (Genet *et al.*, 2011), ecological strategy of the tree species such as the adult stature (tall vs. short species) or the shade tolerance ability (King, 1991; Bohlman & O'Brien, 2006; Sendall *et al.*, 2015) are also determinant. Shade tolerant species are less plastic in term of growth allocation and more morphological plastic (Grime, 1977; Curt *et al.*, 2005), even if with the age individuals became less shade tolerant (Yagi, 2009; Sendall *et al.*, 2015).

In forest, understory trees experiment succession of canopy release and suppression events along their life (Rentch *et al.*, 2010; Trotsiuk *et al.*, 2012). Though these trees do not succeed to reach the canopy layer, they experiment fluctuations of their growth conditions. The strong sensitivity of the diameter growth rate with changes in growth conditions is commonly used by dendrochronology or dendroecology studies. An increase of diameter

growth rate could be interpreted as a better past growth conditions (Dittmar *et al.*, 2003; Lebourgeois *et al.*, 2005) or a canopy release event (Rubino & McCarthy, 2004; Emborg, 2007). In the case of canopy release event, the amount of response depended of the species, the site or whether individual stem diameter (Plauborg, 2004; Skov *et al.*, 2004; Boncina *et al.*, 2007). At the contrary, the age of the tree when the event happen does not impact the intensity of the reaction of the diameter growth rate (Keyser & Brown, 2014).

As growth allocation varies with time, relationship between height and stem diameter at a given time could be not easy to interpret because of the influence of the fluctuant past growth conditions. To study relationship between height and diameter growth rates should provide more robust information but it is just recently studied (Sumida, 2015; Trouvé *et al.*, 2015).

The aim of this study is to evaluate the relationship between the height and diameter growth rates in understory trees. We chose the European beech (*Fagus sylvatica* L.), a shade-tolerant species because it can survive under a high level of inter-tree competition, and can rapidly respond to changes in canopy structure and local irradiance. Ours objectives are: (1) to analyse the growth trajectories of understory trees, (2) to evaluate the relationship between the height and the diameter growth, (3) to study the effect of the variations of diameter growth on the height growth, and (4) to determine the effect of the diameter growth of the past and current year on the height growth. We use retrospective measurements of the height and the diameter growth to reconstruct the growth allocation of along the life of the understory trees. We benefit of the past canopy release events to analyse the effect of a large range of diameter growth on the height growth. In addition to the growth trajectories, we used two approaches to respond to our objectives: a static approach and a temporal approach by the calculation of cross-correlations.

Two hypothesis were tested:

- (**H1**) Understory trees display asymptotic relationship between height and diameter growth;
- (**H2**) Canopy release influences the allocation of the growth and favours diameter growth in the first years.

3.2.2. Material and methods

Study site

The site was a 13-ha-stand in a managed forest in north-eastern France (47.9507°N, 6.3857°E, alt: 470m). The soil was a cambisol dystric to hyperdystric with a luvic layer between the A and S horizons (IUSS Working Group WRB, 2014). Meteorological data came from Aillevillers-et-Lyaumont (French National Climatic Network, Météo-France) 5 km from the stand. Mean annual temperature was 10.3°C and mean annual precipitation was 1218 mm.

The stand had been formerly managed as a coppice-with-standards. In 1955-1956, the stand was thinned and converted to a high forest. Management records show it was further thinned between 1956 and 1995, but the years of thinning were not recorded. After 1995, there was no further thinning. In 2006, the stand was dominated by *Fagus sylvatica* L. (basal area: 21 m^2 ha^{-1}) with another 5.5 m^2 ha^{-1} of *Quercus spp., Fraxinus excelsior* L.*, Acer pseudoplatanus* L.*, Carpinus betulus* L.*, Betula spp., Abies alba* Mill*,* and *Picea abies* L. (H) Karst. Stand density was 513 stem ha^{-1} and the mean height of the overstory trees was 31.6 m.

In fall of 2007, a sample of 42 understory beech trees distributed throughout the stand and at least 18 m from one another was selected for the study. The selected trees originated from seeds and grew up under closed canopy or in small gaps. Sample trees met the following criteria: breast height trunk diameter was 7.5 to 17.5 cm, stems were unforked, leaned < 11°, had fewer than 25 epicormic branches (*sensu* Colin *et al.*, 2012) along the lowest 4 m of stem, had no visible injury, spiral grain, canker, or top dieback. The sample trees was then split into two subsamples with similar mean values for diameter. In winter 2007-2008, one subsample, the half of the total sample, was released by a thinning that removed the trees in competition in a 12 m radius around each target tree and the other subsample of trees, the another half, was left unreleased.

Diameter growth rate

Sample trees were felled in February-March 2014, six years after canopy opening. A 5-cm-thick disk was collected at 1.30 m height from each tree, wrapped in plastic film and was stored at -20°C immediately after harvest. After disks were sanded, four perpendicular radii were imaged by digital camera on each disk. On each radius, the width of each tree-ring (RW, mm) from pith to bark was measured to a precision of 0.01 mm, by image analysis using TSAP-Win (Rinntech, Germany).

Height growth rate

For each tree, successive height annual increments on the main axis were accessed by measuring the length of the annual growth units (LGU, mm) from winter bud scars located on the bark. Each ten growth units, the number of years was checked by counting the number of rings from a disk sampled at the base of the corresponding stem segment. In case of discrepancy between the number of growth units and the number of rings, the stem length was divided in smaller sub-segments and the growth units and rings were counted on each sub-segment until the two estimations were found to be equal. Three trees were finally discarded from the analysis because it was not possible to identify without ambiguity each annual growth unit and each ring on the stem. This method allows to reach a rare precision in terms of dating and value robustness. Tree age was estimated as the number of growth units counted along the trunk.

Data analysis

For each tree, ring width and basal area increment (BAI, cm²) were estimated for each annual ring from the position data for ring boundaries, averaged over the four radii. BAI was estimated as follows:

$$BAI = \pi (r_1^2 - r_2^2) \quad (3.1)$$

where r_1 and r_2 (cm) are the average of the radii from two successive years.

Detection of canopy release events

The dates of the successive canopy release events that occurred for each tree were unknown. Possible release events could be estimated for each tree by visual examination of its ring chronology. However, to standardise the identification of release events among the sample trees, a procedure to automatically detect and date release events was established. The procedure was calibrated against the events identified by visual examination and therefore may not be used as a standard for other studies. However, it may be used as a mean to homogenize the detection of release events among trees that had very different annual growth rates. A two-step-procedure was developed to identify the first year of past release events of the sample trees. The first step aimed at detecting release periods while the second step aimed at identifying the first year after release for each detected period.

In the first step, the percentage of growth change (PGC_1, %) for each year and on each tree is calculated as (Nowacki & Abrams, 1997):

$$PGC = \frac{M_2 - M_1}{M_1} \times 100 \quad (3.2)$$

where M_1 is the median of BAI for the preceding 8 years (excluding target year) and M_2 the median of BAI for the subsequent 4 years (including target year).

PGC_1 was then compared to a threshold value. All years where $PGC_1 > 25\%$ were identified, and time segments with at least 4 successive years above the threshold were considered as release periods. Black and Abrams (2003) used similar threshold values for shade tolerant species and understory trees and observed that it allowed to detect the creation of both large and partial canopy gaps. The minimal duration of the time segments was defined on the basis of a conservative criteria following Emborg (2007).

In the second step, the first year after gap creation was estimated for each release period. Nowacki and Abrams (1997) considered that the peak of PGC indicated the year of canopy disturbance. In our case, we observed important lags between years detected using this criteria and years identified by visual identification (± 4 years) and the approach was discarded. PGC_2 was then computed for each year using Eq. 3.2 with $M_1 = 8$ years and $M_2 = 1$ year. Within each previously detected time segments, the first year where $PGC_2 > 25\%$ was considered as the first year after canopy release.

The earliest release event that could be detected on each tree occurred at the age of 8. However, for each tree, the height that tree had reached at this date was examined, and events corresponding to a height less than 3 meters were discarded, to avoid trees potentially overtopped by neighbouring shrubs. Theoretically, the latest released event that could be detected on each tree occurred in 2009 (i.e. 4 years before the last year taken into account). In fact, the last release event (fall 2007) was not detected because the corresponding 4-year-release period (2008-2011) was not included in the interval taken into account. A total of 120 release events were detected in all trees, and the corresponding years ranged between 1934 and 2005 (Fig. 3.1). Release events appeared to be clustered.

Analysis of growth allocation trajectories

Relationship between tree height (H) and stem radius (R) was analysed using linear mixed-effects model, following:

$$H_{ij} = \beta_1 + \beta_2 \left(b_{ij} + R_{ij}\right) + \varepsilon_{ij} \qquad (3.3)$$

where indices for trees (i) and year (j) were defined as $i = 1, 2, \ldots, 39$ and $j = 1, 2, \ldots, n_i$. β and b terms were parameters to be estimated. ε_{ij} was the model error term, randomly distributed such that $\varepsilon \sim N(0, \sigma_\varepsilon^2)$. β_1 is the intercept, β_2 is the slope. β terms were fixed effects and b term corresponded to a random tree effect which was assumed to be normally distributed, e.g., $b \sim N(0, \sigma_b^2)$, and independent between levels. The model was fitted on 2770 observations, collected on 39 trees.

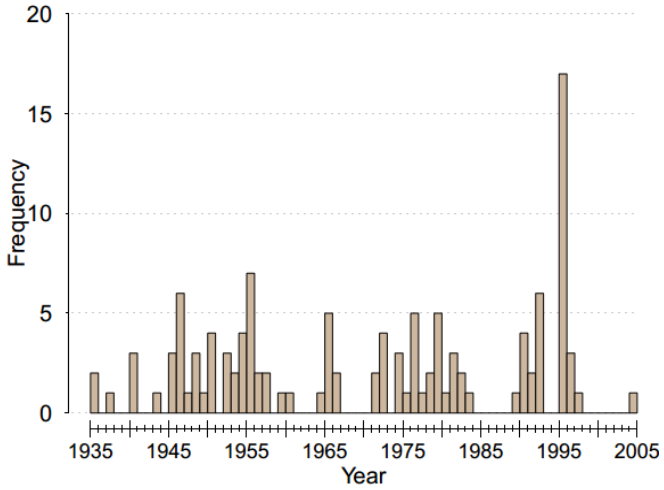

Figure 3.1: Frequency of detected canopy release events per year between 1935 and 2005.

Analysis of growth allocation

Allocation between diameter and height growth was analysed using non-linear mixed-effects models. An asymptotic model was used to describe the relationship between annual ring width (RW) and annual growth unit length (LGU), following:

$$LGU_{ij} = \left(\beta_1 + b_{1,i}\right)\left(1 - e^{\left(-e^{\beta_2\left(RW_{ij}-\beta_3\right)}\right)}\right) + \varepsilon_{ij} \qquad (3.4)$$

where indices for trees (i) and year (j) were defined as i= 1, 2, …, 39 and j= 1, 2, …, n_i. β and b terms were parameters to be estimated. ε_{ij} was the model error term, randomly distributed such that $\varepsilon \sim N(0, \sigma_\varepsilon^2)$. $(\beta_1 + b_{1,i})$ was the asymptote, β_2 the logarithm of the rate constant, and β_3 the value of RW at which LGU=0 (Pinheiro & Bates, 2000). β terms corresponded to fixed effects and $b_{1,i}$ terms to a random tree effect which was assumed to be normally distributed, e.g., $b \sim N(0, \sigma_b^2)$, and independent between levels. The model was fitted on 2770 observations, collected on 39 trees.

In preliminary analyses, random effects (parameters $b_{2,i}$ and $b_{3,i}$) were added to β_2 and β_3, but the parameter values associated to the 3 random effects were highly correlated, and $b_{2,i}$ and $b_{3,i}$ were therefore disregarded and only $b_{1,i}$ was kept in further analyses.

Auto-correlation plots for residuals indicated that the independence assumption was not met. Residual temporal correlation structures were incorporated in the model, using an auto-regressive-moving-average ARMA(1,1) correlation structure (Zuur *et al.*, 2009). The incorporation of the ARMA correlation largely improved the AIC value (35 354 vs. 34 152) and residuals did not display any auto-correlation. However, distribution of model residuals was highly skewed for the model with ARMA correlation. The temporal correlation structure completely absorbed the random tree effect, and it was not possible to disentangle the

individual tree effects from temporal autocorrelation effects. To facilitate interpretation of the results (Bellemare *et al.*, 2015), models without ARMA correlation were finally preferred. Models incorporating ARMA correlation will not presented.

Model residuals were visually checked to ascertain whether any remaining pattern with respect to potential covariates (tree diameter, height and age, number of years since the last canopy release) was to be found. No clear pattern was observed except for the duration since the last canopy release (DR, years).

To analyse the effect of the duration since the last canopy release on growth allometry, the mean of model residuals (MResid, mm) were computed for each DR value ranging between 0 and 25 years, and an asymptotic model was fitted according to:

$$MResid_i = \beta_1 \left(1 - e^{\left(-e^{\beta_2 (DR_i - \beta_3)}\right)}\right) + \varepsilon_i \qquad (3.5)$$

where the index for year was defined as i= 0, 2, …, 25. β terms were parameters to be estimated, defined as in Eq. 3.4, and ε_i was the model error term, randomly distributed such that $\varepsilon \sim N(0, \sigma_\varepsilon^2)$.

To examine temporal correlation between diameter and height growth, cross-correlations (Venables & Ripley, 2002) between RW and LGU were computed for each tree, using Pearson correlation coefficient. A maximum lag of 10 years was set to compute the correlations. For each lag value (ranging between -10 and 10), a Wilcoxon test at 1% was performed to assess whether the median value of the correlation coefficients for all trees pooled differs from 0.

All calculation and statistical analyses were performed using R software (R Core Team, 2015) and asymptotic models were fitted using the nlme package (Pinheiro & Bates, 2000).

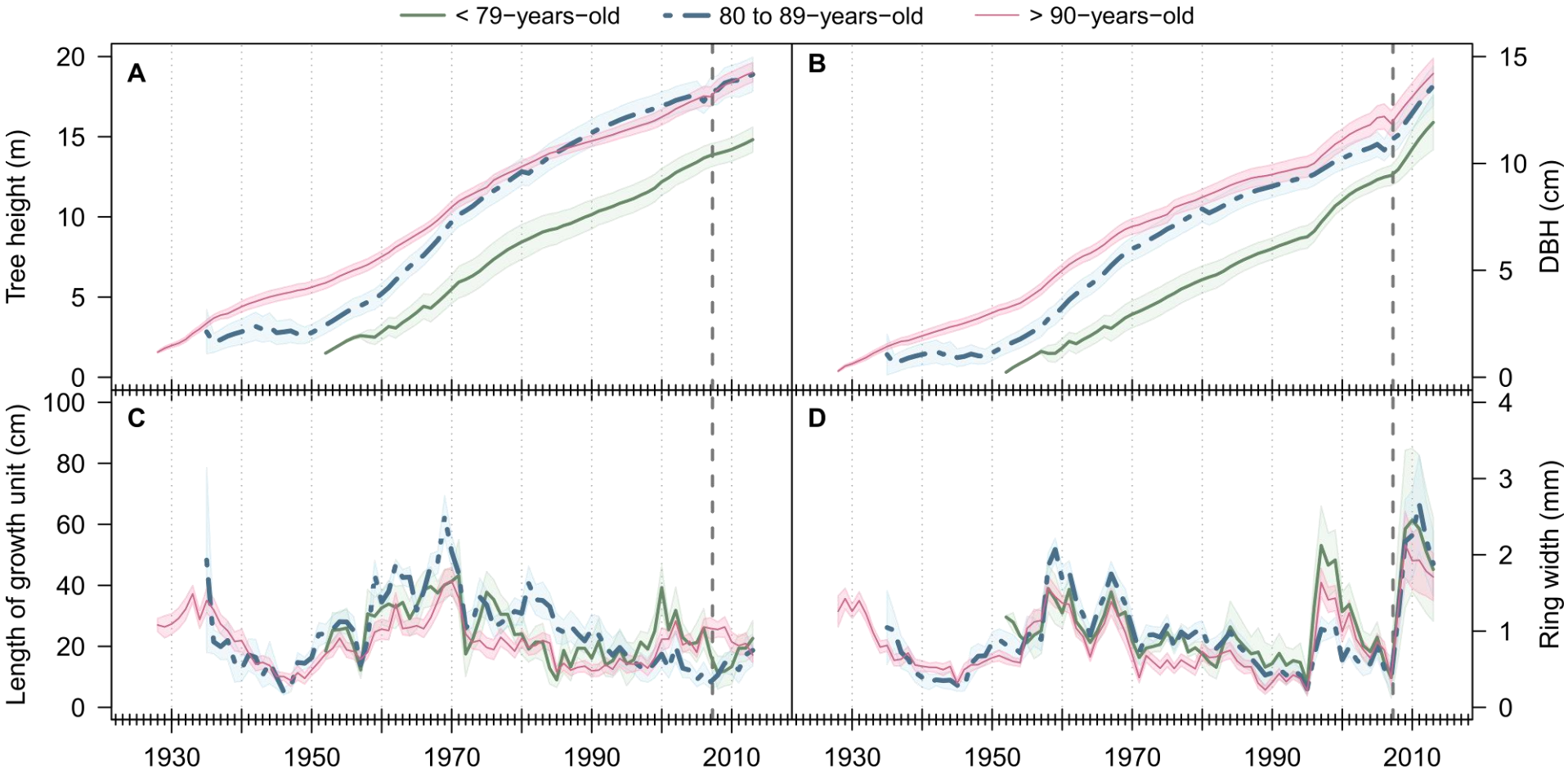

Figure 3.2: Size (A: height; and B: diameter at breast height, DBH) and annual growth (C: length of growth unit, LGU; and D: ring width, RW) of understory trees, over the study period.
Trees were grouped into 3 classes according to their age in 2013: younger than 79-years-old (n=6), from 80 to 89-years-old (n=14), and older than 90-years-old (n=18). Mean ± SE. The grey vertical dotted line shows the canopy release in winter 2007-08.

3.2.1. Results

Growth trajectories

Figure 3.2 presents tree growth trajectories over the study period. In 2013, mean tree height was 14.8, 19.0 and 18.9 m for young, intermediate and old trees, respectively (Fig. 3.2A). Tree height trajectories of intermediate and older trees were similar, except between 1945 and 1965. Mean tree height trajectory of younger trees was always below the trajectories of the 2 other age classes.

In 2013, trees from the 3 classes had no significant different mean stem diameters: 11.9, 14.2 and 13.8 cm for young, intermediate and old trees, respectively (Fig. 3.2B). As for height, intermediate trees showed the highest diameter values and young trees the lowest values.

In 2013, mean LGU was 22.6, 17.3 and 18.0 cm for young, intermediate and old trees, respectively (Fig. 3.2C). Among all years, the maximum value of LGU was 63.9 cm. LGU trajectories displayed large inter-annual variations regardless tree age. Mean RW was 1.8, 2.0 and 1.6 mm in 2013 for young, intermediate and old trees, respectively (Fig. 3.2D). As LGU, several peaks were observed and were synchronous between trees. Globally, Fig. 3.2C and 3.2D showed a succession of high and low growth periods. For high growth periods of 1960, 1968 and 2000, RW peaks seemed to precede LGU increasing.

Allocation between height and diameter growth

Tree height and stem radius are linearly and positively related (Fig. 3.3). The variability in the response variable (tree height) increased with the explanatory variable (stem radius). The slope superior than 1 (2.79 m cm^{-1}) indicated the preferential growth allocation to the height.

LGU and RW were positively related (Fig. 3.4, Table 3.2). Although a large variability was observed in the response variable, the asymptotic model fitted well the data. A negative β_3 indicated a non-null height growth (6.6 cm) when diameter growth is null. The asymptote (32.72 cm) was reached when annual ring width reached 2 mm. Above this width, height growth remained stable. All model parameters were significantly different from 0.

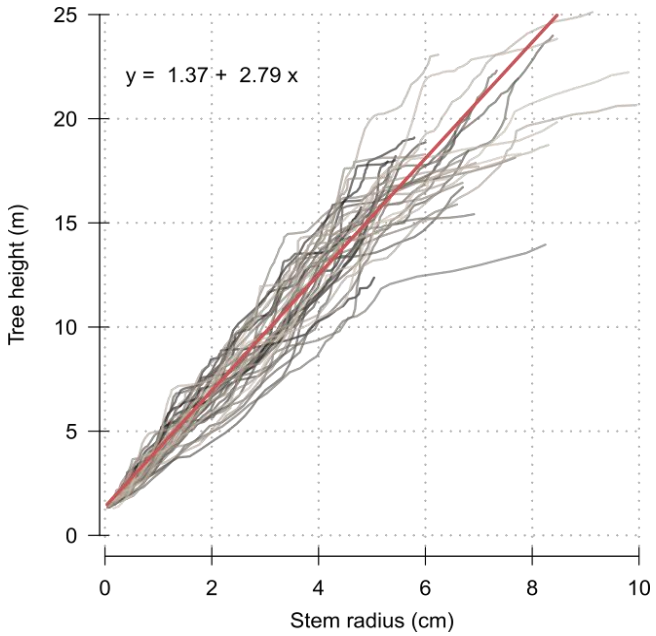

Figure 3.3: Relationship between the tree height (m) and stem radius (cm), for all trees and all years (n=2762).
The red line represents the linear mixed-effects model fitted on the data (Eq. 3.3)

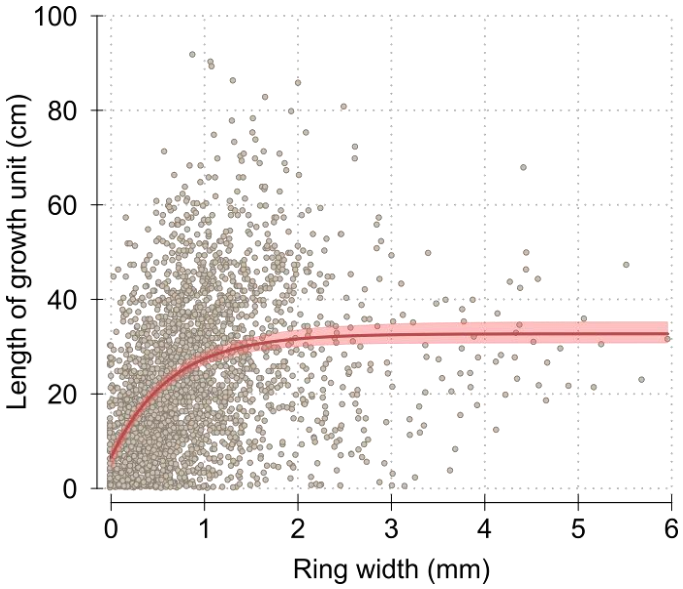

Figure 3.4: Relationship between the length of growth unit (LGU, cm) and ring width (RW, mm), for all trees and all years (n=2762).
The red line represents the asymptotic model fitted on the data (Eq. 3.4, Table 3.2), with 95% confidence interval of the predictor adjusted by bootstrapping.

Table 3.2: Asymptotic model between annual height growth (LGU) and annual diameter growth (RW); and asymptotic model between the mean of model residuals and duration since the last canopy release (DR).

Model	Parameters	Estimate	SE	t value	p value
Eq. 3.4	β_1	32.72	1.15	28.43	< 0.001
LGU vs RW	β_2	0.47	0.10	4.47	< 0.001
	β_3	-0.14	0.04	-4.02	< 0.001
Eq. 3.5	β_1	4.02	0.57	7.04	< 0.001
MResid vs DR	β_2	-1.85	0.21	-8.68	< 0.001
	β_3	6.07	0.64	9.46	< 0.001

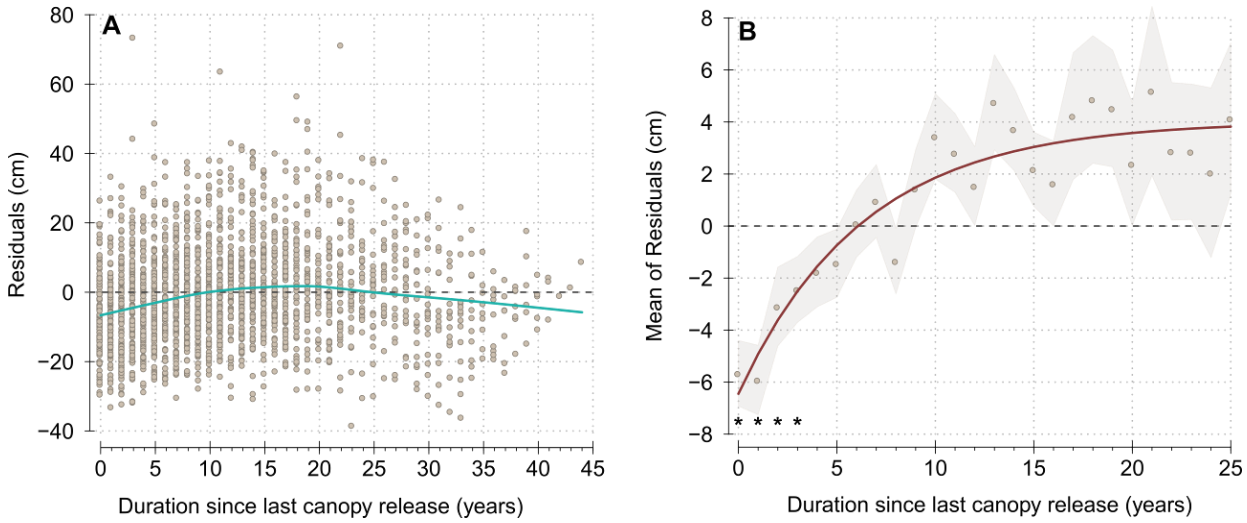

Figure 3.5: Relationship between the duration since the last canopy release (DR) and model residuals.
Year 0 is the year immediately after canopy release. A: model residuals. Blue line represents spline smoothing of the data. B: Mean of the residuals (MResid) ± standard error, computed for each DR value between 0 and 25. Red line represents the asymptotic model fitted on the data (Eq. 3.5, Table 3.2). * Asterisks indicates MResid values that significantly differ from 0 (Wilcoxon-test, $p<0.01$).

Model residuals plotted against the duration after the last canopy release event showed a clear trend, with negative residuals for low DR values (Fig. 3.5A), indicating that trees allocate more diameter growth than to height growth during the first years after canopy release. The mean of model residuals, computed for each DR ranging between 0 and 25 years, showed an asymptotic fit (Fig. 3.5B, Table 3.2) and was significantly different from 0 the first 4 years (from year 0 to year 3). Residuals mean became positive in year 6. The asymptotic model indicated that growth allocation progressively switched from diameter to height following canopy release.

Temporal cross-correlation between RW and LGU were strong (Fig. 3.6). Height growth was positively correlated to diameter growth of the current year (correlation = 0.3) and to diameter growth of the ten previous years. Correlation with the diameter growth in the 5 previous years was higher than for the current year. The mean value of the correlation coefficient between height growth and previous diameter growth were significantly different from 0 for all lag values (ranging 0 and -10 years). Height growth was also positively correlated to diameter growth of the 4 next years but the correlations were smaller, and the mean values significantly differ from 0 only for lag value less than 4 years.

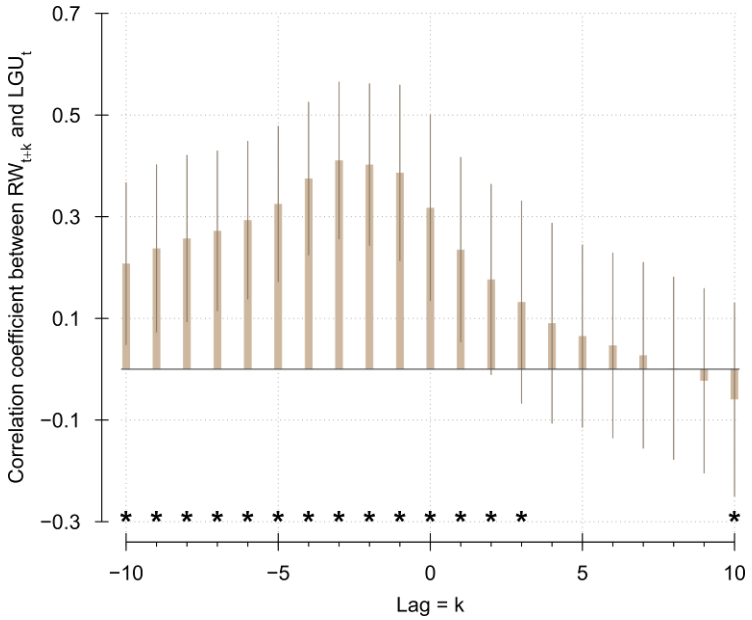

Figure 3.6: Correlation between ring width (RW) in year t+k and growth unit length (LGU) in year t, depending on the applied lag k.
Mean of the correlation coefficient computed on the 39 trees and standard deviation. Asterisks indicates median values that significantly differ from 0 (Wilcoxon test, $p<0.01$).

3.2.2. Discussion

Height and diameter growth rates relationship in understory beech trees

The asymptotic relationship between height and diameter growth rate in understory trees was congruent with previous studies (Sumida *et al.*, 2013; Trouvé *et al.*, 2015). The negative β_3 parameter of the model of growth allocation suggested that height growth did not stop even if it was at the expense of the diameter growth (Table 3.2). This higher investment in height growth than diameter growth could be explained by the high tree competition for light (King, 1990) that resulting in slender trees as a survival strategy to the most limiting resource (Bloom *et al.*, 1985; Poorter *et al.*, 2011). Moreover, understory trees reached in average a height growth rate of 30 cm which corresponded to the range of values observed in overstory 98-year-old beech trees located at 300 km from our stand (Bontemps *et al.*, 2012; Latte *et al.*, 2016). This suggested that even if growth conditions were favourable to an improved growth (e.g. tree-competition), the height growth rate seemed to be driven by another additional important factors. The ecological strategy for a given species as shade tolerance or maximum adult stature (tall vs. short species) could explained by the behaviour of the height growth rate of beech species (Grime, 1977; Bohlman & O'Brien, 2006).

Allometric relationship after canopy release

Despite the asymptotic shape of the mean residuals (Fig 3.5B), canopy release did not significantly impact the growth allocation of understory trees, except for the first years. The overestimation of the height growth rate during the first years after canopy release could be explained by several hypotheses. The first is that the increase of wind movements after canopy release induced thigmomorphogenesis favouring the diameter growth and reducing or stopping the height growth (Pruyn *et al.*, 2000; Telewski, 2006) to improve the biomechanical safety against disturbances. Secondly, in addition to the fact that height growth decreases with tree competition (King, 1990), we can suppose that the canopy release may enhance the development of the lateral growth, i.e. the crown, to improve the light interception and the lateral colonization which is not included in the present work. Moreover, it was demonstrated in seedling that height growth recovery was enhanced the second year after canopy release (Collet *et al.*, 2001). In our case, the delay of height growth recovery would be of 4 years but the response to canopy release at the individual scale could be delayed in term of diameter growth recovery (Hart *et al.*, 2010) and it was possible that the same phenomena happened for the height growth. In addition, the method used to detect canopy release can be failed to detect some small possible canopy releases and induced a bias in the model. Nonetheless, our results suggested that the most important modifications of

tree shape happened during the first 4 years after a canopy release regardless the developmental stage of the tree.

Temporal relationship

Our last objective focused on the temporal correlation between the height growth rate and the diameter growth rate. We found that the height growth rate was positively correlated to the previous years of diameter growth rate (Fig 3.6). As height growth happens at the beginning of the growing season while the diameter growth rate is spread among the growing season, to enhance height growth for a given year, the most important seemed to be the reserves of the past years. Moreover, beech species displayed a deep sapwood area (Granier *et al.*, 2000; Dalsgaard *et al.*, 2011) and the relationship between previous ring width and height growth rate could reflect a compromise between the functional rings and the potential water path length (i.e. height growth) increasing that sapwood area could sustain.

The diameter growth rate of current year impacted less the height growth rate than the diameter growth rate of the first 3 previous years. The height growth may depend mainly on the growing conditions of the previous year in some species (e.g. in conifers, Thornley 1999) whereas the diameter growth rate could depend on the sapwood area of the stem (e.g. in conifers too Galvan et al. 2012) and was mostly sensitive to the current climate (Lebourgeois *et al.*, 2005). In a time-scale, different factors acted on the two growth rates. If the past growth conditions were most decisive for the height growth rate, it was not trivial that the past diameter growth rate contributed too.

3.2.3. Conclusion

The high competition for light enhanced a continuous height growth although the maximum height growth rate seemed to be driven by the ecological strategy of the species. The canopy release impacted the growth allocation. As we suggested that a shade tolerant species as beech should prefer to develop a conservative strategy face to growth conditions changes, it will be interesting to orient the future investigations on the lateral growth or morphological and physiological possible modifications of understory trees to canopy release. Another perspective is to explore the individual trajectories of the relationship of height and diameter growth rates; this could be bringing some information about the dynamic of understory trees growth. Finally, we showed that the ten previous years of diameter growth rate positively impacted the height growth rate. It would be interesting to take account of the diameter growth increment of the previous years instead of the current stem diameter in predicted growth model.

Chapitre 4 : Evolution des performances biomécaniques des perches de hêtres à l'ouverture de la canopée

4.1. Avant-propos

L'ouverture de la canopée implique une augmentation des sollicitations mécaniques auxquelles l'arbre doit s'adapter. Le changement d'allocation de la biomasse entre la croissance radiale et axiale couplé à une anisotropie de la croissance radiale au niveau de la section ou de la modification des propriétés matérielles du bois peuvent impacter les performances biomécaniques de l'arbre. Dans le chapitre précédent, l'accent était mis sur les changements de croissance des arbres à l'ouverture de la canopée. Dans ce chapitre, nous essayons de comprendre quel est l'intérêt de ces modifications pour la biomécanique de l'arbre en nous focalisant sur le contrôle postural et la motricité des tiges. Ce chapitre est divisé en trois parties :

- Dans une **première partie**, nous discutons sur une **méthode** d'évaluation des contraintes de maturation du bois en rétrospectif et de son utilisation dans l'étude à suivre.
- La **deuxième partie** traite des traits liés à la **motricité des tiges** et constitue l'Article 2 qui est en cours de préparation.
- La **troisième partie** est axée sur la **sécurité biomécanique** et est au stade d'avant-projet sous forme d'Article 3.

La contribution des co-auteurs pour chaque ébauche d'article est synthétisée dans le Tableau 4.1.

Tableau 4.1 : Contribution des co-auteurs aux Articles 2 et 3.

Auteurs	**Contribution à l'Article 2**	**Contribution à l'Article 3**
Estelle NOYER	Acquisition des données, analyse des résultats, principale rédactrice de l'article	Acquisition et analyse des données du site du Grand Poiremont, relecture de l'article
Jana DLOUHA	Analyse des résultats (modèle PC) et participation à la discussion et à la rédaction	Analyse des données, principale rédactrice de l'article
Mériem FOURNIER	Participation à la discussion et à la rédaction	Participation à la discussion
Thiéry CONSTANT Catherine COLLET	Participation à la discussion	
François NINGRE	Mise en place du site d'expérimentation du Grand Poiremont	-

4.2. Estimation rétrospective des contraintes de croissance

L'objectif de cette partie est d'évaluer de façon rétrospective les contraintes de croissance du bois de hêtre, qui sont dues au retrait de maturation des cellules du bois et aux contraintes de support. Actuellement, les méthodes du trou unique et des jauges permettent la mesure des contraintes de croissance périphériques (Fournier *et al.*, 1994). La méthode du trou unique évalue indirectement ces contraintes en se basant sur le déplacement mesuré après la libération des contraintes de croissance qui dépend entre autres des propriétés du bois tandis que la méthode des jauges permet une mesure directe de la déformation (déformations résiduelles longitudinales de maturation, DRLM). Après avoir écorcé le tronc, deux pointes sont plantées dans le sens longitudinal à une distance de 45 mm, un capteur développé par le CIRAD est installé (Fig. 4.1a). Un trou de 20 mm de diamètre sur 10 mm de profondeur est réalisé ce qui permet la libération des contraintes et engendre un déplacement des pointes qui est mesuré en µm par le capteur de déplacement (Fig. 4.1b). Une couronne de mesures uniformément réparties autour de la circonférence de l'arbre permet la caractérisation de la répartition des contraintes de croissance sur la périphérie du tronc (Fig. 4.1c).

Figure 4.1 : Mesures des ICC par la méthode du trou unique.
a : mise en place des pointes et du capteur CIRAD. b : réalisation du trou. c : répartition des mesures le long de la périphérie du tronc. (Source : INRA)

Ce déplacement est proportionnel à la déformation longitudinale due à la maturation des cellules nouvellement formées du bois. En connaissant les propriétés du bois, il est possible de convertir le déplacement mesuré en déformation (Sassus, 1998). Ici, nous nous baserons sur la relation observée par Fournier *et al.* (1994) entre les mesures réalisées par la méthode des jauges (mesure directe) et la méthode du trou unique (mesure indirecte) sur le hêtre. Pour cette espèce, la déformation est égale à 15.8 µdef par micromètre de déplacement mesuré. Lorsqu'il s'agit d'une mesure indirecte, le déplacement mesuré en µm est généralement désigné comme indicateur de contraintes de croissance (ICC, ou GSI en anglais) (Clair *et al.*, 2003).

Dassot et al. (2012) proposent une estimation rétrospective des contraintes de croissance du bois de hêtre. En se basant sur la principale caractéristique du bois de tension des angiospermes qui est son état de tension élevé (Trenard & Guéneau, 1975; Fang *et al.*, 2008), et son aspect visuel, *i.e.* l'aspect nacré des fibres G du bois de tension, les auteurs identifient rétrospectivement le pourcentage de bois de tension par cerne (Barbacci *et al.*, 2008). Des photographies des rondelles réalisées sous une lumière rasante permettent de mettre en évidence les plages de bois de tension (Fig. 4.2a). Suite à une analyse d'images, les pixels correspondant au bois de tension apparaissent en bleu tandis que les pixels de bois sans fibres G sont rouges (Fig. 4.2b). En sectorisant la surface des rondelles analysée, la proportion du nombre de pixels bleu permet d'obtenir un pourcentage de bois de tension par secteur (Fig. 4.2c). En combinant ce pourcentage de bois de tension obtenu aux valeurs d'ICC obtenues par la méthode du trou unique, il est possible de calibrer l'état de tension du bois à un pourcentage de bois de tension et *infine* d'obtenir, en rétrospectif, l'état de tension du secteur considéré du cerne.

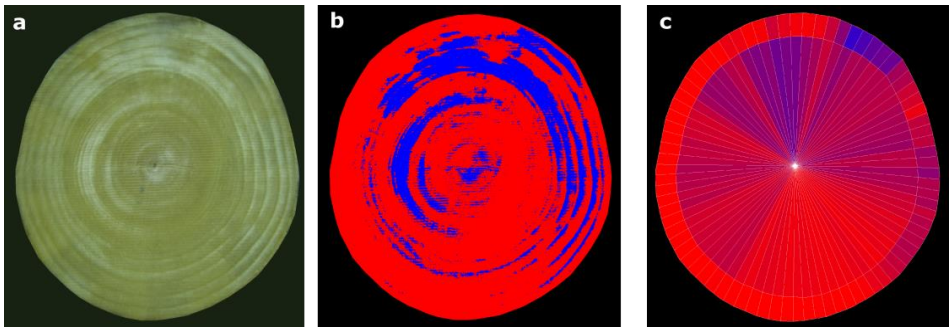

Figure 4.2 : Succession d'étapes permettant la détection du bois de tension sur une rondelle.
a : rondelle originale, le bois de tension présente un aspect nacré. b : étape de seuillage, le bois de tension apparaît en bleu. c : étape de sectorisation radiale et angulaire de la surface de la rondelle, plus le secteur est bleu, plus le pourcentage de bois de tension est élevé. (Source : INRA)

Dans notre étude, les ICC ont été mesurées sur 8 points répartis de façon homogène sur la circonférence du tronc à 1.30 m avant l'abattage (Fig. 4.1c). Une rondelle prélevée à cette hauteur et conservée à -20°C a permis la réalisation de la cartographie du bois de tension. Pour la calibration entre pourcentage de bois de tension et ICC, nous avons délimité des secteurs périphériques lors du traitement des images des rondelles (Fig. 4.2c) pour recaler la position de chaque trou de mesure d'ICC. Différentes tailles de secteurs ont été testées, allant de la taille du trou réalisé (20 mm de longueur d'arc x 10 mm de profondeur) à une taille minimale de 5 mm x 5 mm, de façon à correspondre au mieux à la surface qui contribue le plus à la libération des contraintes de croissance qui est de 8 mm x 8 mm (Sassus, 1998). Finalement, le secteur de 10 mm x 5 mm de profondeur donnant la meilleure qualité de la droite de régression, a été retenu.

La Figure 4.3 présente la droite de régression entre les ICC (µm) et le pourcentage de bois de tension pour les 8 mesures de 42 perches. La relation est significative mais la qualité de l'ajustement est faible ($R^2 = 0.18$). L'origine à l'ordonnée nous informe qu'un bois sans fibres G, i.e. le bois normal, présente une valeur d'ICC de 68.75 µm. La pente est de 1.44. La dispersion des valeurs est très importante surtout pour les secteurs avec un pourcentage limité de bois sans fibres G.

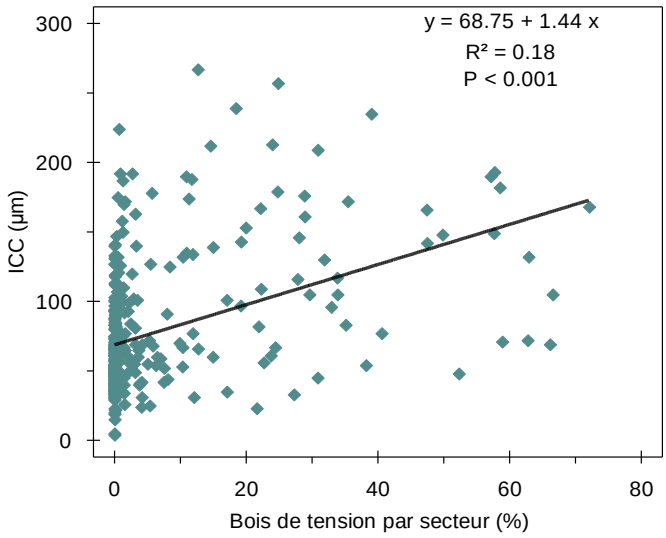

Figure 4.3 : Relation entre les valeurs des ICC (µm) et du pourcentage de bois de tension.

En comparant ces résultats avec Dassot et *al.* (2012), il est observé que les perches présentent une plus forte valeur d'ICC pour le bois normal, ainsi que des ICC maximales plus élevées. Les conditions de croissance de ces deux lots d'arbres sont différentes. Or ce sont les conditions de croissance qui conditionnent la forme de l'arbre. Il a été démontré que la forme de l'arbre, notamment l'asymétrie du houppier ou le ratio hauteur/diamètre, influence l'amplitude des valeurs des ICC, même à l'échelle intraspécifique (Jullien *et al.*, 2013). Nous suggérons donc que ces valeurs sont spécifiques au matériel végétal étudié.

Des fortes valeurs d'ICC ont déjà été observées dans des secteurs avec peu de bois de tension (Trenard & Guéneau, 1975; Fang *et al.*, 2008), et celles-ci ont été attribuées à des hétérogénéités de taux de fibres G. Une mauvaise détection du bois de tension lors du traitement d'images peut aussi en être la cause. En effet, un trop fort seuillage réduit drastiquement le nombre de pixels détectés comme bois de tension. De plus, la qualité de sciage des rondelles altère la qualité des images. Dans notre cas, des coupes anatomiques permettraient d'évaluer le pourcentage de fibres G plus précisément et de s'affranchir des artefacts engendrés par la méthode cartographique. Néanmoins, une telle approche est expérimentalement lourde. Des coupes anatomiques ont été réalisées sur un rayon du bois

normal. La coloration des coupes avec le protocole standard, celui utilisé sur des semis ou des arbres dominants de hêtre, n'est pas adéquate pour le bois de perches de hêtre.

En raison de la faible qualité de la régression entre les ICC et la quantité de bois de tension, nous avons choisi de ne pas estimer rétrospectivement les contraintes de croissance. Les perches dominées présentent de très faibles accroissements radiaux. La profondeur des trous réalisés contient, en moyenne, 15 cernes pour les arbres non libérés et 3 cernes pour les arbres libérés. Par ailleurs, les résultats de Purba *et al.* (2015) démontrent que les ICC à 1m30 ne sont pas modifiés suite à l'ouverture de la canopée. Les valeurs d'ICC mesurées sont donc utilisées comme une valeur moyenne de l'état de tension du bois durant les 13 années étudiées par la suite.

4.3. Article 2 : How trees maintain an erect habit in real managed forests: a theoretical and experimental biomechanical analysis in beech poles (*Fagus sylvatica* L.). (In progress)

Estelle NOYER, Mériem FOURNIER, Thiéry CONSTANT, Catherine COLLET and Jana DLOUHA

LERFoB, INRA, AgroParisTech, F-54000, Nancy, France

Abstract

Context To maintain an erected habit is a vital need for tree regardless its growth condition. Limited access to light may induce a tortuous or tilted habit however once the competition is released, this habit has no more functionality.

Aims In this study, we examined whether beech poles growing in understory with limited access to light exhibit a risk of sagging and if they are able to restore their verticality after a sudden competition release.

Methods To assess the posture control at the tree level, we need to pool together many traits measured at different scales. Stem curvature and lean were measured by TLS (Terrestrial LiDAR Scanner) scans before the release and 6 years after. Tree biomass distribution and taper were determined during tree harvest. Height and radial increment were retrospectively estimated. Concerning wood properties, GSI (growth stress indicator) and wood density were measured. From these traits, theoretical tropic curvature rate and change in lean angle were computed and compared to the lean change estimated from TLS scans.

Results Even under highly constrained environment, two thirds of beech poles were able to counterbalance gravitational curvature and avoid sagging. After release, beech poles with high initial lean angle were up-righting while beech poles with lean angle lower than 6° did not move much. The theoretical tropic curvature rate increased after release to slow down after two years likely due to the stem diameter increase. Theoretical model overestimated lean correction. Technical obstacles likely responsible for this overestimation, are discussed.

Keywords

Posture control; *Fagus sylvatica*; competition release

4.3.2. Introduction

Gravitropism is the capacity of plant to reorient their stem and control their posture during the growth phase. As stated by Darwin (Darwin & Darwin, 1880), movement is a basic necessity of plant life (Whippo & Hangarter, 2009; Moulia & Fournier, 2009). Actually, without gravitropism that allows plants to counteract gravitational forces, growth, which represents an increasing of both the self-weight and the height of the centre of mass, would be mechanically unstable (Moulia *et al.*, 2006). Among plants, trees, which are high, extremely slender and long living, could not maintain their erected habit, with a dramatically increasing of trunk lean during tree life (Fournier *et al.*, 2013).

Biomechanics and mechanobiology study how plants sense signals associated to gravity (Telewski, 2006) or their own shape (Hamant & Moulia, 2016) to right themselves smartly. As tree stems are mainly made of lignified, dead, and stiff wood, biomechanics pays also attention to how growth and cell differentiation at the stem periphery can produce enough energy to reorient so rigid bodies. Differentiation of the secondary cell wall in wood, associated to polymerization shrinkage, can generate forces of high enough magnitude (Archer, 1987; Moulia & Fournier, 2009). When the force between the two sides of the stem is asymmetric, due to reaction wood formation, it can provoke upward bending, i.e. a gravitropic curvature opposed to the gravitational one, which lead to downward bending and increasing lean (Wilson & Archer, 1979; Moulia & Fournier, 2009).

Then, the challenge of erected tree stem habit is figured out as a balance between gravitational and gravitropic curvatures. The ratio of the gravitropic curvature to the gravitational one represents the performance of the gravitropic process i.e. its ability to change significantly the stem habit (Fournier *et al.*, 2013). Going further in biomechanical modelling, the effects of several variables that influence the gravitropic movement can be disentangled (Alméras *et al.*, 2005a; Alméras & Fournier, 2009): the gravitropic curvature has been modelled as a curvature rate per unit of radial growth. It varies as a function of both section size (diameter) and independent to tree size variables (wood maturation strain asymmetry or eccentricity of radial growth). The gravitropic curvature per unit of radial growth represents the efficiency of the gravitropic process in respect to the investment in radial growth.

This theoretical framework removes some obstacles for studying the ecological relevance of gravitropic processes. First, it formalizes how gravitropic processes (i.e. the energy production to counteract gravity) are always and necessarily stimulated in the field, even in the lack of movement, when gravitropic energy just compensates gravitational downward bending. For example, Huang *et al.* (2010) use biomechanical models of gravitropic curvature

to discuss how branches can maintain their habit over time. Secondly, it proposes key traits, related to tree morphology or to wood tissue mechanical properties, involved in gravitropic efficiency and performance, that can compensate themselves with formalized trade-offs. For example, Dassot *et al.* (2012) examined in several silvicultural conditions whether radial growth and reaction wood properties can compensate the great constraint of increasing thickness, since the model states that gravitropic efficiency scales as the inverse of the square of the stem diameter (Dassot *et al.*, 2012). Investigating why advanced regeneration of *Fagus sylvatica* is more efficient than the seed bank to insure forest resilience and regrowth after a strong gap opening, Collet *et al.* (2011) demonstrated that beech saplings restore efficiently and quickly a vertical trunk, useful in light foraging in open conditions, after having survived several decades with an oblique trunk and tree shape, typical of shade tolerance, and efficient in the previous poor light conditions. Lastly, the biomechanical traits involved in gravitropic efficiency and performance formalize a capacity of movement, quite independently of peculiar experimental conditions. Therefore, observations of gravitropic movements in greenhouse tilting experiments can be used to assess more generically the gravitropic performance of a population of trees. For instance, Alméras *et al.* (2009) discussed the functional diversity of gravitropic performance among a set of tropical species, although they observed movements in peculiar conditions of gravitropic stimulus or available resources. In the same vein, Sierra-de-Grado *et al.* (2008) proposed to use the gravitropic efficiency estimated from tilting experiments, rather than the trunk straightness itself, which is too variable and linked to too many processes, in breeding programs of maritime pine.

The validation of models faces three technical obstacles. Firstly, the movements expected by models are usually quite slow (excepted in tilting experiments in young small stems). Moreover, the relevant variable of movement is the rate of curvature with growth, i.e. the time derivative of the spatial derivative of lean along the stem (Moulia & Fournier, 2009). Therefore, very accurate measurements of stem longitudinal shape over time are required, which are cumbersome in the field and on tall trees over long periods. Secondly, the observed movement is the superimposition of both gravitropic and gravitational bending, and the validation of both theoretical models of curvature involves a lot of parameters (e.g. Alméras *et al.*, 2009; Huang *et al.*, 2010). For instance, modelling gravitational curvature involves generally unknown data about how both the total mass and the centre of mass height vary during growth. Thirdly, models involve wood properties as maturation strains or modulus of elasticity, and geometrical properties (eccentricity of radial growth) that cannot be assessed without destructive experiments in wood science labs.

For these three reasons, experimental studies which have used the biomechanical models to link wood or stem morphological properties to observed stem movements have concerned mainly on one hand, small and young stems easy to manipulate and of fast movements, and on the second hand, artificially tilted stems, where gravitropism is strongly stimulated, so that the gravitropic curvature is much greater than the gravitational one, which can then be neglected (e.g. Coutand *et al.*, 2007; Sierra-de-Grado *et al.*, 2008) or roughly assessed (Alméras *et al.*, 2009). Due to the great number of tedious to measure parameters, authors usually inversed the model to estimate unmeasured traits of the gravitropic performance or efficiency.

In this study, we will study gravitropic efficiency and performance of beech trees in field conditions. Gravitropic reactions are assumed to be stimulated by thinning after a long period of growth in dense high forests. This assumption is supported by results of Collet *et al.* (2011), although the tree ages will be older, and environmental conditions quite different, representative of a silvicultural disturbance rather than large gaps.

Thanks to the terrestrial laser scanner (TLS) technology, it is the first study that monitors accurately stem movements in tall and big trees on the field, and can then compare these observed movements to the model prediction from parameters measured independently on wood after tree harvesting.

The questions addressed are therefore the following:

- (**Q1**) Is very low radial growth before thinning compensated by other traits of gravitropic performance to maintain the capacity of the tree to control habit? Or can we suspect that unthinned trees could become mechanically unstable?
- (**Q2**) Do trees move upright after thinning? If yes, what is the main drivers of these movements, higher radial growth alone or a more complex synergy with traits related to wood properties.
- (**Q3**) Is the biomechanical model, previously used for the prediction of the capacity of movement of big stems (e.g. Dassot *et al.*, 2012), and mainly validated by movements observed in young tilted stems (e.g. Alméras *et al.*, 2009), definitely able to capture the reality of stem movement of big old trees in the field?

4.3.3. Material and Methods

Study sites and plant material

The site was a broadleaved 13-ha-stand in north-eastern France (47.9507°N, 6.3857°E, alt: 470m) formerly managed as a coppice-with-standards. In 1955-1956, stand was thinned, converting it to a high forest. Records show it was further thinned between 1956 and 1995, but the years of thinning were not recorded. After 1995, there was no further thinning.

In fall of 2007, a sample of 42 understory beech trees distributed throughout the stand and at least 18 m from one another were selected for study. The trees originated from seeds and grew up under closed canopy or in small gaps. Sample trees met the following criteria: breast height trunk diameter was 7.5 to 17.5 cm, stems were unforked, leaned < 11°, had fewer than 25 epicormic branches (sensu Colin *et al.*, 2012) along the lowest 4 m of stem, and had no visible injury, spiral grain, canker, or top dieback. The sample trees were then split into two subsamples with similar mean values for diameter, height and relative vertical crown length (see Noyer *et al.*, 2017 for more details). In winter 2007-2008, one subsample was released by a thinning that removed the trees within competition in a 12-m radius around each target tree (hereafter referred to as “thinned” trees) and the other subsample of trees was left unreleased (“control” trees) (Ningre *et al.*, 2011). Two trees that exhibited an abrupt increase in lean angle and two trees with errors in TLS images were excluded from the study so that 18 control and 20 thinned trees were investigated. Six years after thinning in winter 2013-2014, all trees were harvested.

TLS scans and characterisation of tree shape and lean

Tree morphology was recorded using a terrestrial laser scanner (TLS). From December 2007 to March 2008 and from December 2013 to January 2014, one scan per tree was performed using a phase-shift FARO Photon 120 scanner (FARO, USA) mounted on a tripod at a distance of 6 m of the tree. For each tree, the location (distance and azimuth) of the TLS was identical for the scans performed in 2007-08 just before the thinning and in 2013-14. On each scan, the target tree was isolated by using FARO Scene 4.5 software as primary clean step, and Polyworks software (PolyWorks, InnovMetric Software Inc.) to isolate more precisely crowns of understory trees from neighbour trees.

Computree (computree.onf.fr) was then used to describe stem morphology. Horizontal circles were adjusted every 10 cm along the stem, and the neutral line of the stem was defined as the line passing through the centres of the successive circles. Lean angle at different heights was computed from the coordinates of the neutral line points. To compute the lean angle at a given height, three successive points at the base of the tree and at a given height were used.

Osculating circles, or curvature circles, were calculated for each horizontal circle from its centre by best taking account of the five above and below horizontal circles alignment, i.e. 50-cm-length on both side of the trunk shape. The inverse of the osculating circle radius was the local curvature of the trunk at this point. For the horizontal circles, recorded data were the radius, the *x*, *y* and *z* coordinates of the centre circles. For the osculating circles, the *x*, *y* and *z* coordinates, the curve abscissa was given.

Growth stress measurement

Before tree harvesting peripheral growth stress indicators (GSI, µm) were measured at breast height of the stem by the single-hole method (Fournier *et al.*, 1994) using CIRAD's sensor. This method consists in measuring the relative displacement of two pins inserted in wood after drilling a hole between them and so releasing the longitudinal growth stresses in the outmost layer of wood. Eight measurements equally distributed along the stem circumference were performed, the first being located on the upper side of maximal local lean angle. After bark removal, two nails separated by 45 mm in the longitudinal direction were tapped at each location. Each value was then converted in deformation by the calibration done by Fournier et al. (1994), where $GSI(\varepsilon) = GSI(\mu m) \times 15.8\ 10^{-6}$. Due to very narrow growth rings in our trees (0.4 mm for control trees and 3.1 mm in thinned trees), attempts to use image analysis based on photographs under a particular light incidence that makes the TW shiny (Barbacci *et al.*, 2008) to access retrospectively the amount of TW generated each year were not conclusive. As the GSI measurement by the single hole-method encounters cca 8 mm outmost wood layer of wood (Sassus, 1998) which corresponds to cca 15 growth ring in control and 3 growth rings in thinned trees and as nor average GSI value nor the TW intensity were affected by thinning (Purba *et al.*, 2015), measured values were considered as average values for all years examined in the retrospective analysis of biomechanical traits.

Biomass distribution and stem taper

After harvest, tree stems were divided into six successive segments. The basal segment measured 2m; other five segments were of equal length. To increase accuracy of log-log models of taper (*n*) and biomass distribution along the height (*m*) according to Jaouen *et al.* (2007), the two distal segments were cut again in two segments of equal length. For each segment, we measured the length, the two perpendicular basal cross-section diameters and segment and branches weight. These data together with the coordinates of neutral line were also used to compute the height of the centre of mass (H_{CG}). For the computation of PC trait (Postural Control), H_{CG} of the distal part where the GSI are measured were used while for

comparison between modelled lean change and lean change measured by TLS scanner, H_{CG} of the whole tree more representative of the global lean of a tree was used.

Retrospective analysis of tree axial and radial growth and wood density

For each tree, successive height annual increments along the stem were estimated through measurements of the length of the successive growth units (LGU, mm) based on the bud scars observed on the bark. The age of the growth units was checked by counting the annual ring on disks sampled every 10 GUs and, in case of observed discrepancy between GU age and the number of rings, GU and rings were measured again.

Five-cm-thick disks were collected at 1.35m-height just above the GSI measurement from each tree for micro-density measurements. The disks were wrapped in plastic film and were stored at -20°C immediately after harvest. After disks have been sanded, four perpendicular radii were identified in regard to GSI values. The radius corresponding to the highest GSI values observed on the tree was designated as tension wood (TW) radius, the opposite one as opposite wood (OW) radius while the last two perpendicular radii as normal wood (NW) radii. On each radius, the width of each tree-ring (RW, mm) from pith to bark was measured to a precision of 0.01 mm, by image analysis using TSAP-Win (Rinntech, Germany) for last 13 years to allow for growth analysis 6 years before and 6 years after the thinning. From ring width, disk diameter between TW and OW radii was used for the calculation of growth asymmetry (parameter k_m). After ring width measurements, a NW radius without knots or visible damage was selected. A radial strip (2.5 x 5 cm², T x L) was cut in the selected radius and conditioned for one month at 12% relative humidity at ambient temperature. Then, a radial slice (1.0 x 0.2 cm², T x L) was cut for X-ray micro-densitometry measurements with a microfocus X-ray source (Hamamatsu L9181-02 130 kV) and a digital X-ray detector (Varian PaxScan 4030R). The Crad and Cerd software suite was used to compute radial wood density (WD, kg m^{-3}) profiles (Mothe *et al.*, 1998). Wood density was used to estimate elastic modulus according to Guitard and Fournier (1994).

Biomechanical traits

Integrative approach proposed by Fournier et al. (2013) was used to estimate the motricity traits at the whole tree level combining data measured at different scales. Measured data allow for retrospective analysis of both traits in view to compare predicted lean angle change with measured lean angle change.

The tropic motion velocity (MV) defined as the theoretical curvature rate of the stem tropic movement was calculated as:

$$MV = -4 \ \frac{F_m \Delta\alpha}{D^2} \frac{dD}{dt} \qquad (4.1)$$

where F_m is the radial growth asymmetry motor, Δα is the GSI asymmetry (μdef), D is stem diameter at breast height (m), dD/dt is the annual radial growth increment (m).

F_m represents interaction between maturation strains and radial growth asymmetry and is defined from Alméras et al. (2005) as:

$$F_m = 1 + 2.k_m.\frac{\overline{\alpha}}{\Delta\alpha} \quad (4.2)$$

where k_m is the asymmetry of radial growth and ᾱ the average of GSI values (μdef).

The posture control (PC) is the ratio of active up-righting curvature and gravitational curvature due to an increase in biomass. As growth stresses generating the active up-righting curvature were measured at breast height, only the distal part of a tree above the breast height was considered for the computation of PC:

$$PC = \frac{-dC_m}{dC_g} = \frac{E\Delta\alpha}{4(1+b)\rho_T g\, sin\varphi}\frac{F_m}{F_g}\frac{D}{H^2} \quad (4.3)$$

where E is Young's modulus (N m^{-2}), b is the ratio of axial (dH/H) to radial (dD/D) increment, ρ_T is total fresh biomass supported, including leaves, trunk, and branches, per unit of trunk volume (kg m^{-3}), g is gravity acceleration (N kg^{-1}), φ is the lean angle (°), H is the height of the distal part of the tree (m) and F_g is the growing weight form factor calculated as:

$$F_g = \frac{2}{(m+1)(2n+1)} \quad (4.4)$$

where m is the biomass distribution and n is taper.

PC higher than unity means that the tree is up-righting i.e. the curvature rate generated by the maturation strains of the growing stem per unit of growth (dC_{mat}/dD) is higher than the curvature rate due to gravity (dC_g/dD). Active up-righting curvature rate and gravitational curvature rate are computed as follows:

$$\frac{dC_{mat}}{dD} = -4\,\frac{F_m\,\Delta\alpha}{D^2} \quad (4.5)$$

$$\frac{dC_g}{dD} = 16(1+b)\,F_g\,\sin\varphi\,\frac{\rho_T\,g}{E}\frac{H^2}{D^3} \quad (4.6)$$

To allow retrospective analysis, the relative height of the centre of mass of the distal part was determined for 2013 and used to compute the position of H_{CG} in previous in previous years based on the height of a given year. Further, the lean angle of previous year was corrected for the change in lean angle generated according to the PC during a given year.

Variance decomposition

The variance decomposition was realized for MV. We analysed the relative contribution of each parameter: dimensions (diameter D), growth (dD/dt), material properties (magnitude

of GSI Δα) and shape (F_m). After a log-transformation of the equation 1, we estimated the variability due to the treatment (Var_{treat}) and due to inter- tree variability inside the treatment ($Var_{tree/treat}$) as:

$$Var(\ln MV) = Var_{\frac{tree}{treat}}(-2\ln D) + Var_{\frac{tree}{treat}}\left(\ln\frac{dD}{dt}\right) + Var_{\frac{tree}{treat}}(\ln \Delta\alpha) + Var_{\frac{tree}{treat}}(\ln F_m) +$$
$$Var_{treat}(-2\ln D) + Var_{treat}\left(\ln\frac{dD}{dt}\right) + Var_{treat}(\ln \Delta\alpha) + Var_{treat}(\ln F_m) \quad (4.7)$$

Statistical analysis

Linear regressions were adjusted by the ordinary least-squares to obtain the adjusted-R^2. P-values were obtained by t-test.

To test the effect of the release on the lean changes, a linear model was built with the initial lean (i.e. 2007) as explanatory co-variable. Due to the precision of the lean measurement from TLS, the significant threshold was 0.1.

For MV, and for each year, treatment levels were compared using a Kruskal-Wallis test with a significant threshold where $P < 0.05$. All statistical analyses were performed using R software version 3.2.3 (R Core Team 2015).

4.3.4. Results

Measured changes in stem lean at 2-m height and at the height of centre of mass of the tree

Relationships between the stem lean angle in 2007 and 2013 at 2-m height and HG are displayed in Fig. 4.4. For both group of trees, linear regressions were significant ($P < 0.001$) what is the height analysed. Ten trees (4 thinned and 6 controls) were above the sagging line. At 2-m height and for both years, lean angle of control trees was not significantly different than the lean angle of thinned trees (5.82° and 5.48° in control trees and 5.17° and 4.70° in thinned trees, in 2007 and 2013 respectively, Table 4.2). At H_{CG}, only 4 trees had an inclination superior than 8° in 2007. Most of trees had an inclination inferior than 7° for both years (Fig. 4.4). Mean lean angle for control trees were significantly different than those of thinned trees (4.13° and 3.98° for control trees and 4.03° and 3.50° for thinned trees, in 2007 and 2013 respectively, Table 4.2). In control trees, slope of linear regression was lower at 2 m (0.91) than at H_{CG} (0.97). For thinned trees, it was the opposite: slope was higher at 2 m (0.89) than at H_{CG} (0.8, Fig. 4.4).

The lean changes between 2007 and 2013 were not significantly correlated to the initial lean in 2007 for both treatments at 2-m height (Fig. 4.5). At H_{CG}, the correlation was significant only for thinned trees ($R^2 = 0.24$, $P = 0.0162$, Fig. 4.5) and its slope was negative (slope = -

0.20). After 6 years of treatment, thinned trees may change their lean angle until 3.38° at 2-m height and 2.41° at H_{CG}. When we compare the mean lean changes of both treatments, a significant difference was found for H_{CG} but not for 2-m height (Table 4.2).

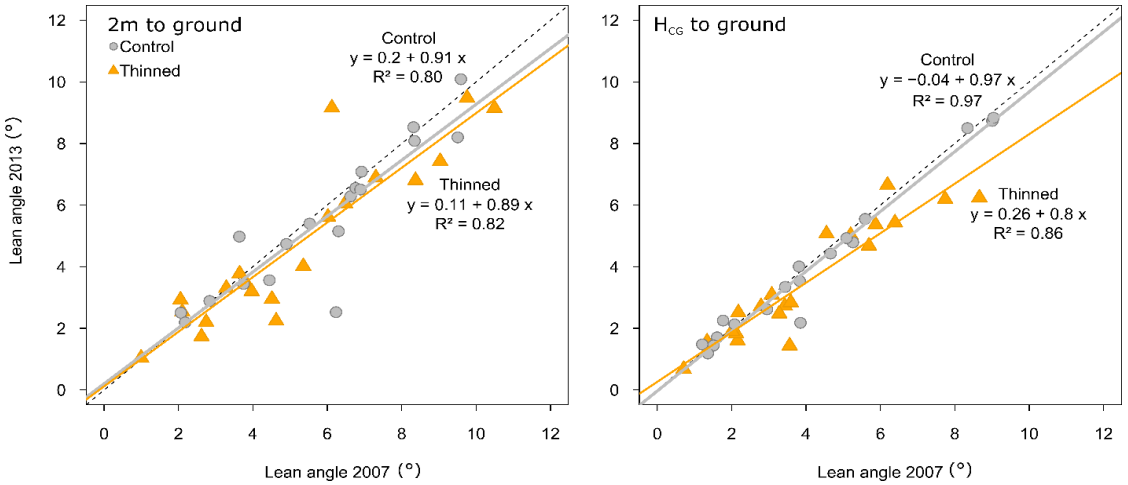

Figure 4.4: Relationship between the stem lean (°) deduced from TLS scans at 2-m height (left) and at the height of the centre of mass (right) in 2007 and 2013 of control and thinned poles.
Grey circles correspond to control poles and orange triangles to thinned poles. Black dotted line represents sagging line. Linear regressions for both groups of trees and for the two heights are significant ($P < 0.001$).

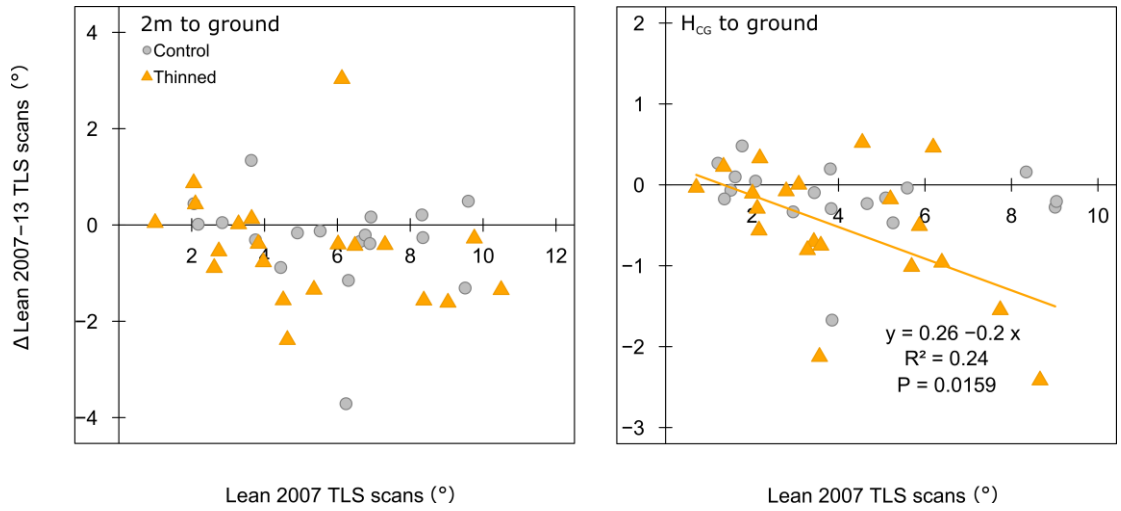

Figure 4.5: Relationship between the change in lean angle (°) between 2007 and 2013 and the initial lean angle in 2007 at 2-m height (left) and at the height of the centre of mass of the tree (right).
Grey circles correspond to control poles and orange triangles to thinning poles. No significant relationship was found for control trees at the two height tested. Significant relationship was found for thinned at the height of the centre of mass of the tree ($P < 0.001$).

Table 4.2: Mean ± standard error (SE) of stem lean angle, relative and absolute lean angle changes between 2007 and 2013 measured with TLS scans, and stem lean angle changes predicted with model.

Different letters indicate a significant difference at 0.1 between control and thinned trees for a same height.

Height	Treatment	Stem lean angle (°)		% of change between 2007 and 2013	Δ Lean angle TLS (°)	Δ Lean angle predicted (°)
		2007	2013			
2-m-height	Control	5.82 ± 0.55	5.48 ± 0.55	-5.84 %	-0.34 ± 0.24	-0.17 ± 0.04
	Thinned	5.17 ± 0.61	4.70 ± 0.59	-9.09 %	-0.47 ± 0.26	-1.47 ± 0.23
H_{CG}	Control	4.13 ± 0.6	3.98 ± 0.6	-3.63 %	-0.15 ± 0.11 a	-0.51 ± 0.12
	Thinned	4.03 ± 0.49	3.50 ± 0.42	-13.15 %	-0.53 ± 0.18 b	-4.22 ± 0.58

Table 4.3: Variance decomposition of parameter groups (S: shape, G: growth, D: dimensions, M: material) between trees inside a same treatment (Tree) and between treatments (Treatment) of MV trait in 2013.

	Variance				Covariance						Total
	S	G	D	M	S,G	S,D	S,M	G,D	G,M	D,M	
Tree	1.76%	31.55%	8.17%	29.53%	4.13%	-0.33%	-6.49%	-2.03%	-8.52%	2.04%	59.8%
Treatment	0.00%	76.41%	3.02%	0.46%	-0.06%	0.31%	-0.02%	-30.37%	-11.92%	2.37%	40.2%
Total	1.76%	107.96%	11.19%	30.00%	4.07%	-0.02%	-6.51%	-32.41%	-20.43%	4.41%	100.0%

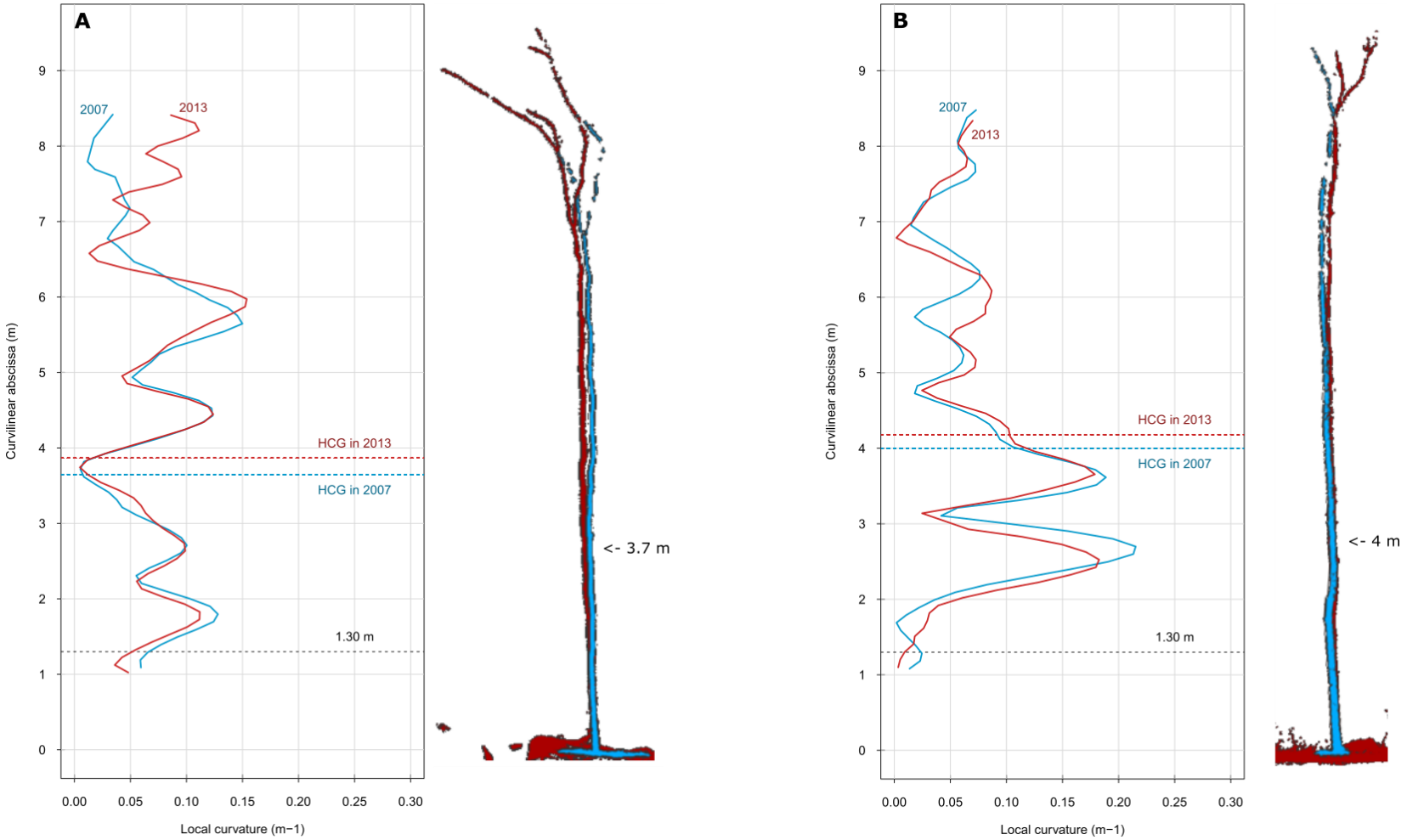

Figure 4.6: Example of local curvature variations along the main axis and tree shape in 2007 (blue) and 2013 (red) for two thinned trees that model overestimated the gravitropic curvature.
Data and images came from TLS scans. The height of the centre of mass of the tree (H_{CG}) are indicated by blue and red dotted line in 2007 and 2013, respectively. Black dotted line indicated 1.3–m-height, i.e. the location of material properties measurements.

Complexity of stem lean and stem shape

Despite significant relationship between lean angle at 2-m-height and H_{CG}, the coefficient of correlation was low ($R^2 = 0.49$, Fig. 4.7) showing that an extrapolation of stem lean angle at 2-m-height to taller in the tree is difficult and no general pattern could be established as illustrated by the Fig. 4.6. The 2 selected thinned trees presented complex shape with high variation in local curvatures. For the first tree (Fig. 4.6A), we noted the tilted branches and main axis reflecting a possible asymmetric crown. The maximal curvature is located around 5.8-m-height. For the second tree (Fig. 4.6B), stem presented 2 mains curvatures at 2.5-m-height and at 3.5-m-height.

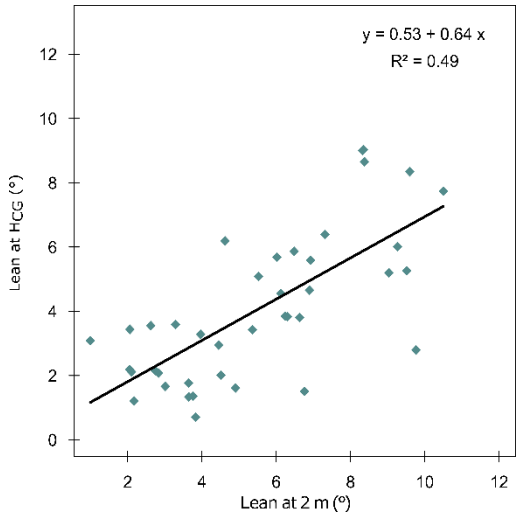

Figure 4.7: Relationship between lean angle (°) at HCG and 2-m-height in 2007.
In black, the linear regression is significant ($P < 0.001$).

Theoretical stem motricity

Up-righting curvature rate

Thinned beech poles increased strongly and significantly their theoretical MV values the two first year after thinning to reach 3.07 10^{-3} against 0.32 10^{-3} m^{-1} $year^{-1}$ for control poles in 2009 (Fig. 4.8). After 2009, MV of thinned poles decreased until 1.66 10^{-3} m^{-1} $year^{-1}$ in 2013. For this year, the MV variability in thinned poles was mainly due to the growth improvement (76.4 %, Table 4.3). Material properties contributed only inside a same radial growth interval (29.5%), where value was close to growth contribution (31.6%). The total covariance between growth and material properties was of -20.43% (-8.52% between trees inside treatment, and -11.92% between treatments). The variability due to trees was higher than this to treatment (59.8% and 40.2% respectively).

The ratio between the geometrical up-righting motor (dD) and brake (D^2) reflects how far growth increment is efficient in counteracting the inertia of the diameter. The Fig. 4.9

showed a positive and significant relationship between MV and the geometrical factor dD/D² ($R^2 = 0.49$, $P < 0.001$).

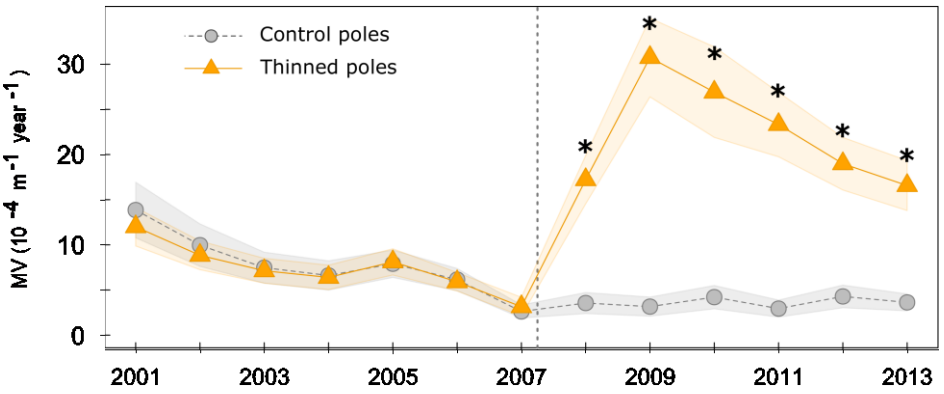

Figure 4.8: Evolution of tropic motion velocity (MV) of control poles (grey, dotted line) and thinned poles (orange, solid line) from 2001 to 2013 (mean ± SE).
Vertical dotted line represented the date of thinning. Symbol * indicated a significant difference between control and thinned poles (Kruskal-Wallis test, $P < 0.05$).

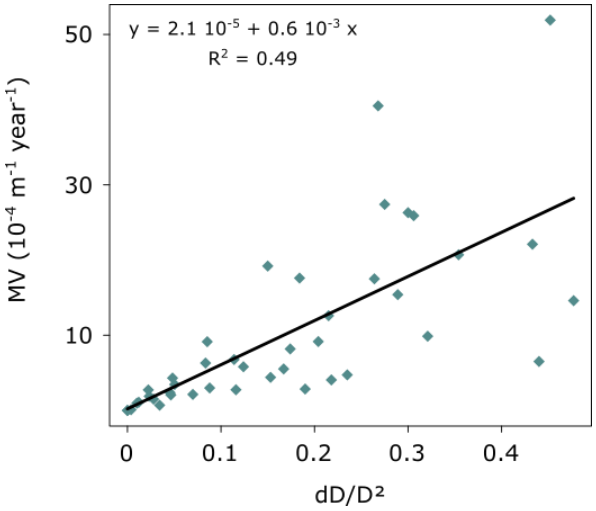

Figure 4.9: Link between tropic motion velocity MV and geometrical brake dD/D² (diameter increment on the trunk diameter squared) in 2013.
In black, the linear regression is significant ($P < 0.001$).

Relationship between gravitropic and gravitational curvatures

The relationship in 2013 between the gravitropic curvature (dC$_{mat}$) and the gravitational curvature (dC$_g$) is significant ($R^2 = 0.42$, $P < 0.001$, Fig. 4.10), the slope is different than the unity (-9.4) and the intercept is not significantly different to zero (-0.01). Contrary to the Fig. 4.4, no trees are above the sagging threshold. Then, trees close or on the sagging threshold presented low dC$_g$ values. Surprisingly, trees with high lean angle did not enhance high dC$_{mat}$ values and trees with lean angle superior than 6°, except one, generated high C$_g$.

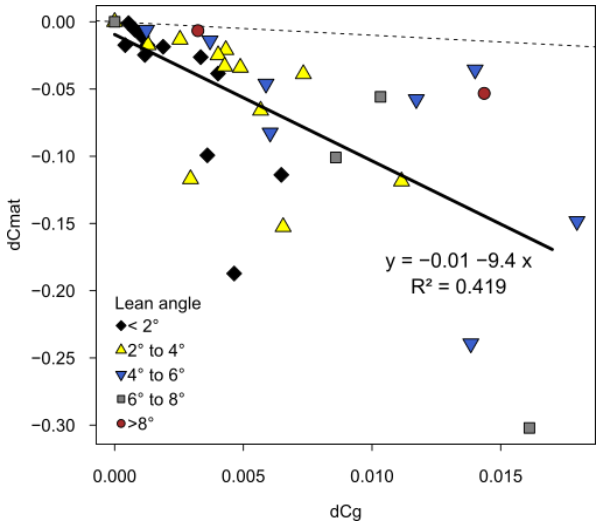

Figure 4.10: Relationship between gravitropic curvature (dC_{mat}) and gravitational curvature (dC_g) in regard to lean angle at HCG of the stem in 2013.
Lean angle inferior than 2° (black diamonds), between 2 and 4° (yellow triangles), 4 and 6° (blue inverse triangles), 6 and 8° (grey squares), superior than 8° (red circles). Black dotted line represents sagging line. In black, the linear regression is significant ($P < 0.001$).

Comparison between predicted and observed stem lean change

The Fig. 4.11 shows the relationship between stem lean changes at H_{CG} predicted by PC model and deduced from the TLS data. Linear regression is significant ($P < 0.05$) however the coefficient of determination is relatively low (0.10), the slope higher than unity (1.39) and intercept relatively far from zero (-1.97) showing that predicted lean change is largely overestimated as summarized in Table 4.2.

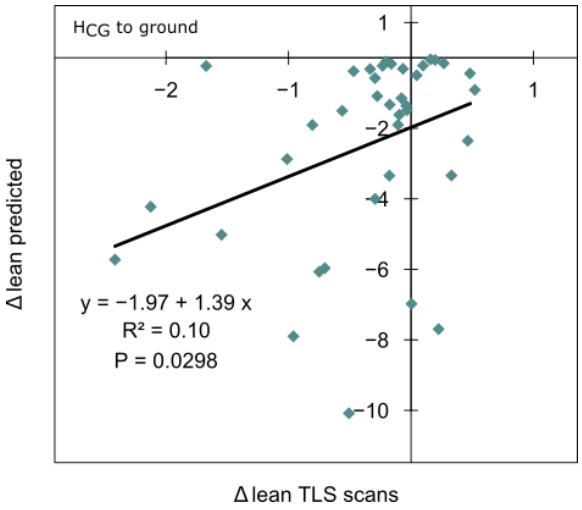

Figure 4.11: Link between lean angle changes (°) predicted by computation of the model from the H_{CG} to the ground and measured from TLS scans.
In black, the linear regression is significant ($P < 0.05$).

4.3.5. Discussion

Control of stem lean in different growth conditions

When we compare the lean change in control and thinned trees, we can see that at 2 m-height both groups of trees move with similar magnitude (Table 4.2) and this movement is independent of initial lean (Fig. 4.5). On the contrary at CG-height, which may be understood from the biomechanical viewpoint as a simplified proxy of the tree global lean, thinned trees move more than control trees (Fig. 4.5, Table 4.2). One third of control trees is above sagging threshold and trees with relatively high lean of the stem (>8°) struggle to maintain a fixed lean angle (Fig. 4.5). However, we do not expect control trees to upright their stem in a significant way as they are constrained by the presence of light gaps to access the light (i.e. phototropism). It is interesting to note that despite their very low radial growth (0.36 mm in average), two thirds of control trees remain able to avoid sagging which means that posture control is one of the priorities even in very constrained growth condition. After the release of competition from neighbours, trees clearly try to up-right their stems (Fig. 4.5, Table 4.2) and trees with high lean in 2007 invest more in the stem lean correction than trees with low lean in 2007. Is it reasonable to expect that thinned trees will achieve completely vertical stems? Some reports mention that for light capture, it may be beneficial to keep lean angle different from the vertical (Ishii & Higashi, 1997) which may be interesting for trees after thinning whose foliage needs to acclimate to the new environment. The only report we found with experimental data of tree lean change after competition release in big trees was the work done by Constant *et al.* (2006). In this study, no global behaviour of trees after release could be identified and measured reactions were very small and complex.

Tropic curvature rate after release is increased ten times mainly due to the growth rate increase

Theoretical MV values of control poles were close to previous results obtained in beech poles with similar stem diameter (Dassot *et al.*, 2012). After the thinning however, MV increased up to 10-fold despite the increase in stem diameter which represents a geometrical break in up-righting process (Eq. 4.1). Increase in stem diameter may however explain the slowdown of the theoretical tropic curvature rate after the second year after thinning (Fig. 4.8). As we can see from Fig. 4.9, considering the growth increment and diameter explains already 49% of the MV variability. As average value of GSI as well as the intensity of TW were not affected by thinning (Purba *et al.*, 2015), the difference in MV due to the thinning results mainly from the increase in growth rate. Nevertheless, inside the same treatment, contribution of GSI intensity is of the same order as the growth increment when decomposition of MV variance is performed (Table 4.3).

Why simple biomechanical model of up-righting process does not work well for big trees and how can we improve it?

In biomechanical model of tree posture control, lean angle used in the computation is the lean angle of the distal part in respect to the height of GSI measurement. However, when we look at the complexity of tree curvature and lean variation along the height in big trees (Fig. 4.6, 4.7), one may wonder how representative this proxy is of the global or local loading at a given height of the stem. Moreover, it is interesting to see how dC_{mat} and dC_g are related because it shows if dC_{mat} is used to counterbalance the bending moment we expect it to counterbalance. Sagged trees observed in experimental measurements at CG-height (Fig. 4.4) did not appear when we computed curvatures at the base of the distal part (Fig. 4.10). The applied hypothesis beside the estimation of the gravitropic curvature is that all TW detected in the section at the base of the segment allows for the distal segment up-righting. In this way, high dC_{mat} values should (i) correspond to high loading and (ii) be related to the presence of TW (Eq. 4.5). In our case, the absence of the detection of sagged trees such as the overestimation of the gravitropic curvature could be explained by the high quantity of TW in the section at 1.30-m-height. As in beech saplings, only one-third of the up-righting is induced by the stem basal part movements (Collet *et al.*, 2011), a part of produced TW might not contribute to up-righting process and be involved at a more local level. Moreover, the azimuth of the stem curvature was not included in the calculation. The computed gravitropic curvature might be not in the same azimuth that the GSI and growth asymmetry causing bias in calculation.

In saplings, lean angle is in general very high (58°) as well as its change (18°) thanks to small stem inertia (Collet *et al.*, 2011). Further, the variation of curvature along the sapling's height presents in general at maximum one peak corresponding to a change in lean angle (Almeras *et al.* 2009). In big trees that evolved in constrained condition, the lean angle does not exceed 10° at CG-height, the change in lean angle is of 0.53° in average and the stem curvature variation along the tree height is complex (Fig. 4.6). Moreover, the lean angle significantly varies along the tree height in a non-systematic way which makes it difficult to predict (for example the lean at the CG-height from the lean 2-m-height) (Fig. 4.5). Another problem with big trees is that they may generate a torsion moment due to for example the rotation of a crown especially after thinning where the light access become suddenly homogeneous (Constant *et al.*, 2006) and crown, often asymmetric, is free to evolve in a symmetric way again while in saplings, the up-righting process is generally contained in one vertical plane even if it can be also helped by establishment of relay axes as it was for example observed for *Acer pseudoplatanus* saplings (Collet *et al.*, 2011). Crown movements could explain the low dC_{mat} coupled to high dC_g in Fig. 4.10. Unfortunately, in big trees,

crown data are complicated to access contrary to saplings. Several TLS scans per trees will be necessary. This technology limits the description of tree architecture to the winter period without leaves on branches.

Considering the data used for the computation of active curvature, GSI and ring width measurements including the growth eccentricity, which are the main factors driving the active up-righting curvature change (Almeras, Thibaut & Gril 2005), are very local. To see what happens higher in the tree or, for example at the height where the achieved change in curvature is maximal, one should measure GSI and ring widths at this location. Such measurements may help to better understand how the tree lean and curvature change is controlled along the tree height. Another option, unfortunately not investigated in this study, is to separate maturation stresses and "spring-back" strain (strains due to the load) which allows to characterize the gravitational moment due to the lean or asymmetric growth as done for example in Hung *et al.* (2016). This will allow for characterization of the load locally "sensed" by the stem and give a clue for the choice of the best geometrical descriptor of the tree shape to determine the loading inducing the gravitational curvature but also used as an input to correct by active curvature. Finally, this method will also permit the characterisation of crown asymmetry.

4.3.6. Conclusion

This work showed that posture control is one of the priorities for trees even under high growth constraints. For big trees, the up-righting movements were enhanced at CG-height at the contrary of small trees from the literature where movements were detected at the stem base. In addition, the intensity of the up-righting movements increased with the initial stem lean for thinned trees. From theoretical tropic curvature rate calculation, we stated that this increase was due to the boosted radial growth rate which was also the cause of the observed slowdown by the increase of the stem diameter. The application of existing model to predict retrospectively the stem lean overestimated the gravitropic curvature. Because of the complexity of tree shape, we suggested that the tension wood included in the calculation of the model more acted at the local level and might not fully participate to the up-righting process of the distal part. Moreover, crown movements could be also involved in the up-righting process or in the loading of the basal part. As perspectives, we proposed (i) to include the azimuth of the stem curvature and the GSI, (ii) to realise several TLS scans per trees, (iii) to measure GSI and ring widths at the location of maximal curvature changes and (iv) to measure "spring-back" strains.

4.4. Article 3 : Safety against self-buckling and against wind-break in beech poles after competition release. (In progress)

Jana DLOUHA, Estelle NOYER, Thiéry CONSTANT, Catherine COLLET, François NINGRE and Mériem FOURNIER

LERFoB, INRA, AgroParisTech, F-54000, Nancy, France

4.4.1. Introduction

In understory trees or saplings growing under a dense forest cover the risk of self-buckling may be high. In such environment, trees may partially rely on their neighbours for mechanical support, they are sheltered from wind forces and foraging for light is the main environmental constraint. To access the light, trees allocate their biomass preferentially to height growth instead of radial growth achieving very slender structures. In some cases, they can become nonself-supporting as described by Jaouen et al. (2007) in saplings from tropical forest understorey. While the tree size has the greatest effect on self-buckling risk, form factor including the taper and biomass distribution along the stem height needs also to be considered.

Once an understory tree is released from its neighbours' competition, wind penetrates more easily to the tree and mechanical loading due to the wind becomes more important. Moreover, access to light and to other nutriments allows for the crown development which increases the sailing area exposed to the wind. From thigmomorphogenetic studies we know that when a plant is submitted to longitudinal bending, axial growth is stopped and radial growth is boosted (Coutand, 2010). Bonnesoeur *et al*. (internal report, 2016) observed an increase of radial growth of 44% to 67% in young beech poles after the release depending on the meteorological condition of the year. This explains why decrease in slenderness is observed in trees after the competition release (Mitchell, 2000) and also why trees from windy habitats evolve typically short and thick stems with reduced crown area such as a flag tree (Telewski, 2012). Increase in diameter is essential to resist the wind forces because the stem resistance in bending scales with the third power of diameter while the effect of height acting as an arm level is only proportional (Peltola, 2006).

In the present study, we examine the change in biomechanical safety traits, namely safety against self-buckling and against wind-break on a sample of beech understorey trees submitted to a long compression period and released in 2007. In winter 2009, fifteen of released beech trees were broken by the wind. Final sample consists therefore of 21 control trees, 21 released trees unharmed in 2009 and 15 released trees broken in 2009. The aim is to examine how trees acclimated to an increased mechanical loading in terms of shape

change (slenderness, taper, biomass distribution) and material properties change. Further, the relevance of safety against wind-break trait based solely on allometric comparison will be discussed. Two other samples were used to discuss the variability of biomechanical safety traits in beech in function of growth condition: canopy trees from a regular stand and standard trees from a coppice with standards site.

4.4.2. Material and methods

Study sites

Two distinc sites were used in this study.

Site 1 was a broadleaved 13-ha-stand in north-eastern France (47.9507°N, 6.3857°E, alt: 470m) formerly managed as a coppice-with-standards. In 1955-1956, stand was thinned, converting it to a high forest. Records show it was further thinned between 1956 and 1995, but the years of thinning were not recorded. After 1995, there was no further thinning. In fall of 2007, a sample of 72 understory beech trees distributed throughout the stand and at least 18 m from one another were selected for study. The trees originated from seeds and grew up under closed canopy or in small gaps. Sample trees met the following criteria: breast height trunk diameter was 7.5 to 17.5 cm, stems were unforked, leaned < 11°, had fewer than 25 epicormic branches (sensu Colin *et al.*, 2012) along the lowest 4 m of stem, and had no visible injury, spiral grain, canker, or top dieback. The sample trees were then split into two subsamples with similar mean values for diameter, height and relative vertical crown length. In winter 2007-2008, one subsample was released by a thinning that removed the trees within competition in a 12-m radius around each target tree (hereafter referred to as "released" trees) and the other subsample of trees was left unreleased ("control" trees) (Ningre *et al.*, 2011). From thirty-six released understorey trees, fifteen were broken by the wind in winter 2009 and twenty-one remained unharmed. For wind-broken released trees, we have only the initial measurement of tree morphology while released trees were followed until harvested in winter of 2013-2014.

Site 2 was situated in Montiers-sur-Saulx in north-eastern France (48.538 N, 5.305 E). On this site, two stands were used for sampling. The first stand was a regular mixed *F. sylvatica* and *A. pseudoplatanus* even-aged high forest and the second one a coppice-with-standards stand. Thirty-two trees *F. sylvatica* canopy trees from the regular stand and three standard trees from the coppice-with-standards stand were sampled in 2009 and 2010 during an experimental campaign of ANR EMERGE project which aimed to evaluate the available forest biomass in France (p37-46, Gamblin, 2013).

Tree measurements

For understorey beech trees from site 1, retrospective analysis of radial and axial growths as well as the determination of biomass distribution parameter and taper parameter was performed according to the procedure detailed in §4.3.3 Further, horizontal crown projections were measured for all trees at 2007, 2010 and 2013 by a four-radii method.

For beech trees from site 2, only values measured during the tree harvesting were available. Taper parameter was fitted at the same manner as for site 1. During EMERGE project, biomass distribution along the trunk was measured for all branches with diameter higher than 7cm while smaller axes were weighted all together. To obtain biomass distribution parameter m, weights of sections smaller than 7cm were distributed along the stem proportionally to the weight of branches with higher diameter. For some trees, branch data was not of a good quality so that only twenty-one canopy tree and three standard trees were used for the study. Crown projections are missing for site 2. Therefore, we used diameters of branches at insertion to predict the length of branches according to Constant & Morisset (2015). Length was converted into projected length using average angle at insertion according to Kint et al. (2010) and average of at least three branches was used as an average crown radius. When less than three branches was recorded on the tree, crown radius was not computed which reduced the number of trees for which we could estimated the crown radius to 9 canopy trees and 3 standard trees. Basic morphological characteristics by tree type are summarized in Table 4.4.

Biomechanical integrative traits

Biomechanical safety traits were computed according to Fournier *et al*. (2013). Safety against self-buckling was estimated as follows:

$$SB = 0.836H^{-3/4}D^{1/2}E^{1/4}(\rho_T g)^{-1/4}(2n+1)^{-1/4}F_b^{1/2} \quad (4.8)$$

where H is the tree height, D is the basal diameter, E is the wood elastic modulus, ρ_T is the ratio of total fresh biomass including branches to the volume of the stem, g is the gravitational acceleration, n is the taper parameter and F_b is the shape factor which is computed as follows:

$$F_b = 0.1785(|m-4n+2|)\cdot(2n+1)\cdot J^{-1}_{\frac{4n-1}{m-4n+2}} \quad (4.9)$$

where m is the biomass distribution coefficient and $J^{-1}_{\frac{4n-1}{m-4n+2}}$ is the first root of Bessel function that can be solved using linear regressions fitted by Jaouen et al. (2007).

Safety against the wind-break was estimated as:

$$SW = \frac{\pi\sigma D^3}{16 A_c H k_w} \quad (4.10)$$

where σ is the wood strength, D is the tree diameter at breast height, A_c is the crown area and Hk_w is the height of the centre of pressure *i.e.* the centre of mass that we can obtain from the biomass distribution along the trunk.

As for beech trees from site 2 we did not have data about the wood properties and the center of the pressure, simplified version of SW was computed without these parameters designated in the following as SW1 using horizontal projection as a crown area. Bonnesoeur *et al.* (2013) suggested to compute the bending moment applied on the tree crown assumed to have a diamond shape as R_cH^2 where R_c is the crown radius and H is the tree height. Using this expression of the bending moment, SW can be also calculated as follows:

$$SW2 = D^3/(R_c H^2). \quad (4.11)$$

Variance decomposition

In order to estimate the weight of each parameter on the total variance of SB trait, we did the variance decomposition. First, Eq. 4.8 was log-transformed and parameters were grouped according to their nature as follows:

$$Log\ SB = \log 0.836 + log(H/D)^{-3/4} + \log\left(D^{-\frac{1}{4}}\right) + \log\left(E^{\frac{1}{4}}\right) + log(\rho_T g)^{-1/4} + log\left((2n+1)^{-1/4} \cdot F_b^{1/2}\right) \quad (4.12)$$

where S = slenderness = $\log(H/D)^{\cdot 3/4}$

D = diameter = log ($D^{1/4}$)

E = elastic modulus = log ($E^{1/4}$)

L = load ratio by biomass = log $(\rho_T \cdot g)^{\cdot 1/4}$

F = shape = log $((2n+1)^{\cdot 1/4} \cdot F_b^{1/2})$

Variance of the linearized form of SB trait (Eq. 4.12) was decomposed to obtain the contribution of each parameter and to separate the variance due to the treatment and variance due to individual trees inside each treatment.

Statistical analysis

Statistical analyses were performed with the Origin software. A Student's t-test at specified level of significance was used to assess the difference between treatments.

Table 4.4: Morphological characteristics of *F. sylvatica* trees from different growth conditions in 2013.

H/D_{130} and H/D_{basal} are the tree slenderness ratios taking the diameter at breast height (D_{130}) and the tree basal diameter (D_{basal}) respectively, as a reference value for diameter.

	Nb	Age (yrs)	Height (m)		D_{basal} (m)		D_{130} (m)		H/D_{basal}		H/D_{130}		Crown area (m²)	
		Mean	Mean	S.D.	Mean	S.D.	Mean	S.D.	Mean	S.D.	Mean	S.D.	Mean	S.D.
Control	21	86.0	18.3	3.34	0.16	0.04	0.13	0.03	113.8	11.9	144.6	12.7	30.7	14.0
Released	21	84.8	18.4	3.32	0.19	0.03	0.15	0.03	96.9	17.6	121.0	18.0	35.5	13.4
Canopy trees	21	52.4	22.2	2.06	0.36	0.09	0.30	0.08	66.6	17.0	78.3	19.9	341.4	147.5
Standards	3	140	26.3	0.93	0.84	0.12	0.71	0.05	31.6	3.8	37.3	1.6	432.5	243.5

Table 4.5: Biomechanical traits of *F. sylvatica* trees from different growth conditions.

ρ_T is the load factor, n is the taper, m is the distribution of biomass factor, Fb is the shape factor, SB is the safety against self-buckling, SW_1 is the safety against wind break according to Fournier *et al*. (2013) and SW_2 is the safety against wind break according to Bonnesoeur *et al*. (2011).

	ρ_T (kg m^{-3})		n		m		F_b		SB		SW_1		SW_2	
	Mean	S.D.	Mean	S.D.	Mean	S.D.	Mean	S.D.	Mean	S.D.	Mean	S.D.	Mean	S.D.
Control	1285	175	0.97	0.11	2.72	0.28	3.01	0.32	1.68	0.11	9.2E-06	5.9E-06	4.1E-06	1.5E-06
Released	1357	119	0.98	0.12	2.75	0.26	3.06	0.27	1.82	0.24	1.2E-05	4.4E-06	6.6E-06	3.1E-06
Canopy trees	1475	186	0.95	0.14	3.15	0.32	3.63	0.40	2.08	0.25	8.2E-06	4.7E-06	1.1E-05	6.0E-06
Standards	2038	217	1.17	0.10	3.76	0.30	4.42	0.43	2.90	0.13	5.9E-05	2.2E-05	7.7E-05	2.0E-05

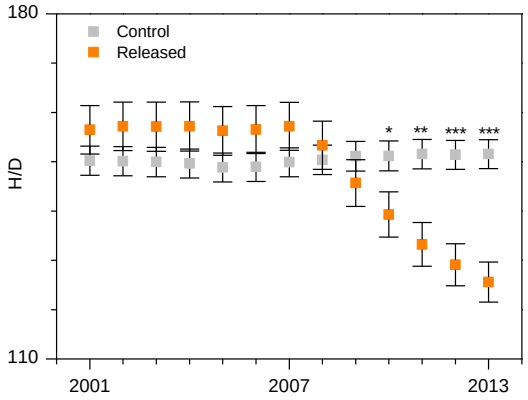

Figure 4.12: Change in slenderness ratio (H/D_{130}) in control and released beech poles from 2001 to 2013.
Stars designate positive result of t-test at 0.001 (***), 0.01 (**) or 0.05 (*) level of significance.

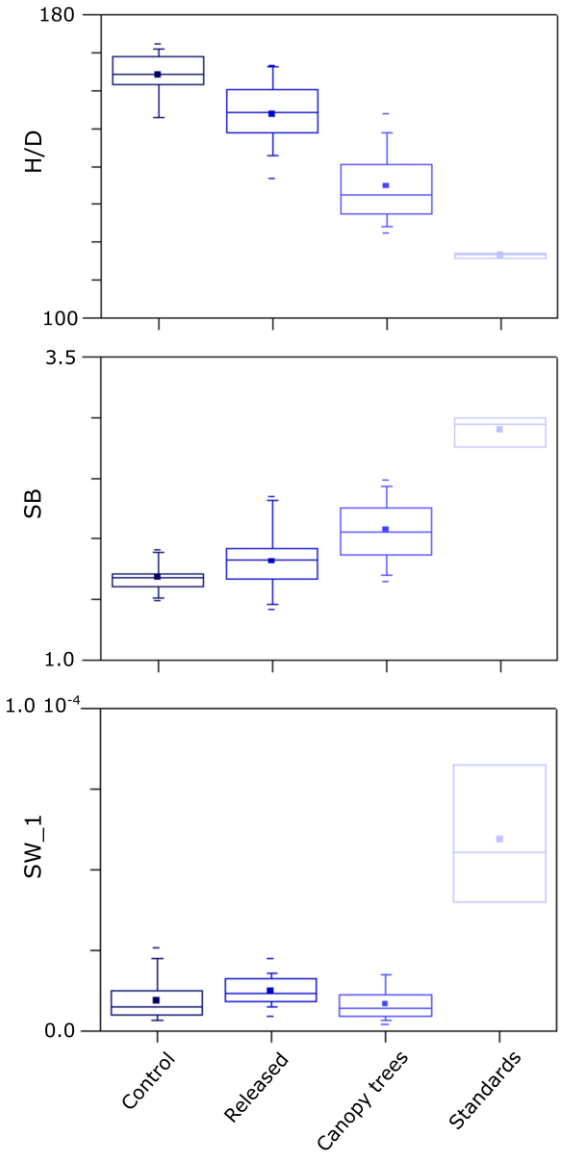

Figure 4.13: Slenderness ratio (H/D_{130}), safety against self-buckling (SB) and safety against wind-break (SW) in beech trees from different growth conditions.

4.4.3. Results

Morphology changes of beech understorey trees after the release

We found that beech trees evolving during their whole life in the forest undrestorey exhibited very high slenderness ratio. During the six years after the release, slenderness ratio has been continously decreasing (Fig. 4.12) and no stabilisation was reached. The slenderness ratio of released poles in 2013 was in average 16.3% lower when compared to control poles (Table 4.4, slenderness ratio with the diameter at breast height is taken as a reference). Increase in crown area was not significant six years after the release.

Morphology of beech trees from different growth conditions

Canopy trees exhibited significantly lower slenderness (*p-value* < 0.001) and larger crowns (*p-value* < 0.001) than understorey trees of similar height. Biomass distribution factor was higher (Table 4.5, *p-value* < 0.01) while taper factor did not significantly differ between canopy and understorey trees. Standard trees from the coppice-with-standards site growing without competition for light but submitted to wind loads exhibited very thick stems, low slenderness ratio (Fig. 4.13) and large crown areas.

Biomechanical traits in beech trees from different growth conditions

We found that safety against self-buckling was low in understorey trees (1.68) and significantly increased after the release (Table 4.5, Fig. 4.13, *p-value* < 0.05). This increase was mainly driven by changes in slenderness and in diameter; the weight of other factors on SB change after the release was lower than 0.3% (Table 4.6). It is interesting to note that inter-tree variance was very high between undrestorey trees (Table 4.6). When comparing understorey trees with canopy and standard trees, we can note significant increase in SB trait (2.08 and 2.90 for canopy and standard trees respectively, Fig. 4.13). While slenderness and diameter factors are again the main drivers of observed difference in SB traits for different growth conditions, shape factor variance becomes more important than for the release change. Shape factor variation is mainly due to change in biomass distribution (parameter m, Table 4.5) while surprisingly, taper factor seems to be less affected by growth conditions.

Table 4.6: Variance decomposition of SB trait.

S stands for slenderness, D for diameter, E for elastic modulus, L for load and F for shape factor.
First part of the table represents variance decomposition of SB trait in understorey trees after release for all factors separating the variance due to individuals in the same group (tree) and due to the release (treatment) while second part of the table represents variance decompositin of SB trait in different growth conditions (status = understorey, canopy or standard tree).

		S	**D**	**E**	**L**	**F**	**Total**
Release	Tree	56.4%	11.3%	1.5%	3.3%	6.0%	78%
	Treatment	18.9%	2.3%	0.1%	0.2%	0.0%	22%
	Total	75.3%	13.6%	1.6%	3.5%	6.1%	100%
Status	Tree	15.4%	3.0%	0.2%	0.7%	1.2%	21%
	Status	63.3%	12.4%	0.5%	0.7%	2.4%	79%
	Total	78.8%	15.5%	0.7%	1.5%	3.6%	100%

Table 4.7: Morphological characteristics and safety against wind of released *F. sylvatica* understorey trees.

D_{130} is the tree diameter at breast height, H/D_{130} is the tree slenderness ratio, SW1 is the safety against wind break according to Fournier *et al.* (2013) and SW2 is the safety against wind break according to Bonnesoeur *et al.* (2011).

	Nb	Height (m)		D_{130} (m)		H/D_{130}		Crown area (m²)		SW1		SW2	
		Mean	S.D.	Mean	S.D.	Mean	S.D.	Mean	S.D.	Mean	S.D.	Mean	S.D.
Unharmed	21	16.5	3.6	0.12	0.03	144.2	21.6	27.9	12.8	4.3E-06	2.3E-06	2.4E-06	7.6E-07
Wind-break	15	17.6	2.4	0.13	0.02	136.3	19.5	40.0	16.1	3.9E-06	1.1E-06	2.5E-06	6.7E-07

Safety against wind-break was found to significantly increase in understorey trees after the release when computed according to Fournier *et al.* (2013) (SW1, Table 4.7, *p-value* < 0.01) but the difference was not significant if SW2 was considered. Safety against wind-break was high in standard trees but when comparing understorey released and canopy trees, it depended on the method used for SW determination. From the comparison of the morphology of released understorey trees broken by the wind in winter 2009 and unharmed released trees we can see that broken trees exhibited higher crown area (*p-value* < 0.05) and thicker stems (*p-value* < 0.1) but slenderness ratio was not significantly different. Estimation of the safety against wind-break based on allometric parameters did not allow for discrimination of broken trees.

4.4.4. Discussion

The safety against self-buckling in understorey trees was comparable to saplings from the tropical forest where Jaouen *et al.* (2007) observed an average value of 1.56 ± 0.23. It shows that self-buckling risk is present not only for small saplings but also for relatively large understorey trees, the main factor being the density of forest cover. From allocation of tree biomass after the release, we can see that beech understorey trees allocated more biomass to radial growth. This allowed for reduction of slenderness (Fig. 4.12) which was identified as the main driver of the safety against self-buckling change after the release (Table 4.6). Jaouen *et al.* (2007) reported that shape factor was the second most important factor of intraspecific variance (7.6%) of the safety against self-buckling. In this study, the shape factor accounted for 6% of total variance mainly due to the intertree variance but was not significantly affected by the release, likely because it is difficult to significantly modify the taper or biomass distribution in relatively large established trees.

More surprisingly when compared beech trees from different growth conditions, the shape factor, exhibiting the result of long-term acclimation to different wind and light regimes, accounted only for 2.4% of the total SB variance (Table 4.6). While distribution of biomass was significantly affected by the growth conditions, taper factor did not differ between canopy and understorey trees (Table 4.5). If thinning is known to affect the stem taper (Baldwin Jr *et al.* 2000), Makinen & Isomäki (2004) reported that in case of late thinning this effect is not significant. This only confirms that small saplings can rapidly change their geometry by an increase in diameter growth while this is more difficult for large trees: Collet *et al.* (2011) reported that beech saplings doubled their diameter in four years after the release while in our study we observed an increase in diameter of 18.8% in six years.

Slenderness ratio is also often used as a proxy of wind firmness (Mitchell 2000). Slenderness significantly decreased after the release and was still not stabilized six years after the

release. Safety against the wind-break (SW1) increased after the release in understorey trees however high variability was observed among trees in comparison for example with the SB trait (Table 4.5). This likely comes from the difficulty to properly asses the crown surface exposed to the wind. The crown surface used in this study was the horizontal projection of the crown. We also tried to compute vertical projection which is more appropriate in the case of wind loading however considering the very diverse crown shapes of understorey trees, it was not really possible to describe them in a simple geometric way. Unfortunately, we did not have an operational routine to treat TLS scans to obtain better information about the crown profile. From the comparison of released understorey trees broken by the wind (no windthrow was observed) and unharmed released understorey trees (Table 4.7), it is clear that estimate SW based solely on allometric comparison is not satisfactory because it does not allow to discriminate trees exposed to higher risk. To assess properly the risk of wind-break, it seems necessary to take into account the local topology that can largely affect the wind flow and thus the wind load applied on an individual tree.

Chapitre 5 : Changements des traits du bois du hêtre à l'ouverture de la canopée

5.1. Avant-propos

Pour ce dernier chapitre, les résultats présentés sont axés sur l'échelle tissulaire. Ce chapitre est divisé en deux parties :

- La **première partie** décrit la **plasticité du bois** de hêtre en réponse à l'ouverture de la canopée en prenant en compte les caractéristiques anatomiques initiales du bois et la taille de la section de la tige (diamètre). Les résultats suivants décrivent les traits du bois (taille et distribution des vaisseaux, surface de cernes, densité du bois) et les propriétés hydrauliques potentielles du cerne (diamètre hydraulique des vaisseaux, conductivité hydraulique spécifique potentielle et conductivité hydraulique potentielle du cerne annuel). Cette partie sous forme d'article constitue l'Article 4 de cette thèse.
- La **seconde partie** s'axera sur une **analyse statistique** pour estimer la contribution relative des traits structuraux sur la conductivité hydraulique potentielle du cerne annuel chez les différents groupes d'arbres étudiés dans l'Article 4. L'effet des variations annuelles, du statut social et de l'ouverture de la canopée sur la répartition de la contribution relative de chaque trait sera analysé.

Tableau 5.1 : Contribution des co-auteurs à l'Article 4.

Auteurs	**Contribution à l'Article 4**
Estelle NOYER	Acquisition et analyses des données, principale rédactrice de l'article
Barbara LACHENBRUCH Jana DLOUHA Catherine COLLET Mériem FOURNIER	Contribution à la discussion et à la rédaction de l'article
Julien RUELLE	Développement des outils d'analyse d'images et contributions à la discussion
François NINGRE	Mise en place du site d'expérimentation du Grand Poiremont

5.2. Article 4 : Xylem traits in European beech (Fagus sylvatica L.) display a large plasticity in response to canopy

Estelle NOYER[1], Barbara LACHENBRUCH[2], Jana DLOUHA[1], Catherine COLLET[1], Julien RUELLE[1], François NINGRE[1], Mériem FOURNIER[1]

[1] LERFoB, INRA, AgroParisTech, F-54000, Nancy, France

[2] Department of Forest Ecosystems & Society, Oregon State University, Corvallis, OR-97333, USA

Article accepté dans *Annals of Forest Sciences*

Abstract

Context Forest canopies are frequently submitted to disturbances that allow understory trees to access the upper canopy. The effect of canopy release on xylem anatomy has been assessed in juvenile trees and saplings while the potential acclimation of larger trees remains poorly-documented.

Aims We estimated the potential hydraulic conductivity of growth rings in large understory trees compared to overstory trees and evaluated the responses to canopy release in large trees and in saplings.

Methods We recorded radial growth, wood density and vessel structure in beech trees according to their position within the canopy and their size. Xylem traits were followed during six years after canopy release for large trees and during two years for saplings. Vessel diameter and frequency as well as ring area were used to compute the potential annual ring hydraulic conductivity.

Results Large understory trees displayed lower radial growth increments, lower potential annual ring hydraulic conductivity than overstory trees. After canopy release, potential annual ring hydraulic conductivity increased in large trees due exclusively to increased radial growth without any change in specific hydraulic conductivity. It increased in saplings due to both increased radial growth and increased specific conductivity.

Conclusion Tree size impacted xylem structure and resulted in plasticity of the potential hydraulic conductivity of the annual tree ring following canopy release.

Keywords

xylem anatomy, vessel, potential hydraulic conductivity, radial growth, wood density.

5.2.1. Introduction

Trees face changing environments throughout their lifetime because their locations may experience environmental change, and also because they sample locations differently as they grow. By examining modifications in stem structure as microclimate changes, ecophysiological responses may be uncovered. The present work focuses on plasticity in xylem traits of stems in response to tree position within the canopy. European beech (*Fagus sylvatica* L.), a diffuse-porous species with a wide functional sapwood area (Gasson, 1985), was chosen as the model species because of its known plasticity to growth conditions (Stojnic *et al.*, 2013; Eilmann *et al.*, 2014; Schuldt *et al.*, 2016). It is a shade-tolerant species that can survive under a high level of inter-tree competition, and can rapidly respond to changes in canopy structure and local irradiance (Lemoine et al. 2002a, 2002b; Caquet et al. 2009a).

The potential specific hydraulic conductivity at tissue level (K_S) is a function of vessel diameter and frequency (Tyree & Zimmermann, 2002). Slight modifications in vessel diameter have a large impact on hydraulic properties (Gartner, 1991; Badel *et al.*, 2015). Trees can also alter the conductivity in the whole stem by increasing sapwood width or by increasing the width of the new growth rings (Maherali *et al.*, 1997), independently of any change in K_S.

Understory trees grow under lower irradiance levels, lower wind speeds and lower extremes in air temperature and vapor pressure deficit (VPD) (Parker *et al.*, 1995; Aussenac, 2000). They are shorter, exhibit smaller stem diameters, narrower annual growth increments, lower sapwood area (Nicolini *et al.*, 2001; Löf *et al.*, 2005; Petritan *et al.*, 2009; Klopcic & Boncina, 2010; Fajardo, 2016) and may have access to less water than overstory trees (Bréda *et al.*, 1995). While modifications in xylem traits reflect tree acclimation (Fonti *et al.*, 2010; Anderegg & Meinzer, 2015), there is little literature on xylem anatomy and function in overstory vs. understory trees from temperate forests. Most studies focus on sun exposed and shaded branches on the same individual (Lemoine *et al.*, 2002a; Gebauer *et al.*, 2014) which is not representative of acclimation at tree level. Some studies suggest that because of lower access of understory trees to water, it would be to their advantage to display a larger resistance to soil water shortage than overstory trees. And because of lower irradiance (Hacke, 2014), shorter path length (Preston *et al.*, 2006) and possibly lower dry growth conditions (Hajek *et al.*, 2016), smaller vessels might occur in understory trees. However, other studies suggest that the lower evaporative demand and shorter stem could lead to lower tension in the xylem column of understory trees (Granier *et al.*, 2000) and, therefore, wider vessels.

Another case in which xylem plasticity could play an important role is after understory trees are released from inter-tree competition. Natural or anthropogenic disturbances periodically affect most forest ecosystems (Rentch *et al.*, 2010) and provide the opportunity for understory trees to reach the canopy (Webster & Lorimer, 2005). Such released understory trees then have to cope with severe and sudden changes in their environment. To our knowledge, the acclimation process of stem xylem after canopy release, including the timing and nature of changes in xylem traits has not been fully characterized. Various studies analyzing xylem traits of released angiosperm trees focus on the instant response to canopy release. While some authors observed an increase in vessel diameter and a decrease in vessel frequency (Hoffmann & Schweingruber, 2002; Caquet *et al.*, 2009), others did not observe such changes (Maherali *et al.*, 1997). Moreover, enhanced radial growth following canopy release was repeatedly observed (Collet *et al.*, 2001; Hartmann & Messier, 2011). Large-diameter trees have a greater potential than smaller trees to increase stem conductivity through enhanced radial growth, due to wider annual rings (Caquet *et al.*, 2010; Klopcic & Boncina, 2010) and larger relative basal area increments. Therefore, the relative importance of changes in xylem structure vs. changes in ring width for altering water transport capacity may depend on tree size.

The study focuses on the response of stem xylem traits to tree position within the canopy and to canopy release, assessed in experimental sites with either large or small beech trees. We recorded xylem structure and growth increment to reconstruct hydraulic conductivity of tree-rings in the past. Such a retrospective approach does not allow any direct measurement of stem conductivity nor to access past sapwood width or total stem conductance. Thus, we concentrated on changes in potential hydraulic conductivity at tree ring level. We test the following hypotheses:

- (**H1**) understory trees display a xylem structure with smaller vessel diameter and higher vessel frequency;
- (**H2**) because of lower year-to-year variation in the micro-environment, understory trees exhibit a more stable xylem structure from year to year than overstory trees;
- (**H3**) after canopy release, understory trees increase the conducting area and change the number and size of vessels and attain similar potential annual ring hydraulic conductivity than overstory trees within a few years;
- (**H4**) after canopy release, small trees display larger adjustments in xylem anatomy in addition to radial growth as a basis for increased potential ring conductivity than large trees which have larger tree-ring sections.

5.2.2. Material and methods

Study sites and plant material

Large trees

The site for large trees was a 13-ha-stand in a managed forest in north-eastern France (47.9507°N, 6.3857°E, alt: 470m). The soil was dystric to hyperdystric cambisol with a luvic layer between the A and S horizons (IUSS Working Group WRB, 2014). Meteorological data were recorded from 2001 to 2013 from the Aillevillers-et-Lyaumont weather station (French National Climatic Network, Météo-France) 5 km from the stand. Over that period, the mean annual temperature was 10.3°C (Online Resource 1). The mean annual precipitation was 1218 mm. During 2003 and 2011, years with very dry summers in Europe, temperatures were slightly higher and precipitation slightly, but not significantly, lower than long term means.

The broadleaved stand had formerly been managed as a coppice-with-standards. In 1955-1956, however, the stand was thinned and converted to a high forest. Records show it was further thinned between 1956 and 1995, but the years of thinning were not recorded. After 1995, there was no further thinning. In 2006, the stand was dominated by *Fagus sylvatica* L. (basal area: 21 m^2 ha^{-1}) with another 5.5 m^2 ha^{-1} of *Quercus spp., Fraxinus excelsior* L.*, Acer pseudoplatanus* L.*, Carpinus betulus* L.*, Betula spp., Abies alba* Mill, and *Picea abies* L. (H) Karst. Stand density was 513 stems ha^{-1} and the mean height of the overstory trees was 31.6 m.

During fall 2007, we selected a sample of 42 understory beech trees distributed throughout the stand and at least 18 m from one another was selected. The trees originated from seeds and grew under closed canopy or in small gaps. Sample trees met the following criteria: DBH was 7.5 to 17.5 cm, stems were unforked, leaned < 11°, had fewer than 25 epicormic branches (sensu Colin *et al.*, 2012) along the lowest 4 m of stem, and had no visible injury, spiral grain, canker, or top dieback. The sample trees were then split into two subsamples with similar mean values for diameter, height and relative vertical crown length (Table 1). During winter 2007-2008, one subsample was released by a thinning that removed the competing trees in a 12-m radius around each target tree (hereafter referred to as “released” trees) and the other subsample of trees was left unreleased (“suppressed” trees) (Ningre *et al.*, 2011).

Five overstory, healthy and relatively straight beech trees were also selected. They were later found to be among the oldest canopy trees of the stand (Table 5.2).

Saplings

The site for the saplings (49.0778°N, 6.0172°E) (Caquet *et al.*, 2009, 2010) is at a distance of about 150 km from the large tree site and at a similar altitude (300 m). The soil is a calcisol (40-60 cm depth). Mean annual temperature is 10.1°C and annual precipitation is 745 mm (French National Climatic Network, Météo-France).

The stand was formerly a broadleaved coppice-with-standards converted to a high forest during the 1960s. In 1999, a storm created scattered canopy gaps. In 2006, the forest canopy was mainly composed of *Fagus. sylvatica*, *Acer pseudoplatanus L.*, *Acer platanoides L.*, *Carpinus betula* L. and *Quercus spp.*

During January 2005, four advanced regeneration patches were selected under closed canopy and at least 300 m from one another. Canopy gaps of 500 to 1900 m² were created by removal of all overstory trees above two patches (leaving the "released" understory saplings) and the two other patches were left unthinned ("suppressed" saplings). Two 0.5- to 1-m-tall beech saplings were selected for measurement in each patch. Additionally, four beech saplings were selected in gaps that had been created by the 1999 storm ("acclimated" saplings) (Table 5.2). During summer 2005, relative irradiance (with respect to the irradiance above canopy) was estimated above each selected sapling with hemispherical photography. It reached, on average, 5, 31 and 60% for the suppressed, released and acclimated saplings, respectively (Caquet *et al.*, 2010).

Measurements

Large trees

The released and suppressed understory trees were felled during March 2014, six years after canopy release. Two 5-cm-thick disks were collected at a height of 1.30 m from each tree and wrapped in plastic film. The first disk, used for anatomical measurements, was stored at 4°C immediately after harvesting. Using growth stress indicator measurements (Fournier *et al.*, 1994), we identified the radial position of expected tension-wood (Purba *et al.*, 2015). Radii perpendicular to the tension-wood zone and without knots were considered to be normal wood. A radial strip (0.5 cm x 1.8 cm, T x L) was then cut in the normal wood zone and divided into successive 1.5-cm-long segments. Each segment was embedded in successive polyethylene glycol baths (30%, 50% and 100% w/v). Twelve-µm-thick cross-sections were cut from each segment with a sliding microtome. They were double-stained with a specific staining procedure as follows.

Table 5.2: Sample tree characteristics (number of trees, age and tree height range, mean ± standard error of stem diameter and cross-section area) in 2013 for large trees and in 2006 for saplings.

	Large trees			**Sapling**		
	Overstory	Understory suppressed	Understory released	Acclimated	Understory suppressed	Understory released
Number of trees	5	21	21	4	4	4
Age	83-117*	54-108			11-18	
Tree height (m)	27.7-31.6	12.4-25.1			0.5-1.0	
Stem diameter (cm)	52.60 ± 0.91	12.13 ± 0.52	14.98 ± 0.57	0.92 ± 0.48	0.50 ± 0.04	0.74 ± 0.07
Stem cross-section area (cm²)	2150.8 ± 150.5	132.93 ± 16.01	181.29 ± 13.68	0.68 ± 0.11	0.20 ± 0.03	0.44 ± 0.08

* at breast height (1.30 m).

They were first stained for 1 min in aqueous Safranin (1% w/v), treated with hydrochloric alcohol for 1 min, rinsed with distilled water, then stained with Astra blue (1% w/v) for 5 min, rinsed with distilled water, and dehydrated sequentially with 96% and absolute ethanol. Finally, the sections were mounted on glass slides in Histolaque LMR©. Each section was then imaged at x10 magnification with a digital camera (Sony XCD-U100CR) through a light microscope (Zeiss AxioImagerM2) with image acquisition software (Archimed software, Microvision Instruments, France). For each image, three to six sectors bounded by rays were defined per ring to collect data related to vessel number and geometry. Sectors typically contained 25 to 200 vessels.The second disk was used for ring width and wood density measurements. It was stored at -20°C immediately after harvest. After disks were sanded, four perpendicular radii were imaged by digital camera. On each radius, the width of each ring (RW, mm) from pith to bark was measured to a precision of 0.01 mm, by image analysis using TSAP-Win (Rinntech, Germany).

One of the normal wood radii was used for wood density measurements. A radial strip (2.5 cm x 5 cm, T x L) was cut and conditioned for one month at 12% relative humidity at ambient temperature. A radial slice (1.0 x 0.2 cm^2, T x L) was then cut for X-ray micro-densitometry measurements with a microfocus X-ray source (Hamamatsu L9181-02 130 kV) and a digital X-ray detector (Varian PaxScan 4030R). Pixel size varied between 20 to 30 µm. The Crad and Cerd software suite was used to compute radial wood density (WD, kg m^{-3}) profiles (Mothe *et al.*, 1998).

The selected overstory trees were sampled with an increment borer. In June 2015, two 5-mm-diameter cores were collected at 1.30 m in height. Cores were stored at 4°C. These cores were used for anatomical and X-ray micro-densitometry measurements, using a protocol similar to the one used for understory trees. Ring widths for the overstory trees were estimated from X-ray data.

Saplings

Understory saplings were harvested from late August to mid-September 2006, two growing seasons after treatments had been applied. A 2- to 3-cm-long stem portion was cut from each sapling from just above the ground level. It was stored at -20°C until it was analyzed.

A 12-µm-thick cross-section was then cut from each stem portion using a sliding microtome (SM2000, Leica Jung, Nussloch, Germany). Sections were double-stained like for the large trees, and mounted on slides with Canada balsam. Images were taken and analyzed as above, to measure ring width. Vessel number and geometry were measured in three to six sectors bounded by rays in each of the three most recent (youngest) growth rings.

Data analysis

For each tree and sapling, annual ring width and annual basal area increment (BAI, cm²) was estimated from the position data for ring boundaries, averaged over the four radii. BAI was estimated as follows:

$$BAI = \pi\,(r_1^2 - r_2^2) \quad (5.1)$$

where r_1 and r_2 (cm) are the average of the radii from two successive years.

The Hagen-Poiseuille diameter is the vessel diameter which, if multiplied by the observed vessel frequency, gives the same potential specific conductivity as the actual vessel diameter (VD) distribution. Following Steppe and Lemeur (2007), the Hagen-Poiseuille vessel diameter D_{HP} (µm) equation was adjusted for elliptical vessel (Fig. 5.1) and computed as:

$$D_{HP} = \sqrt[4]{\frac{1}{n}\sum_{i=1}^{n}\frac{2a_i^3\,b_i^3}{a_i^2+b_i^2}} \quad (5.2)$$

where n is the number of measured vessels, and a and b (µm) are the two axes of the ellipse (maximum and minimum lumen diameter, respectively).

The potential hydraulic conductivity is the total estimated conductivity of a sample of vessels assuming that their flow is governed by the Hagen-Poiseuille equation. Potential specific hydraulic conductivity K_S (kg m^{-1} s^{-1} MPa^{-1}) was calculated as follows:

$$K_s = \left(\frac{\pi\rho}{128\,\eta}\right).{D_{HP}}^4.VF \quad (5.3)$$

where η is the viscosity of water ($1.002*10^{-9}$ MPa s^{-1}), ρ the density of water (998.21 kg m^3), D_{HP} is the Hagen-Poiseuille vessel diameter (m) and VF (n m^{-2}) is the mean vessel number per square meter.

The potential hydraulic conductivity for a ring K_{ring} (kg m s^{-1} MPa^{-1}) is estimated by:

$$K_{ring} = K_s.BAI \quad (5.4)$$

For each measured or computed trait and for each year, trees or saplings in different treatments were compared using a Kruskal-Wallis test. On large trees, if the associated p-value was below 0.05, a post-hoc Wilcoxon-Mann-Whitney test was made. Large trees and saplings were tested independently. All statistical analyses were performed using R software, version 3.2.3 (R Core Team, 2015).

To identify the variance contribution of each factor (D_{HP}, VF and BAI) to the K_{ring} variation, we computed variance partitioning of log transformed Eq. (5.4) as follows:

$$Var(\log_{10} K_{ring}) = Var(4\log_{10} D_{HP}) + Var(\log_{10} VF) + Var(\log_{10} BAI) + 2\,Cov(4\log_{10} D_{HP}, \log_{10} BAI) + 2\,Cov(4\log_{10} D_{HP}, \log_{10} VF) + 2\,Cov(\log_{10} VF, \log_{10} BAI) \quad (5.5)$$

The covariance factor expresses the interaction between individual factors that can be synergistic (positive value) or compensative (negative value). A covariance value close to zero means that factors are independent.

Results are presented as a relative contribution to total variance and are computed for the second year after release for understory saplings and large trees in comparison to suppressed individuals.

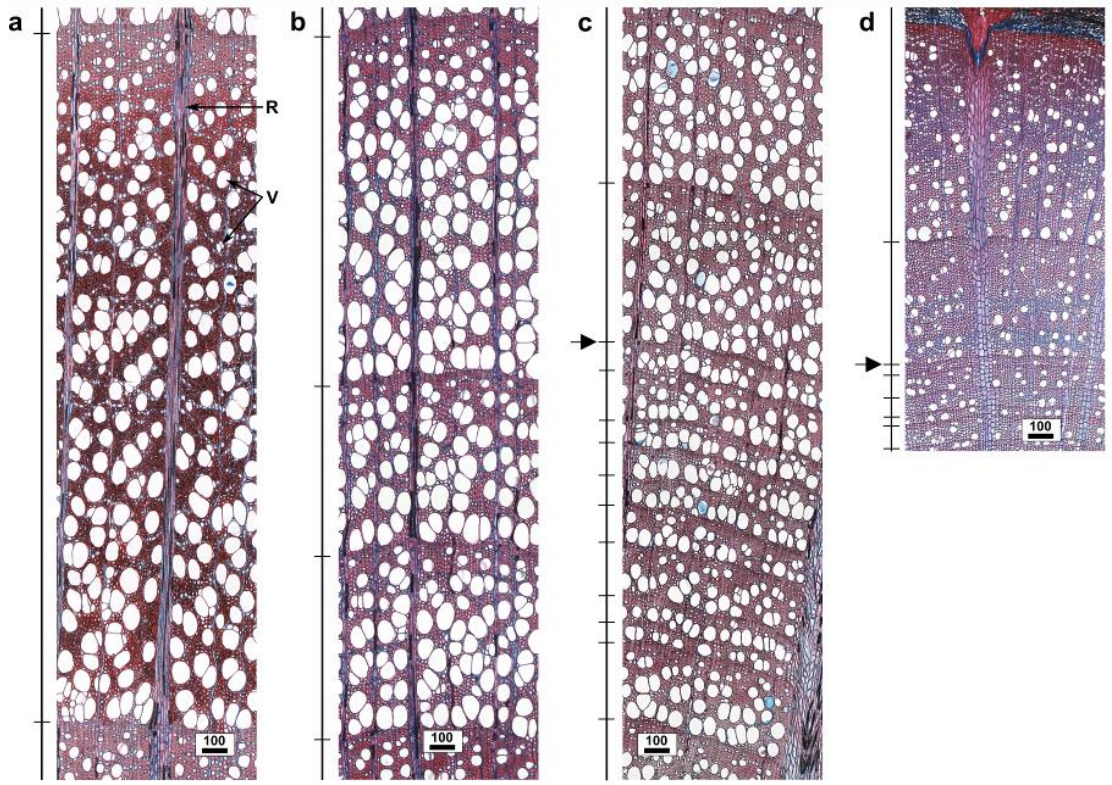

Figure 5.1: Images of large overstory (a and b) and understory (c) trees and saplings (d).
At the left of each image, ticks represent tree-ring boundaries and arrow the ring the first year after a release event. V: vessels; R: ray parenchyma. Bars: 100 µm.

5.2.3. Results

Large trees

BAI of overstory tree varied widely among years (Fig. 5.2a) and BAI was at least 15-fold higher in overstory than in understory trees in all years. Before the release in 2007, understory trees showed stable BAI values. After 2007, BAI of understory suppressed trees remained at 2.1 cm² whereas, for released trees, it significantly increased until 2009 and leveled off at 14.0 cm². However even after stabilization, BAI remained significantly lower for released than for overstory trees (Fig. 5.2a; Table 5.4).

During most years before the release, overstory trees exhibited significantly higher vessel diameter (51.9 to 56.7 µm) than understory trees (40.1 to 45.7 µm). After release, vessel

diameter significantly increased in released trees. In 2009 and afterwards, it was 43.7 and 49.4 µm in suppressed and released understory trees, respectively (Fig. 5.2b; Table 5.4). Vessel frequency was significantly higher in understory trees than in overstory trees and significantly decreased in released trees (Fig. 5.2d; Table 5.4). Wood density was not significantly lower in overstory than understory trees except during in 2004 and 2011 (Fig. 5.2f; Table 5.4). In overstory trees, wood density and BAI displayed similar inter-annual variations.

From 2002 to 2007, D_{HP} and K_S were higher in overstory than understory trees (61.7 to 49.6 µm, 50.6 to 27.6 kg m^{-1} s^{-1} MPa^{-1} respectively) (Fig. 5.2c, e; Table 5.4). After release, D_{HP} showed the same trend as VD: an increase until 2009 followed by a stabilized range of values around 55.7 µm. Annual variations in D_{HP} in suppressed trees were significantly lower than in released trees and overstory trees. K_S fluctuated between 42.5 and 53.9 kg m^{-1} s^{-1} MPa^{-1} in overstory trees whereas it was very stable in understory trees and did not significantly increase after release (Fig. 5.2e; Table 5.4). In all trees, K_{ring} showed inter-annual fluctuations similar to BAI. K_{ring} was significantly higher in overstory ($10.5 * 10^{-2}$ to $23.7 * 10^{-2}$ kg m s^{-1} MPa^{-1}) than in understory trees ($0.9 * 10^{-2}$ kg m s^{-1} MPa^{-1}) (Fig. 5.2g; Table 5.4). K_{ring} of released trees increased after release and stabilized at around $3.9 * 10^{-2}$ kg m s^{-1} MPa^{-1} whereas it remained at $0.65 * 10^{-3}$ kg m s^{-1} MPa^{-1} in suppressed trees (Fig. 5.2g; Table 5.4).

The relative contribution of D_{HP}, VF and BAI, to K_{ring} variation was calculated for 2009, two years after release. Variation of BAI after release contributed up to 101 % to the variation in K_{ring} whereas D_{HP} and VF contributions were low or negative. BAI exhibited a positive covariance with D_{HP} and a negative one with VF (Table 5.3).

Table 5.3: Relative contribution (%) of DHP, VF and BAI to K_{ring} variance in understory released trees and saplings, two years after canopy release.

	D_{HP}	VF	BAI	D_{HP}, BAI	D_{HP}, VF	BAI, VF
Large trees	4.32	4.56	101.10	41.82	-8.88	-42.92
Saplings	38.40	8.25	44.55	82.72	-35.59	-38.34

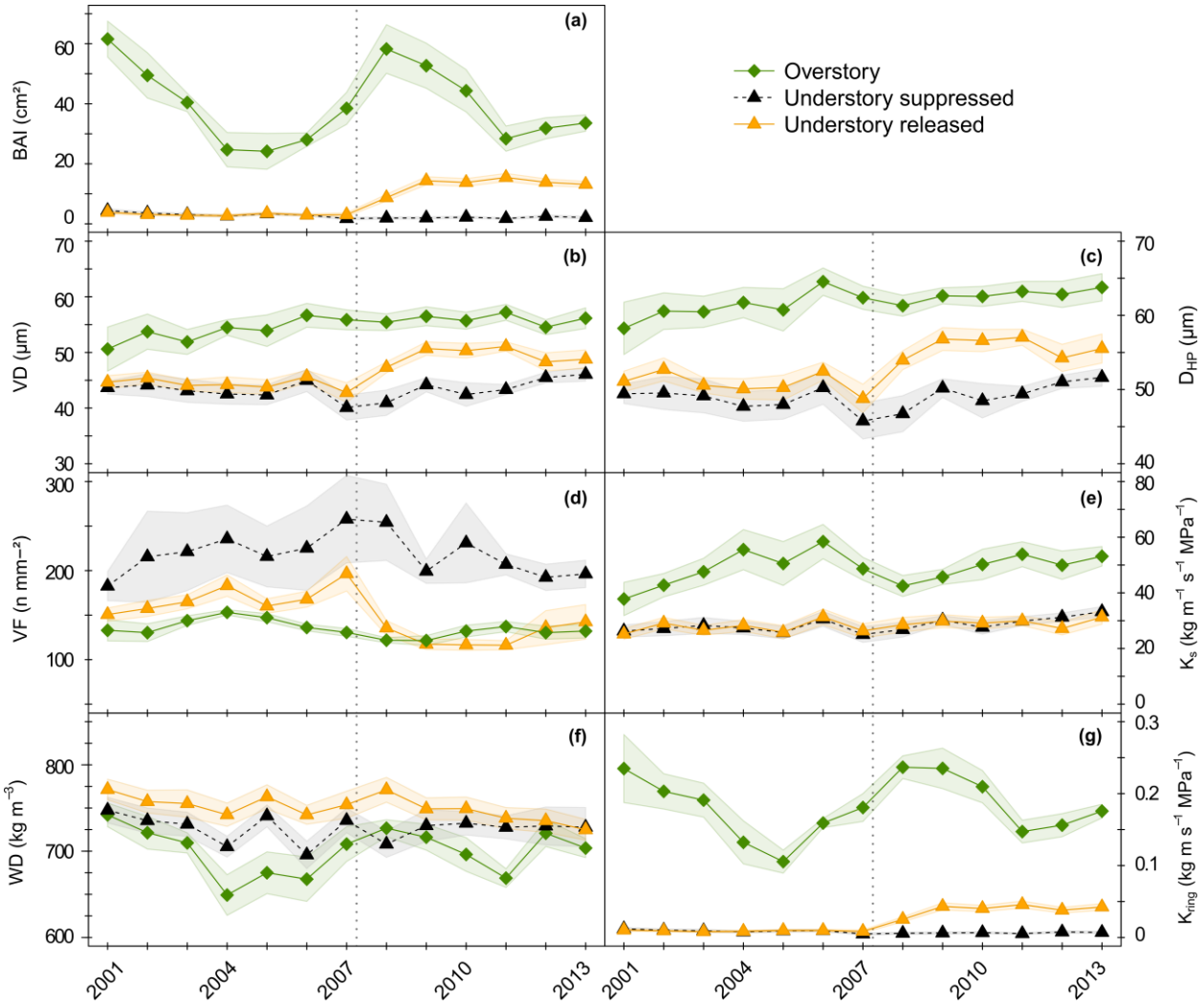

Figure 5.2: Mean (±SE) of xylem traits (a, b, d, f): basal area increment (BAI), vessel diameter (VD), vessel frequency (VF) and wood density (WD); and potential hydraulic performances (c, e, g): vessel conductivity-weight (D_{HP}), potential specific hydraulic conductivity (K_s) and ring conductivity (K_{ring}) of overstory (green) and understory suppressed (black, dotted lines) and released (yellow) large trees. The vertical dotted line shows the canopy release of understory released trees in winter 2007-08.

Table 5.4: Overall treatment effects on anatomic and hydraulic traits for large trees and for each year.

P-values (*P*) are from the Kruskal-Wallis test. Treatments showing significant differences for a year were then tested with a Wilcoxon test. A plus sign (+) indicates significant differences between overstory and understory released (O.R); overstory and understory suppressed (O.S); and understory released-suppressed (R.S) trees.

Year	BAI				VD				VF				D_{HP}				K_s				K_{ring}				WD			
	P	O.R	O.S	R.S	*P*	O.R	O.S	R.S	*P*	O.R	O.S	R.S	*P*	O.R	O.S	R.S	*P*	O.R	O.S	R.S	*P*	O.R	O.S	R.S	*P*	O.R	O.S	R.S
2001	0.0014	+	+		n.s				n.s				n.s				n.s				0.0014	+	+		n.s			
2002	0.0014	+	+		n.s				n.s				0.0269	+	+		0.03	+			0.0014	+	+		n.s			
2003	0.0015	+	+		0.0166	+	+		n.s				0.011	+	+		0.0101	+	+		0.0015	+	+		n.s			
2004	0.0012	+	+		0.0013	+	+		0.0217		+		0.0013	+	+		0.0015	+	+		0.001	+	+		0.0225	+		
2005	0.0011	+	+		0.0097	+	+		n.s				0.0158	+	+		0.0124	+	+		0.001	+	+		0.0297			
2006	0.0008	+	+		0.0023	+	+		0.0164		+		0.0023	+	+		0.003	+	+		0.001	+	+		0.0337			
2007	0.0006	+	+		0.0027	+	+		0.0048	+	+		0.005	+	+		0.0098	+	+		0.001	+	+		n.s			
2008	0	+	+	+	0	+	+	+	0		+	+	0	+	+	+	0.0036	+	+		0	+	+	+	n.s			
2009	0	+	+	+	0.0001	+	+	+	0		+	+	0.0004	+	+	+	0.0039	+	+		0	+	+	+	n.s			
2010	0	+	+	+	0		+	+	0		+	+	0.0001	+	+	+	0.0032	+	+		0	+	+	+	n.s			
2011	0	+	+	+	0	+	+	+	0		+	+	0	+	+	+	0,0024	+	+		0	+	+	+	0.0130	+		
2012	0	+	+	+	0.0011		+	+	0.001			+	0.0005	+	+	+	0.0019	+	+		0	+	+	+	n.s			
2013	0	+	+	+	0.0002	+	+	+	0.0012			+	0.0001	+	+	+	0.0018	+	+		0	+	+	+	n.s			

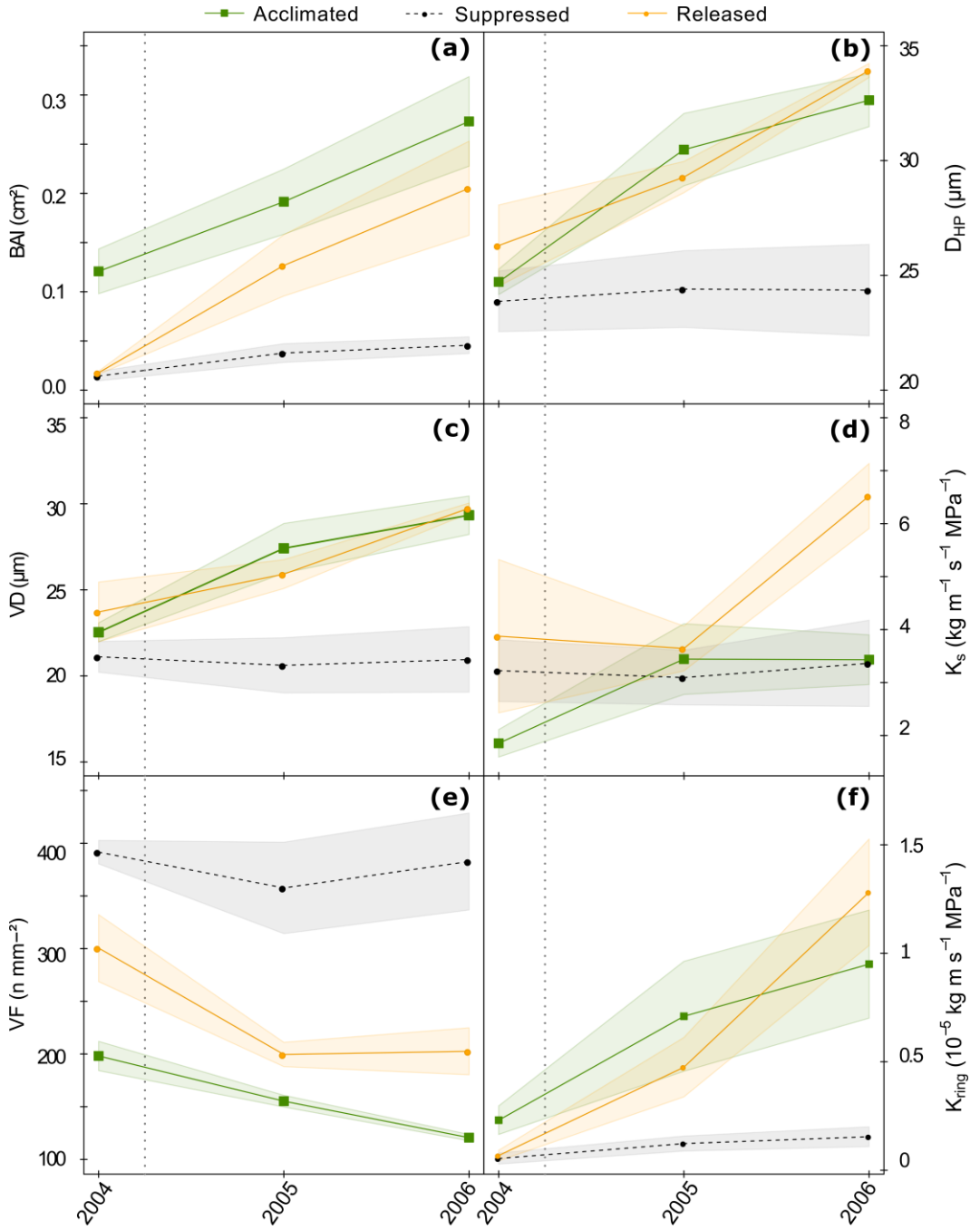

Figure 5.3: Mean (±SE) of xylem traits (a, c, e): basal area increment (BAI), vessel diameter (VD) and vessel frequency (VF); and potential hydraulic performances (b, d, f): vessel conductivity-weight (D_{HP}), potential specific hydraulic conductivity (K_s) and ring conductivity (K_{ring}) of acclimated (green), understory suppressed (black, dotted lines) and understory released (yellow) saplings. The vertical dotted line shows the canopy release of released saplings in January 2005.

Saplings

In all saplings, BAI increased between 2004 and 2006, from an average of 0.121 to 0.273 cm², from 0.014 to 0.046 cm² and from 0.014 to 0.205 cm², in acclimated, suppressed and released saplings, respectively (Fig. 5.3a). Differences among treatments were statistically significant in all years (Table 5.5).

In 2004, average VD was 22.5 µm in all saplings (Fig. 5.3c). Acclimated and released saplings showed an increase in VD of up to 29.3 µm and 29.7 µm, respectively, in 2006, whereas VD remained stable in suppressed saplings and was significantly lower than in acclimated and released saplings (Table 5.5). In 2004, VF was higher in acclimated than in suppressed and released saplings. In 2005 and 2006, values were stable in suppressed saplings, and significantly decreased in released and acclimated saplings (Fig. 5.3e; Table 5.5). In 2006, released and acclimated saplings had 203 and 121 vessels mm^{-2}, respectively.

D_{HP} increased each year in acclimated (from 24.7 to 32.6 µm) and released (from 26.3 to 33.9 µm) saplings. Suppressed saplings showed stable D_{HP} of around 24.2 µm in all years (Fig. 5.3b; Table 5.5). K_s of acclimated saplings increased in 2005 (from 1.9 to 3.4 kg m^{-1} s^{-1} MPa^{-1}), whereas K_S of released saplings increased in 2006, the second growing season after release (6.5 kg m^{-1} s^{-1} MPa^{-1}) (Fig. 3d; Table 4). Similar to the other measured variables, suppressed saplings had very stable values of K_S (Fig. 5.3d). K_{ring} increased in all years in both acclimated and released saplings, up to 0.95 * 10^{-4} and 1.28 * 10^{-4} kg m s^{-1} MPa^{-1} respectively (Fig. 5.3f; Table 5.5), the result of increases in K_S and BAI.

In saplings, BAI contributed up to 45 % to variation in K_{ring}, whereas D_{HP} contributed up to 38 % and VF 8 %. The covariance between BAI and D_{HP} was 83 %, -36 % between D_{HP} and VF, and -38 % between BAI and VF (Table 5.3).

Table 5.5: Kruskal and Wallis test (p-value) for overall treatment effects (acclimated, understory released, understory suppressed) on xylem structural traits and hydraulic performances for saplings and for each year.

Year	**BAI**	**VD**	**VF**	**D_{HP}**	**K_s**	**K_{ring}**
2004	0.0238	n.s	0.0016	n.s	n.s	0.0458
2005	0.0231	0.0308	0.0073	0.0435	n.s	0.0373
2006	0.0210	0.0244	0.0073	0.0231	0.0373	0.0154

5.2.4. Discussion

Effect of tree position within the canopy on xylem traits in large trees

In large trees, xylem structure strongly differed between understory and overstory trees, except for wood density (Fig. 5.2). As expected, understory trees presented a xylem structure with smaller vessel diameter and higher vessel frequency than overstory trees (Hypothesis 1). Understory trees are simultaneously subjected to lower soil water supply (related to higher inter-tree competition and lower root biomass, Delagrange et al. 2004; Matjaž and Primož 2010) and to lower potential evapotranspiration (related to lower VPD, lower irradiance and lower leaf area, Barigah et al. 2006; Klopcic and Boncina 2010; Hajek et al. 2016) than overstory trees. Schuldt et al. (2016) reported that the reduction of water availability generated narrower vessels. In our case, tree water availability was limited by soil conditions and could have been one of the drivers of reduced xylem vessel size in understory trees.

The consequences of these anatomical differences coupled with stem diameter differences would be a lower potential for water transport through the annual ring in understory trees compared to overstory trees. As stated in previous studies (McCulloh *et al.*, 2010, 2015), a small stem diameter induces reduced potential specific conductivity and potential ring conductivity, although xylem structure adjustments that resulted in smaller D_{HP} (through vessel diameter and vessel frequency) also contributed. Furthermore, the differences in xylem anatomy of understory vs. overstory trees may be also related to the longer water path length from roots to canopies overstory trees (Preston *et al.*, 2006; Fan *et al.*, 2012).

As expected, the growth and wood traits displayed smaller inter-annual variations in understory than overstory trees (Hypothesis 2, Fig. 5.2). The largest differences between understory and overstory trees were observed in annual fluctuation in wood density, BAI and in K_{ring} which is strongly related to BAI. Through wood density adjustments, overstory trees may modulate their water transport capacity in regard to annual growth conditions (Stratton *et al.*, 2000; Anderegg & Meinzer, 2015). The relationship between BAI and wood density reflects hydraulic adjustments in many situations (Preston *et al.*, 2006), but it can also reflect developmental constraints, such as fast cambial growth involving shorter cell wall thickening stages (Cuny et al. (2012) on gymnosperms) that produce thinner cell walls, or thinner slowly growing stems that require mechanically stiffer and stronger wood (Lei *et al.*, 1997). Our finding of the relatively constant xylem structure and potential specific conductivity suggests that the understory trees, in their

less fluctuating environment, did not receive sufficient signals to adjust xylem structure from year to year (Fonti *et al.*, 2010) and/or the trees' reactions were constrained by a limited growth potential. In contrast, the larger overstory trees, in their more fluctuating environments, showed adjustments of their BAI and potential water transport ability each year.

Effects of canopy release on xylem traits of large trees

After understory trees are released, one would expect xylem adjustments reflecting the acclimation to the new environmental conditions. Contrary to our hypothesis, xylem structure and potential hydraulic conductivity of released understory trees approached but did not reach those of overstory trees, even six years after release (Hypothesis 3). Although potential tree-ring conductivity of released trees was far from that of overstory trees and was probably limited by tree size (Poorter *et al.*, 2010; Fan *et al.*, 2012), all xylem traits as well as basal area growth remained stable after two years. Changes that occurred during the first two years post-release were apparently sufficient to supply the main hydraulic demands for tree survival, although we are unable to conclude whether and to what extent hydraulic properties actually limited tree growth after release. It is difficult to discuss the dynamics and duration of the acclimation of hydraulic properties because existing studies focused in general on the initial few years after canopy release in saplings or branches (Maherali *et al.*, 1997; Hoffmann & Schweingruber, 2002; Lemoine *et al.*, 2002b; Gebauer *et al.*, 2014).

Observed increases in D_{HP} after canopy release may be related to a higher irradiance (Barigah *et al.*, 2006; Hacke, 2014) and wind movements in the foliage that increase the potential evapotranspiration: the wider vessels would support an increased demand while limiting the increase of tension in the xylem sap. However, an increase in D_{HP} was compensated for by lower vessel frequency, so that at the tissue scale, potential hydraulic conductivity (K_S) did not change. This observation may seem contradictory with large changes observed in the xylem anatomy of beech saplings after canopy release and may be related to differences in tree size, as discussed below.

Saplings vs large trees

Even if the relative change in K_{ring} after release was similar in saplings and in large trees, the contribution of K_s to K_{ring} release-induced changes was significant only in saplings (Hypothesis 4, Table 5.3). This indicates that the gain of sapwood area with same intrinsic property (K_S) may be sufficient to sustain the increased evaporative demand in large trees whereas saplings equally rely on adjustments in both the tissue quantity (BAI) and quality (especially D_{HP}). This difference in the nature of the transport adjustment in saplings and large trees may be partly explained by the difference in the relative contribution of one new growth ring in a species such as beech with its diffuse-porous wood and deep sapwood in which sap flow occurs throughout many growth rings (Granier *et al.*, 2000; Luttschwager & Remus, 2007; Dalsgaard *et al.*, 2011): the effect of one ring could be much greater in the sapling than the large tree.

Other potential factors could contribute to the observed differences between released large trees and saplings that include differences in water storage and release, relative change in water path length, and specific trajectories of xylem adjustments. Due to their size, large trees may have a greater reliance on water storage and conductivity of older rings (Phillips *et al.*, 2003) than saplings. This hypothesis is obviously only valid for species with wide sapwood area and cannot be generalized for species like oak, known particularly to rely on the last growth ring to ensure sap flow. In fact, Collet et al. (2001, 2011) reported a two-years-differed recovery of axial growth in saplings. As the radial growth rate increases, height increment relative to the total height could be larger in saplings than in large trees, increasing the water path length as well. Consequently, a relatively larger increase in D_{HP} could help saplings to partially offset this effect.

5.2.5. Conclusion

Large understory *Fagus sylvatica* trees display lower specific hydraulic conductivity and ring conductivity than overstory trees, despite their more stable growth environment. We suggest that these differences are driven by the larger hydraulic constraints of overstory trees because of their geometry (longer path lengths and higher canopies) and their growth environment (higher VPD and more light, leading to higher rates of transpiration). Overstory trees presented inter-annual fluctuations in growth, specific conductivity and wood density that could reflect continuous adjustments of their water transport capacity in response to their more fluctuating environments.

After canopy release by thinning, the xylem anatomy of the large understory trees was modified, stabilizing and approaching the trait values of the overstory trees without ever

reaching them. The opposing effects of increased vessel diameter and decreased vessel frequency on conductivity compensated for each other in that there was no significant change in potential specific conductivity after canopy release. The gain in radial growth was sufficient to significantly increase potential stem overall performance (ring conductivity) without modifying the potential specific conductivity. This result contrasts with the saplings, for which the increase in conductivity was equally due to radial growth and changes in potential specific hydraulic conductivity (which resulted mainly from an increase in hydraulic diameter). We suggest that this result is due to a dimensional effect, the relatively larger contribution to the potential water transport of a structure via a new growth increment added to a small vs. a large pre-existing structure. We emphasize that this result may be applicable only to species with considerable sapwood width that are known to use many growth rings for transport (e.g. not for ring-porous species). Further experiments on acclimation after canopy release in species with different wood types, sapwood widths, and radial sap flow patterns could yield interesting information on the role of xylem structure in tree hydraulic performance.

5.2.6. Supplementary data

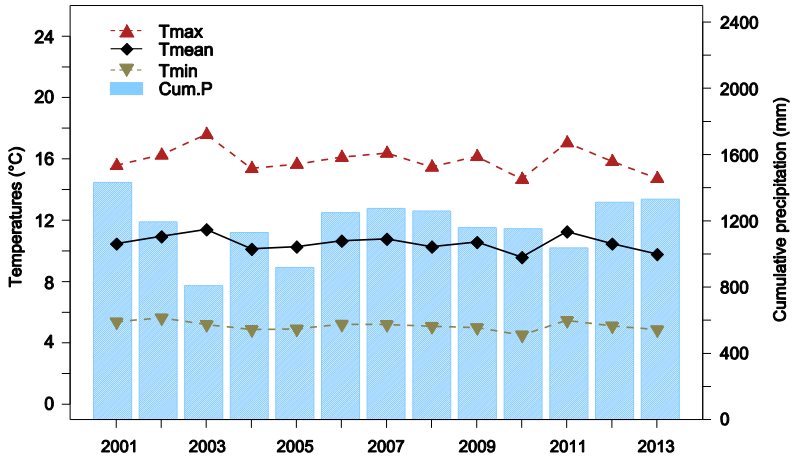

Online Resource 1: Mean (black), minimum (green, dotted line), and maximum (red, dotted line) temperatures and cumulative precipitation (blue bars) at Aillevillers-et-Lyaumont station, near the mature beech stand studied (data from 2001-2013).

5.2.7. Acknowledges

The authors thank Daniel Rittié (INRA, Nancy) for growth measurements, Maryline Harroué (INRA, Nancy) for her assistance in anatomy experimentations, Blandine Caquet for sapling data assessment and her external help and Mathieu Dassot (EcoSustain, Nancy) for his external help.

5.3. Contribution relative des traits structuraux sur la performance hydraulique potentielle du cerne

Afin de quantifier les effets observés dans la partie 5.2 : (i) du statut social, (ii) des variations annuelles et (iii) de la dynamique de réponse à l'ouverture de la canopée sur la stratégie adoptée par les individus, une décomposition de la variance plus précise a été réalisée. En raison du faible nombre d'années et du comportement non constant des semis acclimatés, les résultats sont axés exclusivement sur les grands arbres.

5.3.1. Contribution relative

La contribution relative de chaque paramètre est composée par l'effet du facteur (année, statut social ou ouverture) et par l'effet dû à la variabilité des arbres au sein du facteur décrit. De cette manière, nous obtenons une variance inter-facteur et une variance inter-facteur intra-arbre pour chaque paramètre. La somme des variances et covariances est égale à 100. Une adaptation de l'Eq. 5.5 de l'Article 4 est proposée :

$$Var(log_{10} K_{ring}) = Var_{fac}(4\ log_{10} D_{HP}) + Var_{fac}(log_{10} VF) + Var_{fac}(log_{10} BAI) + Var_{arbre}(4\ log_{10} D_{HP}) + Var_{arbre}(log_{10} VF) + Var_{arbre}(log_{10} BAI) + 2\ Cov_{fac}(4\ log_{10} D_{HP}, log_{10} BAI) + 2\ Cov_{fac}(4\ log_{10} D_{HP}, log_{10} VF) + 2\ Cov_{fac}(log_{10} VF, log_{10} BAI) + 2\ Cov_{arbre}(4\ log_{10} D_{HP}, log_{10} BAI) + 2\ Cov_{arbre}(4\ log_{10} D_{HP}, log_{10} VF) + 2\ Cov_{arbre}(log_{10} VF, log_{10} BAI) \quad (5.6)$$

Où Var_{fac} est la variance due au facteur et Var_{arbre} est la variance due à la variabilité entre les arbres au sein du facteur.

5.3.2. Variations annuelles

Le Tableau 5.6 présente les résultats obtenus pour chaque groupe d'arbre appartenant à un même statut social. Les arbres dominés ne comprennent que les individus non libérés et l'analyse a été conduite sur chaque groupe d'arbre séparément (arbres dominants, arbres dominés).

L'année a un plus fort impact sur la contribution relative de la croissance (BAI) à la variabilité de K_{ring} chez les grands arbres dominants que chez les arbres dominés. Au sein d'une même année, lorsque la croissance des arbres dominants augmente, le diamètre hydraulique (D_{HP}) diminue (covariance négative entre BAI et D_{HP}). La tendance inverse est observée chez les arbres dominés. Cependant, celle-ci n'est pas induite par le facteur année, mais par les individus au sein d'une même année.

La contribution relative totale liée à l'année est proche de la contribution relative liée aux individus au sein d'une même année. L'effet des individus est plus important chez les arbres dominés. Leurs traits liés aux vaisseaux (D_{HP} et VF) contribuent peu à la variabilité de K_{ring}.

Tableau 5.6: Effet de l'année et des arbres au sein d'une même année sur la contribution relative du diamètre hydraulique D_{HP}, de la fréquence des vaisseaux VF et la surface annuelle du cerne BAI sur la variabilité de K_{ring} pour les grands arbres dominants, dominés non libérés.

		BAI	D_{HP}	VF	BAI, D_{HP}	BAI, VF	D_{HP}, VF	Total
Arbres dominants	/ année	85.6	9.7	3.4	-24.6	-26.1	-1.3	46.8
	/ arbre	77.2	59.0	7.7	-62.7	0.3	-28.5	53.2
Arbres dominés	/ année	11.1	1.6	0.7	3.0	-4.0	-1.7	10.5
	/ arbre	56.1	48.4	14.4	40.1	-21.7	-47.8	89.5

5.3.3. Statut social

L'effet du statut social est analysé en comparant des arbres dominants aux arbres dominés non libérés (Fig. 5.4). La conductivité hydraulique du cerne plus élevée des arbres dominants par rapport aux arbres dominés est principalement induite par la croissance et ce, quelle que soit l'année analysée. La contribution relative de BAI est proche de 50% et la covariance entre BAI et D_{HP} se situe entre 25 et 40%. La contribution inter-arbre au sein d'un même statut est faible, quel que soit le trait étudié (Fig. 5.4b). La contribution totale due au statut social des arbres (courbe noire, Fig. 5.4a) atteint 75% de contribution relative tandis que la variabilité inter-arbre contribue au maximum à 25% (courbe noire, Fig. 5.4b).

5.3.4. Ouverture de la canopée

L'effet de l'ouverture de la canopée est étudié à partir des arbres dominés libérés et non libérés (Fig. 5.4c, d). Avant ouverture de la canopée, la variabilité de K_{ring} est exclusivement induite par la variabilité inter-arbre (courbe noire, Fig. 5.4c, d). Les principaux traits contribuant à ces résultats sont BAI et D_{HP}. La fréquence des vaisseaux (VF) participe peu à la variabilité de K_{ring} mais est fortement corrélée négativement à D_{HP} chez les grands arbres. Après ouverture, la contribution relative totale due au traitement peut atteindre les 80%.

Les contributions relatives de D_{HP} et de VF sont faibles, stables et identiques à celles d'avant traitement (Fig. 5.4c). La contribution relative de BAI augmente fortement les

deux premières années pilotant ainsi l'augmentation de K_{ring} observée dans l'Article 4. La covariance entre BAI et D_{HP} est d'environ 40% après l'ouverture.

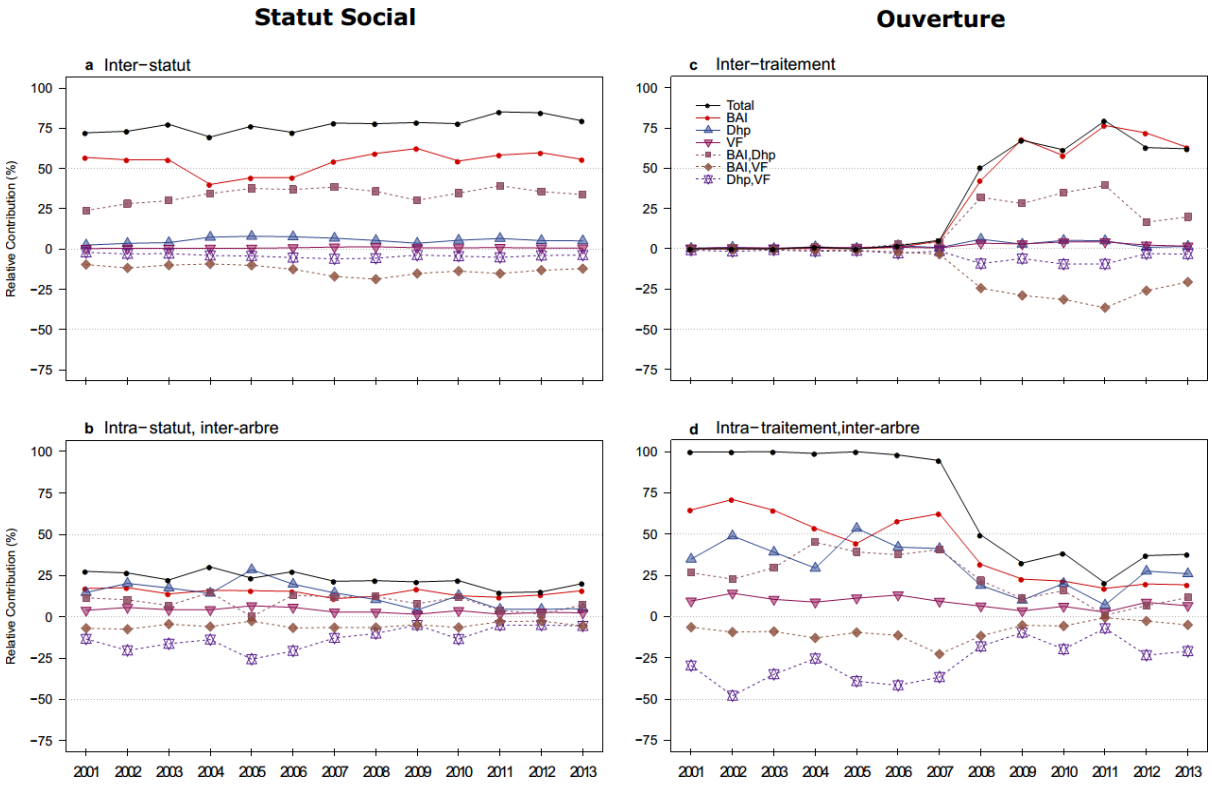

Figure 5.4: Effet du statut social (a et b) et de l'ouverture de la canopée (c et d) sur les contributions relatives de D_{HP}, VF et BAI à la variabilité de K_{ring}.

5.3.5. Discussion

Variations annuelles

Les variations des conditions de croissance entre les années induisent une plus grande variabilité de K_{ring} *via* la croissance chez les arbres dominants (Fig. 5.2a, g ; Tableau 5.6) confirmant ainsi les conclusions avancées dans l'Article 4.

Le peu d'impact des années sur les arbres dominés illustre l'effet « tampon » de la canopée sur le microclimat forestier. En examinant la variabilité intra-arbre au sein d'une même année nous observons que, même si le potentiel de croissance est faible, la contribution relative de ce trait est supérieure à celle du diamètre hydraulique. De plus, la corrélation positive entre ces deux traits nous indique que les arbres dominés qui présentent de plus grandes surfaces de cernes sont aussi ceux dont D_{HP} est le plus élevé suggérant ainsi que la taille initiale de la section n'est pas aussi importante que les conditions de croissance sur la capacité hydraulique potentielle des vaisseaux.

Impact de la vitesse de croissance sur les traits du bois de hêtre

Chez le hêtre, il a déjà été constaté qu'une augmentation de la vitesse de croissance induit des changements de structure du bois en évoluant d'une structure à pore diffus à une structure semi-poreuse (Fig. 5.1, Hoffmann and Schweingruber 2002). De plus, il a été démontré chez des sapins blancs que la vitesse de croissance mais aussi la longueur de la saison de croissance sont plus importantes chez les arbres dominants en comparaison avec des arbres dominés (Rathgeber *et al.*, 2011). La corrélation négative entre BAI et D_{HP} des arbres dominants pourrait donc refléter un changement de texture de cerne (ratio bois initial/bois final) induit par leur vitesse de croissance accrue.

De même, la Fig. 5.4a montre que la contribution relative de BAI est positive ainsi que la covariance entre BAI et D_{HP}, par contre la contribution relative de D_{HP} est faible. En d'autres termes, la variabilité des valeurs de D_{HP} entre les statuts est faible contrairement à celles de BAI. La corrélation positive entre BAI et D_{HP} est explicable par les valeurs plus élevées chez les arbres dominants de ces deux variables en comparaison avec les arbres dominés avec une plus grande différence de valeurs pour BAI entre les deux groupes d'arbres (Fig. 5.2). La principale source de la variabilité de K_{ring} entre les deux statuts est donc due à la différence de vitesse de croissance, i.e. BAI, entre les arbres dominants et dominés.

Chapitre 6 : Discussion générale et perspectives

Tableau 6.1 : Récapitulatif des résultats marquants.

	Perches sous couvert	Perches libérées
Allocation de la croissance	▸ Croissance axiale continue. ▸ Croissance radiale faible voire nulle.	▸ Allocation préférentielle vers la croissance radiale les premières années après ouverture.
Changement d'inclinaison des tiges entre 2007 et 2013	▸ Une partie des perches dominées maintiennent leur inclinaison à 2 m et à hauteur du centre de gravité de l'arbre. ▸ 6 perches s'affaissent.	▸ Maintien de l'inclinaison à 2 m et diminution de l'inclinaison à hauteur du centre de gravité de l'arbre en fonction de l'inclinaison initiale de la tige. ▸ 4 perches libérées s'affaissent.
Sécurité face au flambement (SB)	▸ Valeur faible causée par le fort élancement des tiges et leur faible diamètre.	▸ Augmentation de SB grâce à l'élancement des tiges mais inférieure à celle des arbres dominants. ▸ Diminution de l'élancement des tiges mais non stabilisé après 6 ans et inférieur aux arbres dominants.
Sécurité face au vent (SW)	▸ Valeurs proches de celles des arbres dominants.	▸ Augmentation de SW. ▸ Casse de 15 perches des 36 libérées initialement. ▸ Mauvaise estimation de la sécurité face au vent *via* les modèles allométriques.
Conductivité hydraulique potentielle du cerne (K_{ring})	▸ Faible valeur comparée aux arbres dominants due aux faibles valeurs de croissance radiale et aux plus petits diamètres des vaisseaux. ▸ Valeurs des traits mesurés à l'échelle du bois stable entre les années.	▸ Augmentation de K_{ring} due à la croissance radiale améliorée mais valeurs inférieures aux arbres dominants. ▸ Stabilisation des traits mesurés après 2 ans mais pas de modification de la conductivité hydraulique spécifique potentielle. ▸ Contributions des traits à K_{ring} identiques aux arbres dominants après 2 ans.

6.1. Rappel

L'objectif principal de ce travail était d'étudier la réponse des perches du hêtre à l'ouverture de la canopée et d'en décrire les dynamiques. Nous avons décidé d'aborder cette problématique dans une étude multidisciplinaire et multi-échelle. Les dynamiques de croissance radiale et axiale, d'anatomie et de traits biomécaniques ont été suivies pendant 6 ans après ouverture de la canopée. Chaque discipline a été traitée dans un chapitre indépendant. Le but de cette discussion est donc de faire le lien entre les différentes parties et de proposer des pistes pour les futures investigations entreprises.

6.2. Discussion générale

6.2.1. Comportement des perches dominées et libérées

Nos résultats suggèrent que la compétition pour la lumière est l'un des facteurs environnementaux déterminant l'allocation de la croissance des arbres sous couvert. Il en résulte des tiges très élancées avec une faible sécurité face au flambement (Article 3). Pour rester debout pendant leur course à la lumière, les perches doivent assurer le maintien de la posture de leurs axes et éviter l'augmentation de l'inclinaison de leur tige que pourrait générer un rajout de poids propre sur un axe incliné. De faibles accroissements radiaux produisent de petits moments de flexion qui sont contrebalancés par une production de bois de tension chez deux tiers des perches tandis qu'un tiers des perches s'affaissent (Article 2).

La conductivité hydraulique spécifique potentielle est significativement plus faible chez les arbres dominés en comparaison des dominants. Ceci est due d'une part à un BAI plus fort (en moyenne 70%) mais aussi aux vaisseaux de plus grand diamètre (7%) des arbres dominants (Article 4). Par ailleurs, la fluctuation interannuelle de la conductivité hydraulique spécifique potentielle est faible chez les perches dominées montrant qu'elles sont protégées par la canopée des fluctuations du climat (**chapitre 5**).

Sous le couvert, la compétition pour la lumière force les perches à prendre des risques mécaniques (contrôle postural insuffisant chez un tiers des perches, élancement important). En outre, l'anatomie des vaisseaux chez les perches dominées suggère un accès limité à l'eau.

Une fois libéré, la compétition pour la lumière n'est plus une contrainte. Par contre, l'arbre est exposé au vent. Sa morphologie développée sous couvert, c'est-à-dire protégée du vent, n'est pas adaptée à cette sollicitation. La casse du tronc des 15 perches sur les 36 libérées initialement lors de la deuxième année après ouverture suite à un épisode de vent fort montre clairement la présence de ce risque. Quant à la motricité des tiges, le redressement est observé surtout pour les perches avec une inclinaison initiale supérieure à 6° (Article 2). Les perches ayant une inclinaison inférieure à 6° avant ouverture ne montrent pas de redressement de leur tige même si la production de bois de tension couplée à la croissance en diamètre fortement augmentée pourrait largement assurer le redressement. Il est donc suggéré qu'une faible inclinaison pourrait être un atout pour capter la lumière, ce qui peut être bénéfique en cas de feuillage mal adapté aux nouvelles conditions de croissance (Niinemets, 2010).

L'étude de la conductivité hydraulique potentielle montre que le diamètre des vaisseaux des perches libérées reste largement inférieur à ceux des arbres dominants. Ce qui suggère que les perches libérées sont probablement limitées par leur taille. L'étude hydraulique n'est que partielle : le manque d'informations sur la sécurité du système hydraulique telle que la vulnérabilité à la cavitation ne permet pas d'identifier un risque hydraulique pour les perches après ouverture, ni de le comparer au risque biomécanique.

Lors d'une ouverture, les perches libérées tendent à changer leur priorité biomécanique : le risque biomécanique notamment vis-à-vis du vent semble être une priorité comparée au redressement des tiges pour les perches dont l'inclinaison est inférieure à 6°.

6.2.2. Dynamiques de réponses des perches libérées

Les informations sur les dynamiques de réponses ne sont pas largement répandues dans la littérature. La majorité des études se focalisent surtout sur les premières années d'ouverture (Bréda *et al.*, 1995; Caquet *et al.*, 2009) ou sur l'état des arbres après plusieurs années d'ouverture (Jaakkola *et al.*, 2005; Washusen *et al.*, 2005; Collet *et al.*, 2011; Keyser & Brown, 2014). Le manque de connaissances à cet égard ne permet pas de réflexions quant à la coordination de ces réponses entre elles, ni à la durée nécessaire pour une acclimatation complète. Le travail présent permet d'avancer quelques pistes.

L'analyse originale des accroissements axiaux nous a permis de voir que la croissance en hauteur est diminuée les premières années après ouverture de la canopée (Article 1). Ceci est probablement lié à un effet thigmomorphogénétique (Telewski, 2006). Son effet sur la croissance axiale perdure plus longtemps que sur la croissance radiale qui se stabilise au bout de 2 ans (Article 4). La stabilisation de la croissance radiale peut aussi être liée à une limitation de ressources ou de taille (Mencuccini *et al.*, 2005; Wiley & Helliker, 2012; Fichtner *et al.*, 2013;

Palacio *et al.*, 2014). L'effet thigmomorphogénétique permet aussi d'expliquer que la surface du houppier des perches libérées après 6 ans d'ouverture n'est pas significativement plus élevée que celle des perches dominées. La combinaison des deux dynamiques de croissance fait que l'élancement (ratio hauteur/diamètre) n'a pas atteint de stabilisation à la fin de la période de 6 ans (Article 3). Ces résultats concordent avec ceux de Mitchell (2000) qui montrent une acclimatation de l'élancement répartie sur plusieurs années après ouverture de la canopée mais l'étude séparée des dynamiques de croissance axiale et radiale permet de mieux l'expliquer.

Le rapport d'élancement est souvent utilisé comme un estimateur simple de la résistance au vent qui s'est avérée être un risque important chez les perches après une période d'ouverture. Il est aussi envisageable qu'une reprise de la croissance racinaire intervienne en réponse à l'ouverture (Delagrange *et al.*, 2004; Caquet *et al.*, 2009) pour améliorer l'ancrage de l'individu dans le sol et ce, dans le but d'améliorer la résistance au vent (Danjon *et al.*, 2005; Gardiner *et al.*, 2016). Comme aucun dommage par chablis n'a été observé, ce paramètre n'est pas étudié chez les perches. Cependant, il peut s'avérer très pertinent pour des arbres plus grands ou se développant dans des conditions de sol différentes.

En se concentrant sur les traits du bois liés aux performances hydrauliques, l'analyse de la variance apporte des précisions quant à l'état initial des perches dominées et à la mise en place des réponses par les perches libérées en phase de transition. Même si les valeurs absolues de ces traits restent significativement différentes (Fig. 5.2a, c, d, g), d'un point de vue contributif (contribution relative BAI et D_{HP}), les arbres libérés ont atteint le niveau des arbres dominants en 2 ans. Comme nous l'avons observé pour les performances biomécaniques, l'acclimatation est un processus multi-échelle (**chapitre 4**). La stabilisation des traits du bois liés aux performances hydrauliques peut aussi suggérer que le processus d'acclimatation hydraulique s'est axé à une autre échelle (feuilles, Han et al. 2006). En outre, atteindre les valeurs des arbres dominants n'est peut-être pas une priorité pour des arbres libérés qui ont été très contraints par le passé en termes de croissance.

Les processus d'acclimatation sont donc observés autant aux niveaux de la croissance et des traits biomécaniques et hydrauliques. Les perches libérées se redressent, augmentent leur sécurité biomécanique et les traits liés aux performances hydrauliques. Nous avons suggéré que les traits biomécaniques sont encore en plein ajustement après 6 ans d'ouverture tandis que la réponse en termes de performances hydrauliques à l'échelle du cerne est mise en place durant les 2 premières années après ouverture.

6.2.3. Impact de la taille sur les réponses des arbres à l'ouverture

Les résultats de l'Article 4 indiquent clairement que les propriétés du bois (conductivité hydraulique spécifique et densité du bois) ne sont pas affectées par l'ouverture de la canopée. Ces résultats restent surprenants par rapport à la littérature existante sur les semis (redressement (Coutand *et al.*, 2007; Alméras *et al.*, 2009), transport de la sève (Caquet *et al.*, 2009)). Comme détaillée dans le **chapitre 1**, l'évolution de la taille des arbres au cours de leur vie impacte leurs réponses au changement de conditions de croissance (Meinzer *et al.*, 2011) mais aussi aux contraintes mécaniques (Niklas, 2007) et hydrauliques rencontrées (Ryan & Yoder, 1997; Ryan *et al.*, 2006).

D'une part, modifier la forme des tiges d'un grand arbre est plus difficile que chez un semis. Ce fait peut expliquer pourquoi il n'est pas observé de modification de la distribution de la biomasse ou du défilement du tronc chez les perches libérées après 6 ans d'ouverture (Article 3). D'autre part, avec la plus grande inertie de la section des grands arbres, intensifier la production du bois de tension pour générer un mouvement de redressement serait moins efficace. Par ailleurs, la morphologie des perches (tortuosité et inclinaison) avant ouverture de la canopée induisent chez les tiges une grande quantité de bois de tension. Ceci explique le fait que la quantité et la qualité du bois de tension restent inchangées chez les grands arbres après ouverture de la canopée (Purba *et al.*, 2015). Cependant, malgré la difficulté de mise en place d'un processus de redressement chez les grands arbres, un redressement significatif est observé chez les arbres présentant une inclinaison initiale importante (Article 2). Pour ces arbres, un accroissement important de la biomasse sur un axe vertical pourrait représenter un risque biomécanique. L'acclimatation biomécanique des perches consiste donc en des ajustements de l'allocation de la croissance et non des propriétés matérielles.

Pareillement aux performances biomécaniques, chez les perches libérées, la conductivité hydraulique potentielle du cerne est gérée presque uniquement par l'augmentation de la quantité de tissu et non par la qualité (Article 4). La capacité de stockage de l'eau dans le tronc peut augmenter avec la taille de la section (Phillips *et al.*, 2003; Scholz *et al.*, 2011) permettant ainsi aux grands arbres de limiter les modifications des propriétés du tissu. Cela peut s'ajouter à une surface d'aubier plus importante chez les grands arbres (Dalsgaard *et al.*, 2011).

L'impact de la taille des individus dans les mécanismes des réponses à l'ouverture amène à reconsidérer les analyses se basant exclusivement sur les caractéristiques anatomiques ou matérielles du bois comme marqueur de l'ouverture de la canopée. L'approche intégrative a clairement démontré la nécessité d'inclure l'effet de la taille et de la forme dans l'étude de réponse à une ouverture et a permis de comprendre certaines divergences observées dans la littérature.

6.3. Perspectives

Comme nous l'avons démontré, les processus d'acclimatation sont répartis sur plusieurs échelles. Si les processus d'acclimatation diffèrent en fonction de la taille des arbres (**chapitres 4** et **5**), il est probable que la stratégie écologique ou encore la structure du bois (pores diffus *vs.* zone poreuse) impactent les dynamiques de réponses. Il serait donc intéressant d'élargir les données récoltées à d'autres espèces. Plusieurs thèmes de recherche peuvent être développés pour de futures investigations. Le travail fourni dans ce mémoire est surtout orienté vers l'acclimatation biomécanique comprenant aussi bien les traits de sécurité que de motricité moins étudiées jusqu'alors. Dans la suite de ce travail, il serait intéressant d'être capable de hiérarchiser les risques encourus (mécaniques et hydrauliques) après une ouverture de la canopée.

6.3.1. Evaluation des performances hydrauliques

Les performances hydrauliques à l'échelle individuelle n'ont pas été évaluées. Tout d'abord, l'efficacité du transport de l'eau peut être aussi estimée par la conductance foliaire spécifique, soit le taux de transpiration sur la surface foliaire totale (E / A_L). Sur de petits arbres, les mesures de transpiration sont facilement réalisables tandis que chez de grands arbres en conditions naturelles les artefacts de mesures peuvent être nombreux et de différentes natures suivant la méthode utilisée (Wullschleger *et al.*, 1998). De plus, il a été montré que chez les arbres feuillus des forêts tempérées, la transpiration est plus dépendante de la conductance stomatique des feuilles que des changements de VPD (Aranda *et al.*, 2012).

Il est néanmoins possible d'estimer l'efficacité de l'utilisation de l'eau en utilisant dans un premier temps la relation allométrique entre surface d'aubier et surface des feuilles. En perfectionnant les protocoles existants, les mesures de surface foliaire peuvent être accessibles par notamment l'utilisation de scanner TLS. Nous pouvons imaginer mettre en place un suivi annuel de l'architecture des arbres *via* la réalisation de plusieurs scans TLS des individus.

La surface d'aubier mais aussi le flux de sève peuvent être acquis *via* les sondes thermiques (Granier, 1985, 1987), avec plusieurs aiguilles sont placées à des profondeurs différentes dans le tronc. La densité de flux de sève est une méthode évaluant l'utilisation de l'eau en intégrant les ajustements de l'échelle de la feuille et les réponses du feuillage entier. Cette variable représente l'utilisation de l'eau à l'échelle de l'arbre entier. La profondeur de l'aubier diffère suivant le statut social d'un arbre (Granier *et al.*, 2000) et impacte la plasticité de l'architecture hydraulique en réponse aux modifications de l'environnement (Anderegg & Meinzer, 2015).

Dans un second temps, la détermination de la conductivité hydraulique spécifique foliaire apporterait des indications quant à la performance de la portion de tronc analysée dans le support du bois vis-à-vis de la demande hydraulique des feuilles en aval. Pour cela, il suffit de diviser la

conductivité hydraulique potentielle estimée à partir des coupes anatomiques par la surface foliaire.

6.3.2. Evaluer la sécurité hydraulique

La régulation du statut hydrique d'un arbre, peut s'effectuer par le contrôle stomatique, la vulnérabilité à la cavitation (bulles d'air dans le lumen des vaisseaux) et le ratio surface des racines / surface foliaire (Maseda & Fernandez, 2006). Le contrôle stomatique est essentiel pour réguler les pertes hydriques et la maintenance du statut hydrique de l'arbre (Aranda *et al.*, 2000). Une baisse de la conductance stomatique induit une baisse de tension de la sève réduisant ainsi le risque de rupture au sein de la colonne d'eau. Il serait donc intéressant d'établir un suivi annuel de la conductance stomatique. Ces données seraient très complémentaires des mesures de flux de sève réalisées à 1.30 m.

Les estimations de conductivité hydraulique spécifique effectuées peuvent fortement surestimer les valeurs réelles : par exemple, la présence de vaisseaux embolisés (présence de bulles d'air à l'intérieur des lumens des vaisseaux) induit une baisse de la conductivité. De plus, la paroi aux extrémités des vaisseaux ainsi que la présence de ponctuations impactent la conductivité hydraulique en modifiant la résistance du tissu au flux d'eau le traversant (Sperry *et al.*, 2006; Lens *et al.*, 2011). Ces deux traits sont aussi déterminants pour la sécurité du transport de l'eau au sein de la colonne d'eau (Hacke *et al.*, 2006)

Concernant la vulnérabilité à la cavitation, les études chez les semis ont montré que lors de la première année, ce trait augmente la première année puis retourne à son niveau pré-ouverture la deuxième année (Caquet *et al.*, 2009). Pour les branches, une augmentation de l'embolie native est aussi observée la première année après ouverture (Lemoine *et al.*, 2002b). La micro-tomographie à rayons X offre des possibilités pour l'acquisition de données sur la structure 3D de la section et aussi sur le taux d'embolie dans les vaisseaux fonctionnels (Choat *et al.*, 2016). Pour le moment, cette technique n'est appliquée qu'à de petites sections (5 mm de diamètre). Des développements seraient donc nécessaires. Les études concernant les relations structure-fonctions ont montré que les ponctuations et la longueur des vaisseaux sont les structures déterminant la vulnérabilité à la cavitation (Choat *et al.*, 2008). Ces données sont accessibles par la réalisation de coupes longitudinales et donc de manière rétrospective.

La biomasse, l'architecture et la physiologie des racines impactent les performances hydrauliques de l'arbre (Markesteijn & Poorter, 2009; Domec *et al.*, 2010; Comas *et al.*, 2013). La profondeur des racines indique la profondeur maximale à laquelle l'arbre peut accéder à l'eau et est la plus importante information fonctionnelle pour la tolérance à la sécheresse (Bréda *et al.*, 2006) et donc *in extenso* la sécurité hydraulique. Pour cela, la distribution verticale des racines fines a besoin d'être connue mais cette variable est l'une des plus difficiles à évaluer de manière fiable.

6.3.3. Améliorer l'estimation de la sécurité vis-à-vis du vent

Les traits de sécurité biomécanique ont été déterminés. Concernant le vent, le trait SW calculé estime le risque de casse de la tige sous l'action du vent ce qui est un des dommages possibles. Les modèles utilisés dans l'Article 3 se sont montré insuffisants pour estimer correctement la sécurité face à la casse. Des développements sont encore nécessaires. Une estimation de la charge due au vent peut être ajoutée au modèle. Pour cela il faut évaluer l'impact d'une ouverture sur les contraintes perçues par les perches dominées et libérées, mesurer le régime de déformation avant et après ouverture de la canopée serait une bonne piste (Bonnesoeur, 2016).

De plus, le déracinement est l'un des autres dommages possibles causé par le vent sur les arbres (Gardiner *et al.*, 2016). L'architecture et la biomasse racinaire sont donc des paramètres non négligeables face au déracinage et donc de la résistance vis-à-vis du vent.

Références

Alméras T, Clair B. **2016**. Critical review on the mechanisms of maturation stress generation in trees. *Journal of The Royal Society Interface* **13**: 20160550.

Alméras T, Derycke M, Jaouen G, Beauchêne J, Fournier M. **2009**. Functional diversity in gravitropic reaction among tropical seedlings in relation to ecological and developmental traits. *Journal of experimental botany* **60**: 4397–4410.

Alméras T, Fournier M. **2009**. Biomechanical design and long-term stability of trees: Morphological and wood traits involved in the balance between weight increase and the gravitropic reaction. *Journal of Theoretical Biology* **256**: 370–381.

Alméras T, Gril J, Yamamoto H. **2005a**. Modelling anisotropic maturation strains in wood in relation to fibre boundary conditions, microstructure and maturation kinetics. *Holzforschung* **59**: 347–353.

Alméras T, Thibaut A, Gril J. **2005b**. Effect of circumferential heterogeneity of wood maturation strain, modulus of elasticity and radial growth on the regulation of stem orientation in trees. *Trees - Structure and Function* **19**: 457–467.

Anderegg WRL, Meinzer FC. **2015**. Wood Anatomy and Plant Hydraulics in a Changing Climate. In: Hacke U, ed. Functional and Ecological Xylem Anatomy. Cham: Springer International Publishing, 235–253.

Aranda I, Forner A, Cuesta B, Valladares F. **2012**. Species-specific water use by forest tree species: From the tree to the stand. *Agricultural Water Management* **114**: 67–77.

Aranda I, Gil L, Pardos J a. 2000. Water relations and gas exchange in Fagus sylvatica L. and Quercus petraea (Mattuschka) Liebl. in a mixed stand at their southern limit of distribution in Europe. *Trees* **14**: 344–352.

Archer RR. **1987**. On the origin of growth stresses in trees. *Wood Science and Technology* **21**: 139–154.

Von Arx G, Graf Pannatier E, Thimonier A, Rebetez M. **2013**. Microclimate in forests with varying leaf area index and soil moisture: Potential implications for seedling establishment in a changing climate. *Journal of Ecology* **101**: 1201–1213.

Aussenac G. **2000**. Interactions between forest stands and microclimate: Ecophysiological aspects and consequences for silviculture. *Annals of Forest Science* **57**: 287–301.

Badel E, Ewers FW, Cochard H, Telewski FW. **2015**. Acclimation of mechanical and hydraulic functions in trees: impact of the thigmomorphogenetic process. *Frontiers in Plant Science* **6**: 266.

Barbacci A, Constant T, Farré E, Harroué M, Nepveu G. **2008**. Shiny beech wood is confirmed as an indicator of tension wood. *IAWA Journal* **29**: 35–46.

Barigah TS, Ibrahim T, Bogard A, Faivre-Vuillin B, Lagneau LA, Montpied P, Dreyer E. **2006**. Irradiance-induced plasticity in the hydraulic properties of saplings of different temperate broad-leaved forest tree species. *Tree physiology* **26**: 1505–16.

Becker P, Meinzer FC, Wullschleger SD. **2000**. Hydraulic limitation of tree height: A critique. *Functional Ecology* **14**: 4–11.

Becker P, Tyree MT, Tsuda M. **1999**. Hydraulic conductances of angiosperms versus conifers: similar transport sufficiency at the whole-plant level. *Tree physiology* **19**: 445–452.

Bellemare MF, Masaki T, Pepinsky TB. **2015**. Lagged Explanatory Variables and the Estimation of Causal Effects. *SSRN Electronic Journal*.

Bergander A, Salmén L. **2000**. Variations in transverse fibre wall properties: Relations between elastic properties and structure. *Holzforschung* **54**: 654–660.

Black BA, Abrams MD. **2003**. Use of boundary-line growth patterns as a basis for dendroecological release criteria. *Ecological Applications* **13**: 1733–1749.

Bloom AJ, Chapin SF, Mooney HA. **1985**. Resource limitation in plants - An economic analogy. *Annual Review of Ecology and Systematics* **16**: 363–392.

Bohlman S, O'Brien S. **2006**. Allometry, adult stature and regeneration requirement of 65 tree species on Barro Colorado Island, Panama. *Journal of Tropical Ecology* **22**: 123–136.

Boncina A, Kadunc A, Robic D. **2007**. Effects of selective thinning on growth and development of beech (Fagus sylvatica L.) forest stands in south-eastern Slovenia. *Annals of Forest Science* **64**: 47–57.

Bonnesoeur V. **2016**.Acclimatation des arbres forestiers au vent : de la perception du vent à ses conséquences sur la croissance et le dimensionnement des tiges. (Doctoral thesis).

Bontemps J-D, Herve J-C, Duplat P, Dhôte J-F. **2012**. Shifts in the height-related competitiveness of tree species following recent climate warming and implications for tree community composition: the case of common beech and sessile oak as predominant broadleaved species in Europe. *Oikos* **121**: 1287–1299.

Booker RE, Sell J. **1998**. The nanostructure of the cell wall of softwoods and its functions in a living tree. *European Journal of Wood and Wood Products* **56**: 1–8.

Brasseur F, De Sloover JR. **1976**. L'extinction du rayonnement dans les gammes spectrales bleu, rouge et rouge lointain. Comparaison de deux pleuplements forestiers de Haute Ardenne.

Bulletin de la Société Royale de Botanique de Belgique **109**: 319–334.

Bréda N, Granier A, Aussenac G. **1995**. Effects of thinning on soil and tree water relations, transpiration and growth in an oak forest (Quercus petraea (Matt.) Liebl.). *Tree Physiology* **15**: 295–306.

Bréda N, Huc R, Granier A, Dreyer E. **2006**. Temperate forest trees and stands under severe drought: a review of ecophysiological responses, adaptation processes and long-term consequences. *Annals of Forest Science* **63**: 625–644.

Brüchert F, Becker G, Speck T. **2000**. The mechanics of Norway spruce [Picea abies (L.) Karst]: mechanical properties of standing trees from different thinning regimes. *Forest Ecology and Management* **135**: 45–62.

Canham CD. **1988**. Growth and canopy architecture of shade-tolerant trees: response to canopy gaps. *Ecological Society of America* **69**: 786–795.

Canham CD. **1989**. Different responses to gaps among shade-tolerant tree species. *Ecology* **70**: 548–550.

Canham CD. **1990**. Suppression and release during canopy opening recruitment in Fagus grandifolia. *bulletin of the torrey botanical club* **117**: 1–7.

Caquet B. **2008**.Réactions de semis naturels de hêtre et d'érable sycomore à l'ouverture du couvert : croissance et ajustements fonctionnels (Doctoral thesis).

Caquet B, Barigah TS, Cochard H, Montpied P, Collet C, Dreyer E, Epron D. **2009**. Hydraulic properties of naturally regenerated beech saplings respond to canopy opening. *Tree physiology* **29**: 1395–405.

Caquet B, Montpied P, Dreyer E, Epron D, Collet C. **2010**. Response to canopy opening does not act as a filter to Fagus sylvatica and Acer sp. advance regeneration in a mixed temperate forest. *Annals of Forest Science* **67**: 105–105.

Chen J, Saunders SC, Crow TR, Naiman RJ, Brosofske KD, Mroz GD, Brookshire BL, Frankling JF. **1999**. Microclimate in forest ecosystem and landscape ecology. *BioScience* **49**: 288–297.

Choat B, Badel E, Burlett R, Delzon S, Cochard H, Jansen S. **2016**. Noninvasive Measurement of Vulnerability to Drought-Induced Embolism by X-Ray Microtomography. *Plant Physiology* **170**: 273–282.

Choat B, Cobb AR, Jansen S. **2008**. Structure and function of bordered pits: New discoveries and impacts on whole-plant hydraulic function. *New Phytologist* **177**: 608–626.

Clair B, Alteyrac J, Gronvold A, Espejo J, Chanson B, Alméras T. **2013**. Patterns of longitudinal and tangential maturation stresses in Eucalyptus nitens plantation trees. *Annals of Forest Science* **70**: 801–811.

Clair B, Ruelle J, Thibaut B. **2003**. Relationship between growth stresses, mechano-physical properties and proportion of fibres with gelatinous layer in chestnut (Castanea Sativa Mill.). *Holzforschung* **57**: 189–195.

Clark JS, Beckage B, Camill P, Cleveland B, Hillerislambers J, Lichter J, McLachlan J, Mohan J, Wyckoff P. **1999**. Interpreting recruitment limitation in forests. *American journal of botany* **86**: 1–16.

Colin F, Sanjines A, Fortin M, Bontemps J-D, Nicolini E. **2012**. Fagus sylvatica trunk epicormics in relation to primary and secondary growth. *Annals of botany* **110**: 995–1005.

Collet C, Fournier M, Ningre F, Hounzandji AP-I, Constant T. **2011**. Growth and posture control strategies in Fagus sylvatica and Acer pseudoplatanus saplings in response to canopy disturbance. *Annals of botany* **107**: 1345–53.

Collet C, Lanter O, Pardos M. **2001**. Effects of canopy opening on height and diameter growth in naturally regenerated beech seedlings. *Annals of Forest Science* **58**: 127–134.

Comas LH, Becker SR, Cruz VM V, Byrne PF, Dierig DA. **2013**. Root traits contributing to plant productivity under drought. *Frontiers in plant science* **4**: 442.

Constant T, Barbacci A, Nepveu G. **2006**. Analysis over a four years period after thinning of the trunk movement linked to the crown development of forty years old European Beech trees. In: 5th Plant Biomechanics Conference.

Coomes DA, Grubb PJ. **1998**. A comparison of 12 species of the Amazon caatinga using growth rates in gaps and understorey, and allometric relationships. *Journal of Ecology* **12**: 426–435.

Coutand C. **2010**. Mechanosensing and thigmomorphogenesis, a physiological and biomechanical point of view. *Plant Science* **179**: 168–182.

Coutand C, Fournier M, Moulia B. **2007**. The gravitropic response of poplar trunks: key roles of prestressed wood regulation and the relative kinetics of cambial growth versus wood maturation. *Plant physiology* **144**: 1166–80.

Cremer KW, Borough CJ, McKinnell FH, Carter PR. **1982**. Effects of stocking and thinning on wind damage in plantations. *New Zealand Journal of Forestry Science* **12**: 244–268.

Cuny HE, Rathgeber CBK, Lebourgeois F, Fortin M, Fournier M. **2012**. Life strategies in intra-annual dynamics of wood formation: Example of three conifer species in a temperate forest

in north-east France. *Tree Physiology* **32**: 612–625.

Curt T, Coll L, Prévosto B, Balandier P, Kunstler G. **2005**. Plasticity in growth, biomass allocation and root morphology in beech seedlings as induced by irradiance and herbaceous competition. *Annals of Forest Science* **62**: 51–60.

Dalsgaard L, Mikkelsen TN, Bastrup-Birk A. **2011**. Sap flow for beech (Fagus sylvatica L.) in a natural and a managed forest-effect of spatial heterogeneity. *Journal of Plant Ecology* **4**: 23–35.

Danjon F, Fourcaud T, Bert D. **2005**. Root architecture and wind- firmness of mature Pinus pinaster. *New Phytologist* **168**: 387–400.

Darwin C, Darwin F. **1880**. *The power of movement in plants* (J Murray, Ed.). London.

Dassot M, Constant T, Ningre F, Fournier M. **2015**. Impact of stand density on tree morphology and growth stresses in young beech (Fagus sylvatica L.) stands. *Trees - Structure and Function* **29**: 583–591.

Dassot M, Fournier M, Ningre F, Constant T. **2012**. Effect of tree size and competition on tension wood production over time in beech plantations and assessing relative gravitropic response with a biomechanical model. *American journal of botany* **99**: 1427–35.

Déjardin A, Laurans F, Arnaud D, Breton C, Pilate G, Leplé J-C. **2010**. Wood formation in Angiosperms. *Comptes rendus biologies* **333**: 325–34.

Delagrange S, Messier C, Lechowicz MJ, Dizengremel P. **2004**. Physiological, morphological and allocational plasticity in understory deciduous trees: importance of plant size and light availability. *Tree physiology* **24**: 775–784.

Diaci J, Kozjek L. **2005**. Beech sapling architecture following small and medium gap disturbances in silver fir-beech old-growth forests in Slovenia. *Schweizerische Zeitschrift fuer Forstwesen* **156**: 481–486.

Dittmar C, Zech W, Elling W. **2003**. Growth variations of Common beech (Fagus sylvatica L.) under different climatic and environmental conditions in Europe — a dendroecological study. *Forest Ecology and Management* **173**: 63–78.

Dixon H, Joly J. **1894**. On the ascent of sap. *Philosophical Transactions of the Royal Society of London B: Biological Sciences* **186**: 563–576.

Dobbertin M. **2005**. Tree growth as indicator of tree vitality and of tree reaction to environmental stress: A review. *European Journal of Forest Research* **124**: 319–333.

Domec JC, Gartner BL. **2002**. Age- and position-related changes in hydraulic versus

mechanical dysfunction of xylem: inferring the design criteria for Douglas-fir wood structure. *Tree physiology* **22**: 91–104.

Domec JC, Schäfer K, Oren R, Kim HS, McCarthy HR. **2010**. Variable conductivity and embolism in roots and branches of four contrasting tree species and their impacts on whole-plant hydraulic performance under future atmospheric CO2 concentration. *Tree Physiology* **30**: 1001–1015.

Eilmann B, Sterck F, Wegner L, De Vries SMG, Von Arx G, Mohren GMJ, Den Ouden J, Sass-Klaassen U. **2014**. Wood structural differences between northern and southern beech provenances growing at a moderate site. *Tree Physiology* **34**: 882–893.

Emborg J. **2007**. Suppression and Release during Canopy Recruitment in Fagus sylvatica and Fraxinus excelsior, a Dendro-Ecological Study of Natural Growth Patterns and Competition. *Ecological Bulletins* **52**: 53–67.

Enquist BJ. **2002**. Universal scaling in tree and vascular plant allometry: toward a general quantitative theory linking plant form and function from cells to ecosystems. *Tree physiology* **22**: 1045–1064.

Evert RF. **2006**. Xylem: Cell Types and Developmental Aspects. In: Esau's Plant Anatomy. Hoboken, NJ, USA: John Wiley & Sons, Inc., 255–290.

Fajardo A. **2016**. Wood density is a poor predictor of competitive ability among individuals of the same species. *Forest Ecology and Management* **372**: 217–225.

Fan ZX, Zhang SB, Hao GY, Ferry Slik JW, Cao KF. **2012**. Hydraulic conductivity traits predict growth rates and adult stature of 40 Asian tropical tree species better than wood density. *Journal of Ecology* **100**: 732–741.

Fang C-H, Guibal D, Clair B, Gril J, Liu Y-M, Liu S-Q. **2008**. Relationships between growth stress and wood properties in poplar I-69 (Populus deltoides Bartr . cv . ' Lux ' ex I-69 / 55). *Annals of Forest Science* **65**: 307.

Fichtner A, Sturm K, Rickert C, von Oheimb G, Härdtle W. **2013**. Crown size-growth relationships of European beech (Fagus sylvatica L.) are driven by the interplay of disturbance intensity and inter-specific competition. *Forest Ecology and Management* **302**: 178–184.

Fisher JB, Marler TE. **2006**. Eccentric growth but no compression wood in a horizontal stem of Cycas micronesica (Cycadales). *IAWA Journal* **27**: 377–382.

Fontaine F, Chaar H, Colin F, Clément C, Burrus M, Druelle J-L. **1999**. Preformation and neoformation of growth units on 3-year-old seedlings of *Quercus petraea*. *Canadian Journal of Botany* **77**: 1623–1631.

Fonti P, Von Arx G, García-González I, Eilmann B, Sass-Klaassen U, Gärtner H, Eckstein D. **2010**. Studying global change through investigation of the plastic responses of xylem anatomy in tree rings. *New Phytologist* **185**: 42–53.

Fournier M, Chanson B, Thibaut B, Guitard D. **1994**. Mesures des déformations résiduelles de croissance à la surface des arbres, en relation avec leur morphologie. Observations sur différentes espèces. *Annales des sciences forestières* **51**: 249–266.

Fournier M, Dlouha J, Jaouen G, Almeras T. **2013**. Integrative biomechanics for tree ecology: beyond wood density and strength. *Journal of Experimental Botany* **64**: 4793–4815.

Franceschini T, Martin-Ducup O, Schneider R. **2016**. Allometric exponents as a tool to study the influence of climate on the trade-off between primary and secondary growth in major north-eastern American tree species. *Annals of Botany* **117**: 551–563.

Franceschini T, Schneider R. **2014**. Influence of shade tolerance and development stage on the allometry of ten temperate tree species. *Oecologia* **176**: 739–749.

De Frenne P, Rodríguez-Sánchez F, Coomes DA, Baeten L, Verstraeten G, Vellend M, Bernhardt-Römermann M, Brown CD, Brunet J, Cornelis J, *et al.* 2013. Microclimate moderates plant responses to macroclimate warming. *Pnas* **110**: 18561–5.

Fritts HC, Swetnam TW. **1989**. Dendroecology: A Tool for Evaulating Variations in Past and Present Forest Environments. *Advances in Ecological Research Vol. 19*: 111–188.

Galvan JD, Camarero JJ, Sangüesa-Barreda G, Alla AQ, Gutiérrez E. **2012**. Sapwood area drives growth in mountain conifer forests. *Journal of Ecology* **100**: 1233–1244.

Gamblin B. **2013**. Dossier EMERGE dendrométrie. *Rendez-vous techniques ONF* **39**–**40**: 1–88.

Gardiner B, Barnett J, Saranpää P, Gril J. **2014**. *The Biology of Reaction Wood* (B Gardiner, J Barnett, P Saranpää, and J Gril, Eds.). Berlin, Heidelberg: Springer Berlin Heidelberg.

Gardiner B, Berry P, Moulia B. **2016**. Review: Wind impacts on plant growth, mechanics and damage. *Plant Science* **245**: 94–118.

Gartner BL. **1991**. Stem hydraulic properties of vines vs. shrubs of western poison oak, Toxicodendron diversilobum. *Oecologia* **87**: 180–189.

Gasson P. **1985**. Automatic measurement of vessel lumen area and diameter with particular reference to pedunculate oak and common beech. *IAWA Bulletin* **6**: 219–237.

Gebauer R, Volařík D, Urban J, Børja I, Nagy NE, Eldhuset TD, Krokene P. **2014**. Altered light conditions following thinning affect xylem structure and potential hydraulic conductivity of Norway spruce shoots. *European Journal of Forest Research* **133**: 111–120.

Genet a., Wernsdörfer H, Jonard M, Pretzsch H, Rauch M, Ponette Q, Nys C, Legout a., Ranger J, Vallet P, *et al.* 2011. Ontogeny partly explains the apparent heterogeneity of published biomass equations for Fagus sylvatica in central Europe. *Forest Ecology and Management* **261**: 1188–1202.

Granier A. 1985. Une nouvelle méthode pour la mesure du flux de sève brute dans le tronc des arbres. *Annales Des Sciences Forestieres* **42**: 193–200.

Granier A. 1987. Mesure du flux de sève brute dans le tronc du Douglas par une nouvelle méthode thermique. *Annales Des Sciences Forestieres* **44**: 1–14.

Granier a, Anfodillo T, Sabatti M, Cochard H, Dreyer E, Tomasi M, Valentini R, Bréda N. 1994. Axial and radial water flow in the trunks of oak trees: a quantitative and qualitative analysis. *Tree physiology* **14**: 1383–96.

Granier A, Biron P, Lemoine D. 2000. Water balance, transpiration and canopy conductance in two beech stands. *Agricultural and Forest Meteorology* **100**: 291–308.

Grattapaglia D, Plomion C, Kirst M, Sederoff RR. 2009. Genomics of growth traits in forest trees. *Current Opinion in Plant Biology* **12**: 148–156.

Grime JP. 1977. Evidence of the existence of three primary strategies in plants and its relevance to ecological and evolutionary theory. *The American Naturalist* **111**: 1169–1194.

Grundmann BM, Bonn S, Roloff A. 2008. Cross-dating of highly sensitive Common beech (Fagus sylvatica L.) tree-ring series with numerous missing rings. *Dendrochronologia* **26**: 109–113.

Guitard D, Fournier M. 1994. Comportement mécanique du bois - Le bois, matériau d'ingénierie -Textes rassemblés par Philippe Jodin - AR BO.

Hacke UG. 2014. Irradiance-induced changes in hydraulic architecture. *Botany* **92**: 437–442.

Hacke UG. 2015. *Functional and ecological xylem anatomy* (UG Hacke, Ed.). Springer.

Hacke UG, Sperry JS. 2001. Functional and ecological xylem anatomy. *Perspectives in Plant Ecology, Evolution and Systematics* **4**: 97–115.

Hacke UG, Sperry JS, Wheeler JK, Castro L. 2006. Scaling of angiosperm xylem structure with safety and efficiency. *Tree physiology* **26**: 689–701.

Hacke UG, Spicer R, Schreiber SG, Plavcov? L. 2017. An ecophysiological and developmental perspective on variation in vessel diameter. *Plant, Cell & Environment* **40**: 831–845.

Hajek P, Kurjak D, von W?hlisch G, Delzon S, Schuldt B. 2016. Intraspecific Variation in

Wood Anatomical, Hydraulic, and Foliar Traits in Ten European Beech Provenances Differing in Growth Yield. *Frontiers in Plant Science* **7**: 1–14.

Hamant O, Moulia B. **2016**. How do plants read their own shapes? *New Phytologist* **212**: 333–337.

Hamilton JR, Thomas CK, Carvell KL. **1985**. Tension Wood Formation Following Release of Upland Oak Advance Reproduction. *Wood and Fiber Science* **17**: 382–390.

Han Q, Araki M, Chiba Y. **2006**. Acclimation to irradiance of leaf photosynthesis and associated nitrogen reallocation in photosynthetic apparatus in the year following thinning of a young stand of Chamaecyparis obtusa. *Photosynthetica* **44**: 523–529.

Hart JL, Austin D a., van de Gevel SL. **2010**. Radial Growth Responses of Three Co-Occurring Species to Small Canopy Disturbances in a Secondary Hardwood Forest on the Cumberland Plateau, Tennessee. *Physical Geography* **31**: 270–291.

Hart JL, Buchanan ML, Clark SL, Torreano SJ. **2012**. Canopy accession strategies and climate-growth relationships in Acer rubrum. *Forest Ecology and Management* **282**: 124–132.

Hartmann H, Messier C. **2011**. Interannual variation in competitive interactions from natural and anthropogenic disturbances in a temperate forest tree species: Implications for ecological interpretation. *Forest Ecology and Management* **261**: 1936–1944.

Hoffmann S, Schweingruber FH. **2002**. Light shortage as a modifying factor for growth dynamics and wood anatomy in young deciduous trees. *IAWA Journal* **23**: 121–141.

Huang YS, Hung LF, Kuo-Huang LL. **2010**. Biomechanical modeling of gravitropic response of branches: Roles of asymmetric periphery growth strain versus self-weight bending effect. *Trees - Structure and Function* **24**: 1151–1161.

Hung LF, Tsai CC, Chen SJ, Huang YS, Kuo-Huang LL. **2016**. Study of tension wood in the artificially inclined seedlings of Koelreuteria henryi Dummer and its biomechanical function of negative gravitropism. *Trees - Structure and Function* **30**: 609–625.

Ishii R, Higashi M. **1997**. Tree coexistence on a slope: an adaptive significance of trunk inclination. *Proceedings of the Royal Society B: Biological Sciences* **264**: 133–139.

IUSS Working Group WRB. **2014**. *World reference base for soil resources 2014. International soil classification system for naming soils and creating legends for soil maps*.

Jaakkola T, Makinen H, Saranpaa P. **2005**. Wood density in Norway spruce: changes with thinning intensity and tree age. *Canadian Journal of Forest Research-Revue Canadienne De Recherche Forestiere* **35**: 1767–1778.

Jaouen G, Alméras T, Coutand C, Fournier M. **2007**. How to determine sapling buckling risk with only a few measurements. *American journal of botany* **94**: 1583–1593.

Jourez B. **1996**. Le Bois de tension 1. Définition et distribution dans l'arbre. *Biotechnol. Agron. Soc. Environ.* **1**: 100–112.

Jullien D, Widmann R, Loup C, Thibaut B. **2013**. Relationship between tree morphology and growth stress in mature European beech stands. *Annals of Forest Science* **70**: 133–142.

Keyser TL, Brown PM. **2014**. Long-term response of yellow-poplar to thinning in the southern Appalachian Mountains. *Forest Ecology and Management* **312**: 148–153.

King DA. **1990**. The adatptive significance of tree height. *The American Naturalist* **135**: 809–828.

King D a. **1991**. Tree allometry, leaf size and adult tree size in old-growth forests of western Oregon. *Tree physiology* **9**: 369–81.

Kint V, Hein S, Campioli M, Muys B. **2010**. Modelling self-pruning and branch attributes for young Quercus robur L. and Fagus sylvatica L. trees. *Forest Ecology and Management* **260**: 2023–2034.

Klopcic M, Boncina A. **2010**. Patterns of tree growth in a single tree selection silver fir–European beech forest. *Journal of Forest Research* **15**: 21–30.

Kubler H. **1988**. Silvicultural control of mechanical stresses in trees. *Can J For Res* **18**: 1215–1225.

Kuprevicius A, Auty D, Achim A, Caspersen JP. **2013**. Quantifying the influence of live crown ratio on the mechanical properties of clear wood. *Forestry* **86**: 361–369.

Lachenbruch B, Mcculloh K a. **2014**. Traits, properties, and performance: how woody plants combine hydraulic and mechanical functions in a cell, tissue, or whole plant. *International journal of pharmaceutics*: 747–764.

Latif ZA, Blackburn GA. **2010**. The effects of gap size on some microclimate variables during late summer and autumn in a temperate broadleaved deciduous forest. *International Journal of Biometeorology* **54**: 119–129.

Latte N, Lebourgeois F, Claessens H. **2016**. Growth partitioning within beech trees (Fagus sylvatica L.) varies in response to summer heat waves and related droughts. *Trees - Structure and Function* **30**: 189–201.

Lebourgeois F, Bréda N, Ulrich E, Granier A. **2005**. Climate-tree-growth relationships of European beech (Fagus sylvatica L.) in the French Permanent Plot Network (RENECOFOR).

Trees - Structure and Function **19**: 385–401.

Lei H, Gartner BL, Milota MR. **1997**. Effect of growth rate on the anatomy, specific gravity, and bending properties of wood from 7-year-old red alder (Alnus rubra). *Canadian Journal of Forest Research* **27**: 80–85.

Lemoine D, Cochard H, Granier A. **2002a**. Within crown variation in hydraulic architecture in beech (Fagus sylvatica L): evidence for a stomatal control of xylem embolism. *Annals of Forest Science* **59**: 19–27.

Lemoine D, Jacquemin S, Granier A. **2002b**. Beech (Fagus sylvatica L .) branches show acclimation of xylem anatomy and hydraulic properties to increased light after thinning. *Annals of Forest Science* **59**: 761–766.

Lens F, Sperry JS, Christman MA, Choat B, Rabaey D, Jansen S. **2011**. Testing hypotheses that link wood anatomy to cavitation resistance and hydraulic conductivity in the genus Acer. *New Phytologist* **190**: 709–723.

Lines ER, Zavala M a., Purves DW, Coomes D a. 2012. Predictable changes in aboveground allometry of trees along gradients of temperature, aridity and competition. *Global Ecology and Biogeography* **21**: 1017–1028.

Löf M, Bolte A, Welander NT. **2005**. Interacting effects of irradiance and water stress on dry weight and biomass partitioning in *Fagus sylvatica* seedlings. *Scandinavian Journal of Forest Research* **20**: 322–328.

Luttschwager D, Remus R. **2007**. Radial distribution of sap flux density in trunks of a mature beech stand. *Annals of Forest Science* **64**: 431–438.

Ma S, Concilio A, Oakley B, North M, Chen J. **2010**. Spatial variability in microclimate in a mixed-conifer forest before and after thinning and burning treatments. *Forest Ecology and Management* **259**: 904–915.

van der Maaten E. **2013**. Thinning prolongs growth duration of European beech (Fagus sylvatica L.) across a valley in southwestern Germany. *Forest Ecology and Management* **306**: 135–141.

Maherali H, DeLucia EH, Sipe TW. **1997**. Hydraulic adjustment of maple saplings to canopy gap formation. *Oecologia* **112**: 472–480.

Markesteijn L, Poorter L. **2009**. Seedling root morphology and biomass allocation of 62 tropical tree species in relation to drought- and shade-tolerance. *Journal of Ecology* **97**: 311–325.

Maseda PH, Fernandez RJ. **2006**. Stay wet or else: three ways in which plants can adjust

hydraulically to their environment. *Journal of Experimental Botany* **57**: 3963–3977.

Matjaž Č, Primož S. **2010**. Root distribution of under-planted European beech (Fagus sylvatica L.) below the canopy of a mature Norway spruce stand as a function of light. *European Journal of Forest Research* **129**: 531–539.

Matsuzaki J, Masumori M, Tange T. **2007**. Phototropic bending of non-elongating and radially growing woody stems results from asymmetrical xylem formation. *Plant, Cell and Environment* **30**: 646–653.

McCulloh KA, Johnson DM, Petitmermet J, McNellis B, Meinzer FC, Lachenbruch B. **2015**. A comparison of hydraulic architecture in three similarly sized woody species differing in their maximum potential height. *Tree Physiology* **35**: 723–731.

McCulloh K, Sperry JS, Lachenbruch B, Meinzer FC, Reich PB, Voelker S. **2010**. Moving water well: comparing hydraulic efficiency in twigs and trunks of coniferous, ring-porous, and diffuse-porous saplings from temperate and tropical forests. *New Phytologist* **186**: 439–450.

McLean JP, Zhang T, Bardet S, Beauchêne J, Thibaut A, Clair B, Thibaut B. **2011**. The decreasing radial wood stiffness pattern of some tropical trees growing in the primary forest is reversed and increases when they are grown in a plantation. *Annals of Forest Science* **68**: 681–688.

Medhurst J, Downes G, Ottenschlaeger M, Harwood C, Evans R, Beadle C. **2012**. Intra-specific competition and the radial development of wood density, microfibril angle and modulus of elasticity in plantation-grown Eucalyptus nitens. *Trees* **26**: 1771–1780.

Meinzer FC, Lachenbruch B, Dawson TE. **2011**. *Size- and Age-Related Changes in Tree Structure and Function* (FC Meinzer, B Lachenbruch, and TE Dawson, Eds.). Dordrecht: Springer Netherlands.

Mencuccini M. **2002**. Hydraulic constraints in the functional scaling of trees. *Tree physiology* **22**: 553–565.

Mencuccini M, Martínez-Vilalta J, Vanderklein D, Hamid HA, Korakaki E, Lee S, Michiels B. **2005**. Size-mediated ageing reduces vigour in trees. *Ecology Letters* **8**: 1183–1190.

Mérian P, Lebourgeois F. **2011**. Size-mediated climate-growth relationships in temperate forests: A multi-species analysis. *Forest Ecology and Management* **261**: 1382–1391.

Messier C, Nikinmaa E. **2000**. Effects of light availability and sapling size on the growth, biomass allocation, and crown morphology of understory sugar maple, yellow birch, and beech. *Ecoscience* **7**: 345–356.

Mitchell SJ. **2000**. Stem growth responses in Douglas-fir and Sitka spruce following thinning: implications for assessing wind-firmness. *Forest Ecology and Management* **135**: 105–114.

Miyashima S, Sebastian J, Lee J-Y, Helariutta Y. **2013**. Stem cell function during plant vascular development. *The EMBO journal* **32**: 178–93.

Motallebi A, Kangur A. **2016**. Are allometric relationships between tree height and diameter dependent on environmental conditions and management? *Trees - Structure and Function* **30**: 1429–1443.

Mothe F, Duchanois G, Zannier B, Leban J-M. **1998**. Analyse microdensitométrique appliquée au bois: méthode de traitement des données utilisée à l'INRA-ERQB (progamme Cerd). *Annals of Forest Science* **55**: 301–313.

Moulia B, Coutand C, Lenne C. **2006**. Posture control and skeletal mechanical acclimation in terrestrial plants: implications for mechanical modeling of plant architecture. *American Journal of Botany* **93**: 1477–1489.

Moulia B, Fournier M. **2009**. The power and control of gravitropic movements in plants: a biomechanical and systems biology view. *Journal of experimental botany* **60**: 461–86.

Myburg AA, Lev-Yadun S, Sederoff RR. **2013**. Xylem Structure and Function. In: eLS. Chichester, UK: John Wiley & Sons, Ltd, 1–9.

Nagel TA, Levanic T, Diaci J. **2007**. A dendroecological reconstruction of disturbance in an old-growth Fagus-Abies forest in Slovenia. *Annals of Forest Science* **64**: 891–897.

Nicholas NS, Gregoire TG, Zedaker SM. **1991**. The reliability of tree crown position classification. *Canadian Journal of Forest Research* **21**: 698–701.

Nicolini E, Chanson B, Bonne F. **2001**. Stem Growth and Epicormic Branch Formation in Understorey Beech Trees (Fagus sylvatica L.). *Annals of Botany* **87**: 737–750.

Niinemets Ü. **2010**. A review of light interception in plant stands from leaf to canopy in different plant functional types and in species with varying shade tolerance. *Ecological Research* **25**: 693–714.

Niklas KJ. **2002**. Wind , Size , and Tree Safety. *Journal of Arboriculture*: 84–93.

Niklas KJ. **2007**. Maximum plant height and the biophysical factors that limit it. *Tree physiology* **27**: 433–440.

Ningre F, Cordonnier T, Piboule A. **2011**. Typologie et réactivité des perches de hêtre en forêt hétérogène. *Forêt Wallonne* **111**: 16–25.

Nowacki GJ, Abrams MD. **1997**. Radial-growth averaging criteria for reconstructing

disturbance histories from presettlement-origin oaks. *Ecological Monographs* **67**: 225–249.

Noyer E, Lachenbruch B, Dlouh? J, Collet C, Ruelle J, Ningre F, Fournier M. **2017**. Xylem traits in European beech (Fagus sylvatica L.) display a large plasticity in response to canopy release. *Annals of Forest Science* **74**: 46.

Palacio S, Hoch G, Sala A, Körner C, Millard P. **2014**. Does carbon storage limit tree growth? *New Phytologist* **201**: 1096–1100.

Parker GG, Lowman MD, Nadkarni NM. **1995**. Structure and microclimate of forest canopies. In: Forest Canopies. 73–106.

Peltola HM. **2006**. Mechanical stability of trees under static loads. *American Journal of Botany* **93**: 1501–1511.

Petritan AM, von Lupke B, Petritan IC. **2009**. Influence of light availability on growth, leaf morphology and plant architecture of beech (Fagus sylvatica L.), maple (Acer pseudoplatanus L.) and ash (Fraxinus excelsior L.) saplings. *European Journal of Forest Research* **128**: 61–74.

Phillips NG, Ryan MG, Bond BJ, McDowell NG, Hinckley TM, Cermák J. **2003**. Reliance on stored water increases with tree size in three species in the Pacific Northwest. *Tree physiology* **23**: 237–245.

Pinheiro JC, Bates DM. **2000**. *Mixed-effects models in S and S-plus*.

Pinheiro MP, de Oliveira Filho JA, França S, Amorim AM, Mielke MS. **2013**. Annual variation in canopy openess, air temperature and humidity in the understory of three forested sites in southern Bahia state, Brazil. *Ciência Florestal* **23**: 107–116.

Plauborg KU. **2004**. Analysis of radial growth responses to changes in stand density for four tree species. *Forest Ecology and Management* **188**: 65–75.

Plomion C, Leprovost G, Stokes A. **2001**. Wood Formation in Trees. *PLANT PHYSIOLOGY* **127**: 1513–1523.

Polge H. **1981**. Influence des éclaircies sur les contraintes de croissance du hêtre. *Annals of Forest Science* **38**: 407–423.

Poorter L, McDonald I, Alarcón A, Fichtler E, Licona J-C, Peña-Claros M, Sterck F, Villegas Z, Sass-Klaassen U. **2010**. The importance of wood traits and hydraulic conductance for the performance and life history strategies of 42 rainforest tree species. *The New phytologist* **185**: 481–92.

Poorter H, Niklas KJ, Reich PB, Oleksyn J, Poot P, Mommer L. **2011**. Biomass allocation to leaves, stems and roots: meta-analysis of interspecific variation and environmental control.

New Phytologist **193**: 30–50.

Preston KA, Cornwell WK, DeNoyer JL. **2006**. Wood density and vessel traits as distinct correlates of ecological strategy in 51 California coast range angiosperms. *New Phytologist* **170**: 807–818.

Pretzsch H. **2010**. *Forest Dynamics, Growth and Yield*. Berlin, Heidelberg: Springer Berlin Heidelberg.

Pretzsch H, Dauber E, Biber P. **2013**. Species-Specific and Ontogeny-Related Stem Allometry of European Forest Trees: Evidence from Extensive Stem Analyses. *Forest Science* **59**: 290–302.

Pruyn ML, Ewers III BJ, Telewski FW. **2000**. Thigmomorphogenesis: changes in the morphology and mechanical properties of two Populus hybrids in response to mechanical perturbation. *Tree physiology* **20**: 535–540.

Purba CYC, Noyer E, Ruelle J, Dlouhá J, Karlinasari L, Fournier M. **2015**. Growth stresses in old beech poles after thinning: distribution and relation with wood anatomy. *Journal of the Indian Academy of Wood Science* **12**: 37–43.

R Core Team. **2015**. R: A language and environment for statistical computing. *R Foundation for Statistical Computing*.

Rambo TR, North MP. **2009**. Canopy microclimate response to pattern and density of thinning in a Sierra Nevada forest. *Forest Ecology and Management* **257**: 435–442.

Rathgeber CBK, Rossi S, Bontemps JD. **2011**. Cambial activity related to tree size in a mature silver-fir plantation. *Annals of Botany* **108**: 429–438.

Read J, Stokes A. **2006**. Plant biomechanics in an ecological context. *American Journal of Botany* **93**: 1546–1565.

Rentch JS, Fajvan MA, Jr RRH. **2003**. Oak establishment and canopy accession strategies in five old-growth stands in the central hardwood forest region. *Forest Ecology and Management* **184**: 285–297.

Rentch JS, Schuler TM, Nowacki GJ, Beane NR, Ford WM. **2010**. Canopy gap dynamics of second-growth red spruce-northern hardwood stands in West Virginia. *Forest Ecology and Management* **260**: 1921–1929.

Ritter E, Dalsgaard L, Einhorn KS. **2005**. Light, temperature and soil moisture regimes following gap formation in a semi-natural beech-dominated forest in Denmark. *Forest Ecology and Management* **206**: 15–33.

Rubino DL, McCarthy BC. **2004**. Comparative analysis of dendroecological methods used to

assess disturbance events. *Dendrochronologia* **21**: 97–115.

Ryan MG, Phillips N, Bond BJ. **2006**. The hydraulic limitation hypothesis revisited. *Plant, Cell and Environment* **29**: 367–381.

Ryan MG, Yoder BJ. **1997**. Hydraulic limits to tree height and tree growth: what keeps trees from growing beyond a certain height? *BioScience* **47**: 235–242.

Salmén L. **2004**. Micromechanical understanding of the cell-wall structure. *Comptes Rendus - Biologies* **327**: 873–880.

Samuels AL, Kaneda M, Rensing KH. **2006**. The cell biology of wood formation : from cambial divisions to mature secondary xylem 1. *Can. J. Bot.* **84**: 631–639.

Sass U, Eckstein D. **1995**. The variability of vessel size in beech (Fagus sylvatica L.) and its ecophysiological interpretation. *Trees* **9**: 247–252.

Sassus F. **1998**.Déformations de maturation et propriétés du bois de tension chez le Hêtre et le Peuplier : mesures et modèles (Doctoral thesis).

Saurat J, Guéneau P. **1976**. Growth stresses in beech. *Wood Science and Technology* **10**: 111–123.

Schindler TM. **1998**. The new view of the primary cell wall. *Zeitschrift für Pflanzenernährung und Bodenkunde* **161**: 499–508.

Scholz FG, Phillips NG, Bucci SJ, Meinzer FC, Goldstein G. **2011**. Hydraulic Capacitance : Biophysics and Functional Significance of Internal Water Sources in Relation to Tree Size. In: Size- and Age-Related Changes in Tree Structure and Fonction. 341–361.

Schuldt B, Knutzen F, Delzon S, Jansen S, Hilmar M. **2016**. How adaptable is the hydraulic system of European beech in the face of climate change-related precipitation reduction? *New Phytologist* **210**: 443–458.

Seki T, Ohta S, Fujiwara T, Nakashizuka T. **2013**. Growth allocation between height and stem diameter in nonsuppressed reproducing Abies mariesii trees. *Plant Species Biology* **28**: 146–155.

Sendall KM, Lusk CH, Reich PB. **2015**. Becoming less tolerant with age: sugar maple, shade, and ontogeny. *Oecologia* **179**: 1011–1021.

Shinozaki K, Yoda K, Hozumi K, Kira T. **1964**. A quantitative analysis of plant form. The Pipe model theory. 1. Basic analysis. *The Ecological Society of Japan* **14**: 97–104.

Sierra-de-Grado R, Pando V, Martínez-Zurimendi P, Peñalvo A, Báscones E, Moulia B. **2008**. Biomechanical differences in the stem straightening process among Pinus pinaster

provenances. A new approach for early selection of stem straightness. *Tree physiology* **28**: 835–846.

Skov KR, Kolb TE, Wallin KF. **2004**. Tree size and drought affect ponderosa pine physiological response to thinning and burning treatments. *Forest Science* **50**: 1–11.

Sperry JS, Hacke UG, Pittermann J. **2006**. Size and Function in Conifer Tracheids and Angiosperm Vessels. *American journal of botany* **93**: 1490–1500.

Steppe K, Lemeur R. **2007**. Effects of ring-porous and diffuse-porous stem wood anatomy on the hydraulic parameters used in a water flow and storage model. *Tree physiology* **27**: 43–52.

Stojnic S, Sass-Klassen U, Orlovic S, Matovic B, Eilmann B. **2013**. Plastic growth response of european beech provenances to dry site conditions. *IAWA Journal* **34**: 475–484.

Stratton L, Goldstein G, Meinzer FC. **2000**. Stem water storage capacity and efficiency of water transport: their functional significance in a Hawaiian dry forest. *Plant, Cell & Environment* **23**: 99–106.

Sumida A. **2015**. The diameter growth-height growth relationship as related to the diameter-height relationship. *Tree Physiology* **35**: 1031–1034.

Sumida A, Miyaura T, Torii H. **2013**. Relationships of tree height and diameter at breast height revisited: Analyses of stem growth using 20-year data of an even-aged Chamaecyparis obtusa stand. *Tree Physiology* **33**: 106–118.

Telewski FW. **2006**. A unified hypothesis of mechanoperception in plants. *American journal of botany* **93**: 1466–76.

Telewski FW. **2012**. Is windswept tree growth negative thigmotropism? *Plant Science* **184**: 20–28.

Thibaut B, Gril J, Fournier M. **2001**. Mechanics of wood and trees: some new highlights for an old story. *Comptes Rendus de l'Académie des Sciences - Series IIB - Mechanics* **329**: 701–716.

Thornley JHM. **1999**. Modelling stem height and diameter growth in plants. *Annals of Botany* **84**: 195–205.

Trenard Y, Guéneau P. **1975**. Relations entre contraintes de croissance longitudinales et bois de tension dans le hêtre (Fagus sylvatica). *Holzforschung* **29**: 217–223.

Trotsiuk V, Hobi ML, Commarmot B. **2012**. Age structure and disturbance dynamics of the relic virgin beech forest Uholka (Ukrainian Carpathians). *Forest Ecology and Management* **265**: 181–190.

Trouvé R, Bontemps J-D, Seynave I, Collet C, Lebourgeois F. **2015**. Stand density, tree

social status and water stress influence allocation in height and diameter growth of Quercus petraea (Liebl.) (A Mäkelä, Ed.). *Tree Physiology* **35**: 1035–1046.

Tyree MT, Zimmermann MH. **2002**. *Xylem structure and the ascent of the sap* (TE Timell, Ed.). Springer-Verlag.

Valinger E, Elfving B, Mörling T. **2000**. Twelve-year growth response of Scots pine to thinning and nitrogen fertilisation. *Forest Ecology and Management* **134**: 45–53.

Venables WN, Ripley BD. **2002**. Modern Applied Statistics with S. *Issues of Accuracy and Scale*: 868.

Violle C, Navas ML, Vile D, Kazakou E, Fortunel C, Hummel I, Garnier E. **2007**. Let the concept of trait be functional! *Oikos* **116**: 882–892.

Wagner S, Collet C, Madsen P, Nakashizuka T, Nyland RD, Sagheb-Talebi K. **2010**. Beech regeneration research: From ecological to silvicultural aspects. *Forest Ecology and Management* **259**: 2172–2182.

Ward JS, Stephens GR. **1993**. Influence of crown class on survival and development of Betulalenta in Connecticut, U.S.A. *Canadian Journal of Forest Research* **26**: 277–288.

Washusen R, Baker T, Menz D, Morrow A. **2005**. Effect of thinning and fertilizer on the cellulose crystallite width of Eucalyptus globulus. *Wood Science and Technology* **39**: 569–578.

Webster CR, Lorimer CG. **2005**. Minimum opening sizes for canopy recruitment of midtolerant tree species: a retrospective approach. *Ecological Applications* **15**: 1245–1262.

Whippo CW, Hangarter RP. **2009**. The 'sensational' power of movement in plants: A Darwinian system for studying the evolution of behavior. *American Journal of Botany* **96**: 2115–2127.

Wiley E, Helliker B. **2012**. A re-evaluation of carbon storage in trees lends greater support for carbon limitation to growth. *New Phytologist* **195**: 285–289.

Wilson BF, Archer RR. **1979**. Tree Design: Some Biological Solutions to Mechanical Problems. *BioScience* **29**: 293–298.

Wimmer R. **2002**. Wood anatomical features in tree-rings as indicators of environmental change. *Dendrochronologia* **20**: 21–36.

Wright EF, Canham CD, Coates KD. **2000**. Effects of suppression and release on sapling growth for 11 tree species of northern, interior British Columbia. *Canadian Journal of Forest Research* **30**: 1571–1580.

Wullschleger S, Meinzer FC, Vertessy R a. **1998**. A review of whole-plant water use studies in tree. *Tree physiology* **18**: 499–512.

Yagi T. **2009**. Ontogenetic strategy shift in sapling architecture of Fagus crenata in the dense understorey vegetation of canopy gaps created by selective cutting. *Canadian Journal of Forest Research* **39**: 1186–1196.

Zuur AF, Ieno EN, Walker N, Saveliev AA, Smith GM. **2009**. *Mixed effects models and extensions in ecology with R*. New York, NY: Springer New York.

Annexes

Annexe 1 : Fosses pédologiques.

a : Localisation des fosses pédologiques sur la parcelle d'étude.

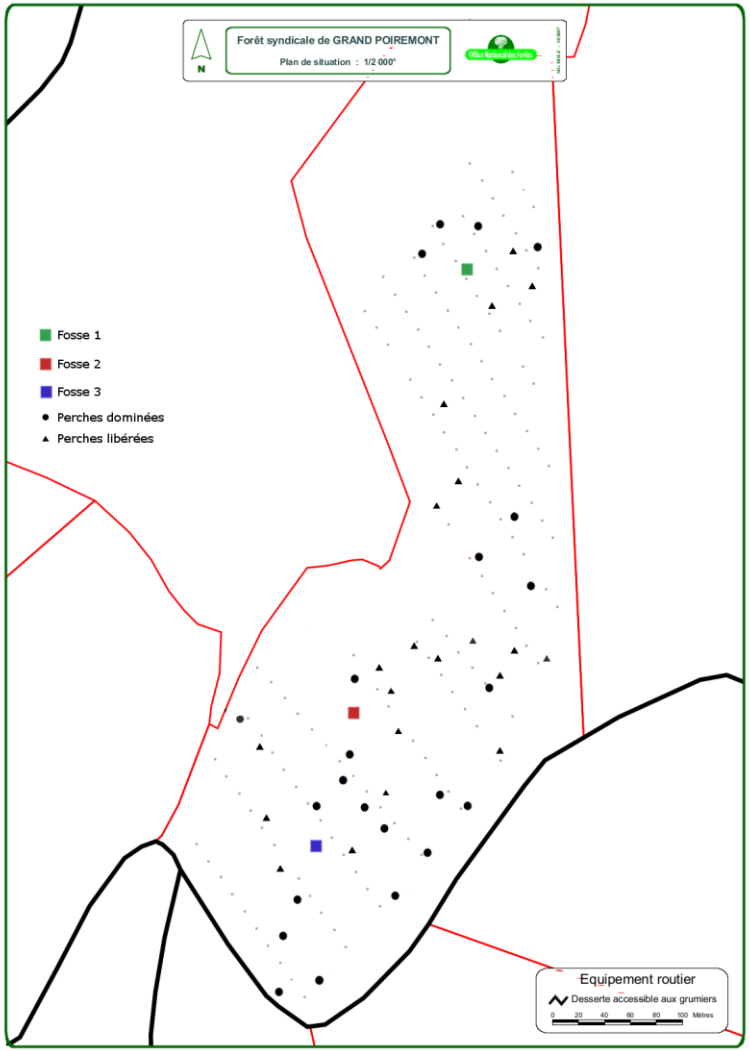

b : Description des 3 fosses pédologiques réalisées.

Suivant la clé de détermination des principales formes d'humus AFES 2008, la forme de l'humus est oligomull.

Fosse	**1**	**2**	**3**
Profondeur (cm)	175	120	160
Nombre horizon	3	3	4
RUM (mm)	225,02	157,81	151,80
RUM (mm) par cm	1,29	1,32	0,95
Horizon 1	LMS	LM	LM
Horizon 2	LMS	LMS	LMS
Horizon 3	SL	LMS	LS
Horizon 4	-	-	SL

LMS : limoneux moyen sableux ; LM : limoneux moyen ; LS : limoneux sableux ; SL : sablo-limoneux.

Type de sol (Référentiel pédologiques franco-français 2008): Brunisols dystriques ou Alocrisols typiques avec une couche luvique.

Type de sol (World Reference 2005 update) : Cambisols dystric/ hyperdystric.

Annexe 2 : Exemples de morphologies des perches dominées et libérées de hêtre acquises à partir des scans T-LIDAR 2013.

Perches dominée n°7

Perches dominée n°11

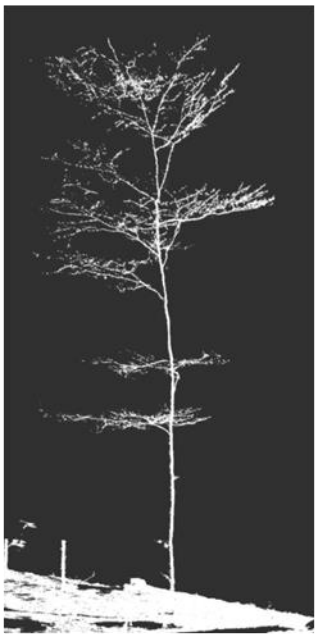

Perches libérée n°32

Perches libérée n°33

Annexe 3 : Récapitulatif des activités.

	Unité	Développement outils / protocoles	Temps moyen manipes	Temps total pour les 42 perches	Nombre total d'intervenants mobilisés
Largeur de cernes et longueur des unités de croissance	1 arbre	Déjà en place	2 jours	3 mois	2
Projection horizontale du houppier	3 arbres	Déjà en place	1 demi-journée	9 jours	1
Abattage[d] : ICC, biomasse, défilement	42 arbres	▸ Mise au point protocole : 2 semaines	▸ ICC : 4 jours ▸ Abattage + biomasse + défilement + conditionnement : 3 semaines	1,5 mois	20
Scans T-LIDAR[d]	42 arbres	▸ Développement plugin : 1 mois ▸ Mise au point protocole : 1 mois	▸ Acquisition images : 3 semaines ▸ Nettoyage des scans : 1 mois ▸ Traitement d'images : 2,5 mois	6 mois	2 (+ 1 stage)
Cartographie du bois de tension[d]	42 arbres	▸ Mise au point du protocole : 2 jours ▸ Développement du plugin : 15 jours	▸ Acquisition des photos et recalage : 1 mois ▸ Traitement d'image : 2 mois	3,5 mois	2 (+ 1 main d'œuvre occasionnelle)

	Unité	Développement outils / protocoles	Temps moyen manipes	Temps total pour les 42 perches	Nombre total d'intervenants mobilisés
Micro-densité du bois[d]	10 arbres*	Déjà en place	▸ Sciage 1 : 1h ▸ Séchage : 1 mois ▸ Sciage 2 : 50 min ▸ Acquisition images : 15 min ▸ Pesée et mesure épaisseur : 10 min ▸ Traitement images et mise en forme données : 12h	1,5 mois (sans séchage)	2
Coupes anatomiques[d]	1 arbre*	▸ Mise au point protocole : 1,5 mois ▸ Développement plugin : 1 jour	▸ Réalisation des coupes + coloration : 30 min à 2h ▸ Acquisition images : 2h ▸ Traitement d'images : 2h	6 mois	3 (+2 stages et 2 main d'œuvre occasionnelle)

***** 1 rayon entier de l'écorce à la moelle

[d] : participation de la doctorante à l'activité

Annexe 4 : Growth stresses in old beech poles after thinning : distribution and relation with wood anatomy.

J Indian Acad Wood Sci (June 2015) 12(1):37–43
DOI 10.1007/s13196-015-0142-6

ORIGINAL ARTICLE

Growth stresses in old beech poles after thinning: distribution and relation with wood anatomy

Citra Yanto Ciki Purba[1,2,3] · Estelle Noyer[1,2] · Julien Ruelle[1,2] · Jana Dlouhá[1,2] · Lina Karlinasari[3] · Meriem Fournier[1,2]

Received: 16 March 2015 / Accepted: 24 April 2015 / Published online: 5 May 2015

Abstract In the present study, we investigated the reaction of small diameter but old beech poles to canopy opening with particular interest in occurrence of growth stresses which allows the tree to maintain or correct its spatial position. We studied the relationships between growth stresses and (i) thinning treatment and (ii) anatomical structure. Forty-two beech poles were used for the study, half of which were thinned in 2007. We measured the growth stresses indicators (GSI) at eight positions around the trunk periphery and wood anatomical characteristics including proportion of G-fibers and vessel characteristics. Surprisingly, thinning treatment did not affect the average growth stress level and intensity of reaction in old beech poles. This rather unexpected result may be related to the high age of these trees and/or the high reaction wood occurrence prior to thinning resulting from the growth in suppressed condition. Considering the relationship between the proportions of G-fiber and the level of growth stresses, a significant positive correlation was found in agreement with previous studies on other species. Further, a negative correlation was found between vessel surface area and GSI level. Vessel frequency was also decreasing with the increasing GSI level and proportion of G-fibers.

Keywords Beech · G-fiber · Growth stress · Thinning

✉ Citra Yanto Ciki Purba
purbacitrayantociki@gmail.com

[1] INRA, UMR 1092 LERFOB, 54280 Champenoux, France

[2] AgroParisTech, UMR 1092 LERFOB, 54000 Nancy, France

[3] Bogor Agricultural University (IPB), 16680 Bogor, Indonesia

Introduction

In contrast with the majority of man-made structures, tree stems exhibit a complex field of internal stresses resulting from the growth process (Kubler 1987). These so-called growth stresses result from an overlap of two components: accumulation of support stresses and maturation stresses. Gradual increase in crown weight induce compression stress (Spatz and Brüchert 2000) while the maturation of the newly formed wood layer lead to the tensile pre-stresses called maturation stress (Fournier et al. 1990). Maturation stresses appear after cell lignification. During the maturation of the newly formed wood, the cells, which grow every year on the stem periphery, contract longitudinally while the lignified wood cells already formed impede this contraction.

Pre-stresses are useful for living trees, since they improve the mechanical resistance of the stem against temporary bending loads. Wood has a high-tensile strength parallel to fiber direction but is relatively weak in compression. When wood is subjected to local axial compression, axial buckling can be avoided by tensile pre-stresses (Bonser and Ennos 1998). Tensile pre-stresses at the tree periphery therefore compensate the relatively low compressive strength of green wood. Pre-stresses are also important for the tree postural control. Its asymmetrical distribution around the tree circumference provides a motor system allowing the postural control of the tree and the stems and branches reorientation.

Trees control the spatial position of their axes (stem or branches) by generation of asymmetrical stress (Fournier et al. 1994; Clair et al. 2013). Asymmetry of maturation stresses induces a bending moment which maintains (growing branches) or corrects (accidentally tilted stem) the spatial position of axes (Alméras et al. 2006). To

achieve an important bending moment, trees are pushed to produce an unusual level of maturation stresses. Tissues with the unusual level of maturation stresses is called reaction wood. Occurrence of reaction wood is most often associated with branches or tilted trees; however, it is also frequently reported in straight stems in a number of species including Beech (Gartner 1997; Washusen et al. 2003; Jullien et al. 2013).

Motor processes of posture control differs between deciduous trees and conifers. While deciduous trees generate highly tensile stressed tissues called tension wood on the upper side of leaning axes, conifers produce so called compression wood on the lower side of leaning axes (Yoshida et al. 2002; Clair et al. 2003; Fang et al. 2008; Abasolo et al. 2009). Apart from the high levels of maturation stresses, tension wood presents some distinctive physical and anatomical features when compared to 'normal wood' (IAWA 1964). Tension wood has high longitudinal shrinkage, wider rings, low lignin, wider cellulose crystallite sand high crystallinity (Ruelle et al. 2007; Mellerowicz and Gorshkova 2012; Washusen and Evans 2001).

In many species of hardwoods such as beech, poplar, oak and chestnut, tension wood contains fibers with a special morphology and chemical composition due to the development of gelatinous layer (Clair et al. 2006, 2010; Fang et al. 2008). This layer usually used as a tool to identify the presence of tension wood in hardwoods. However, this layer is not always observed in the tension wood of some species (Clair et al. 2006). Gelatinous layer has a jelly-like appearance with low MFA (Washusen and Evans 2001; Ruelle et al. 2007), high mesopority (Chang et al. 2009), high crystalline cellulose, and low lignin content (Mellerowicz and Gorshkova 2012).

Previous reports have shown that in chestnut and poplar there is a significant relationship between the proportion of the gelatinous layer and growth stresses. The higher the proportion of the gelatinous layer in tension wood, the higher the growth stress in trees. It indicates that the amount of G-layer largely controls the stress level in trees (Fang et al. 2008; Clair et al. 2003; Dassot et al. 2012). Besides the G-layer, a decrease in the frequency of vessels in tension wood was reported by Ruelle et al. (2006) in 21 tropical tree species and by Jourez et al. (2001) for poplar.

It is well known that silvicultural treatments such as thinning affect the tree morphology. Thinning tends indeed to reduce height growth and stimulates diameter growth which is in general explained by the increased post-thinning wind loads (Evans and Jackson 1972; Mitchell 2000) as thinning will open the canopy, increase the canopy roughness, decrease the sheltering effects from surrounding trees and increase the tree exposure to wind (Zhu et al. 2003). This will lead to higher stress to the stem and may stimulate the tension wood production. However, thinning was reported to improve the tree stability by long-term effects on growth and development of trees (Polge 1981; Ferrand 1982). Some research shows that higher spacing of trees seems to be a good solution to lower the level of growth stress in beech stands and heavy thinning are to be made to reduce growth stresses in beech stands (Polge 1981; Jullien et al. 2013) while some others did not found any effect of thinning treatment or tree spacing (Dassot et al. 2012; Valencia et al. 2011).

In this paper, we focus on the effects of canopy opening on (i) the growth stresses level and intensity of reaction on the tree stem circumference and (ii) on the relationship between growth stress level and anatomical features such as G-fibers proportion and vessels characteristics.

Materials and methods

Site location and tree selection

Trees for the present study were harvested in Grand Poiremont, Haute Saône, France from stands with natural regeneration forest consisting of beech, oak, spruce, maple, and birch. Stands are located at altitude of 470 meters above sea level with 1218 mm rainfall (ONF 2014). Forty-two beech poles aged from 60 to 100 years were used for the study, with diameters ranging from 9.5 to 20.9 cm and heights from 11 to 25 m. Half of them was released from the competition 6 years before harvesting while the other half continued to growth in high competition. Releasing from the competition was done by removal of all competitor trees in a radius of 12 m from the released pole. One of released poles has buckled so that only twenty treated poles are considered in the following analysis.

Growth stress measurement and modeling the distribution of GSI

Stresses growth indicators were measured using the single hole method (Fournier et al. 1994). This method consists in measuring the displacement of two pins (initial distance is 4.5 cm) caused by the stress release after a 2 cm hole has been drilled between the pins. Outer layer up to the cambial layer is removed before the measurement. Two pins are fixed in a stem along the fiber direction using a template. A frame equipped with a micrometer is then mounted on the pins and the micrometer is set to zero. A 10 mm deep hole is drilled between the pins to release the stress leading to displacement of the two pins recorded by the micrometer. This displacement expressed in μm is called growth stress indicator (GSI) and is directly proportional to longitudinal growth stress at the trunk periphery, the conversion factor

depending on each species mechanical properties (Sassus 1998). As such, values of GSI are good indicators of the relative growth stresses level for intraspecific comparison (Clair et al. 2003).

The GSI measurements were done at the 1.3 m height at eight positions equally distributed around the stem circumference (Fig. 1). The objective was to characterize the distribution of the GSI and determine the location of tension wood. The first measurement was done at the upper side of the tree at position of maximal tilt angle estimated with an inclinometer prior to the GSI measurements. The azimuth of the first GSI point was also measured. Measurements were conducted in February–March 2014 before the beginning of the growth season.

As the first position is expected to correspond to tension wood, the distribution of GSI around the stem circumference was described by a cosine function:

$$y = A + B\cos(\theta + \pi)$$

where A is the average value of GSI, B is the difference between the maximal and minimal value of GSI divided by two or the magnitude of GSI asymmetry (intensity of reaction), and θ is the angular difference between the position of the GSI peak as estimated from the tilt measurement and the position of the estimated maximal value. Estimation of the θ value is important for further measurements of the tension wood properties. An example of the distribution of the GSI around the trunk circumference and its modelled values are shown in Fig. 1.

Anatomical measurements

Selection of samples

After the measurement of GSI, trees were felled and a 5 cm thick disc was collected at the breast height. Specimens for the anatomical measurements were selected based on the histogram of all the GSI values recorded. The aim was to cover the complete range of GSI observed in beech poles. GSI values were classified in 14 classes. When possible, 3 thinned and 3 control trees were chosen from each class, and all specimens were used in GSI classes with frequency lower than six. In total, 64 specimens were used for anatomical observations.

Proportion of G-fibers

To characterize the anatomical structure as close as possible to the GSI measurements, small blocks of (0.5 cm × 1.5 cm; R × T) were extracted from the disk. Cross sections approximately 20 µm thick were cut with a microtome and double-stained with safranin and blueastrato highlight the presence of the G-layer in blue as illustrated in Fig. 2b. To determine the proportion of fibers with G-layer i.e., G-fibers, one single image was taken of each sample covering the whole sample surface. Image capture was performed using a digital camera (Sony XCD-U100CR). Image-J software was then used to quantify the area occupied by G-fibers in the section. The algorithm was developed by Badia et al. (2005) and is based on the subtraction of the red component of the image from the blue one. This operation enhances the distinction between G-fibers and other tissues. A common threshold was then used to separate them. The percentage of G-fibers value was deduced without ambiguity from histograms where pixels were identified as belonging to G-fibers and other tissues.

Vessel anatomical characteristics

The samples used were the same sample for proportion of G-fiber but images were taken at a magnification 5× to enable finer analysis of the vessel morphology. Seven photos were taken at 7 different positions distributed

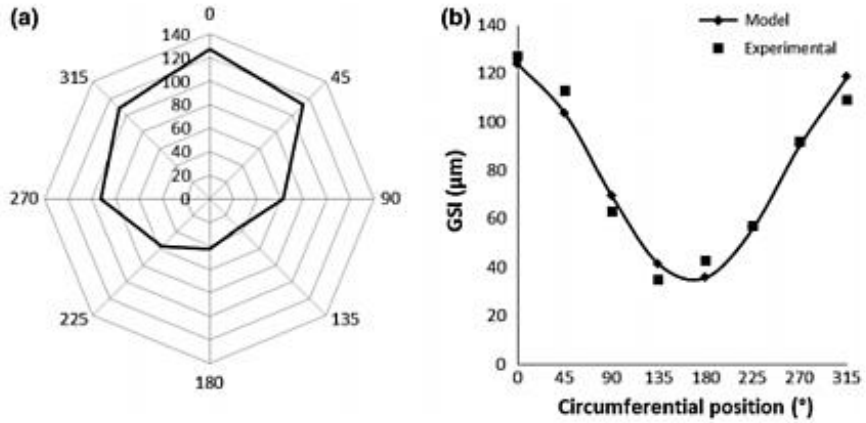

Fig. 1 **a** Distribution of GSI around the stem circumference, position from 0° to 315° indicate the position of GSI measurements, **b** example of the correspondence between the cosine model and experimental values

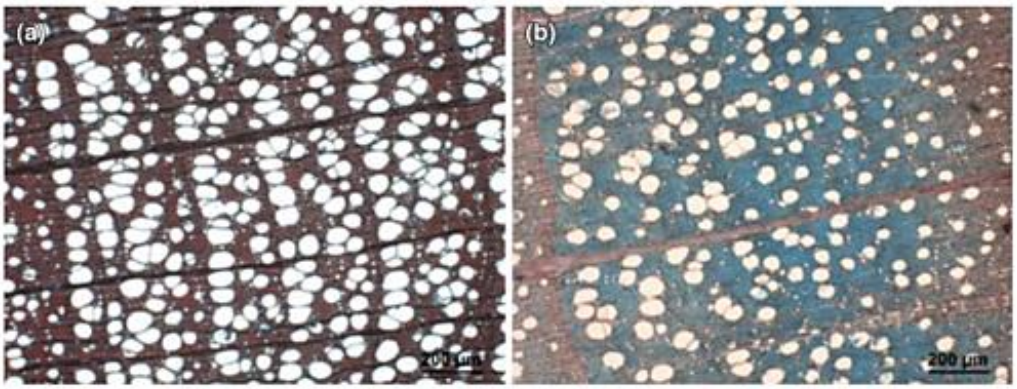

Fig. 2 **a** Transverse sections of wood without G-fibers, **b** transverse sections of wood with G-fibers

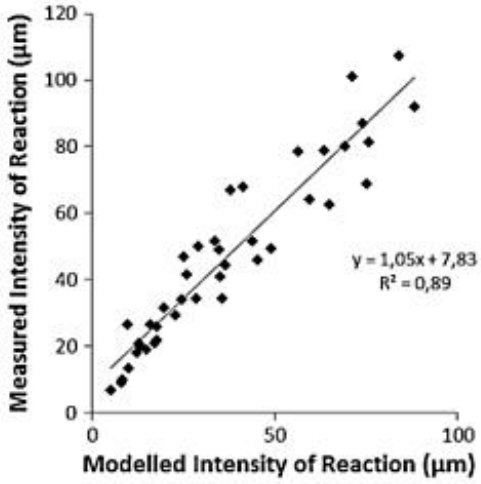

Fig. 3 Agreement between measured and modelled intensity of reaction

evenly on each sample. Proportion of vessel was calculated as total vessel area/total surface of image. Vessels radius and vessel frequency were also calculated to estimate the hydraulic performances of wood tissues.

Results and discussion

Suitability of the cosine model to describe the GSI distribution around the stem circumference

Concerning the agreement between the modeled and experimental values of average GSI (A) and the intensity of reaction (B), the A parameter (modelled) is exactly the average GSI (A measured). The agreement is very good for B values (Fig. 3), showing that globally, a cosine model using three parameters i.e., the average GSI, the difference between maximum and minimum GSI, the azimuth (angle) of the tension wood peak—fits well the experimental data (average $R^2 = 0.64$).

Effect of thinning to GSI distribution

To know whether there is a difference in GSI distribution between thinned and control trees, we compared the average GSI and intensity of reaction in both treatments. Figure 4 shows that there is no statistical difference in GSI average and intensity of reaction wood between thinned and control trees.

Our results show that there is no effect of thinning on the GSI average value and their intensity of reaction. Previous studies concerning this subject show contrasting tendencies. On one hand Polge (1981) found that heavy thinning reduced growth stresses in 35-year-old beech trees that had been thinned 3 times since seedlings. Another report by Jullien et al. (2013) confirms these results. It shows that higher spacing between trees induced higher growth rates related to lower growth stresses. On the other hand, Dassot et al. (2012) studied the tension wood occurrence in spacing trial and highlighted a strong effect of diameter range of trees on the production of tension wood but no additional effect of the tree spacing. Further, Medhurst et al. (2011) showed increase in average value of GSI in 22 years old *E. nitens* trees 16 years after thinning as well as increase of the average GSI value on the wind side of trees similarly to Valencia et al. (2011). Also report by Washusen et al. (2005) suggests increase in tension wood occurrence 4 years after thinning of *E. globulus* trees, 12 years old during tree collection, based on the observation of increased cellulose crystallite width.

The lack of changes in the GSI distribution in our poles may be related to their high age. We can expect that 60–100 years old poles may react differently to the canopy

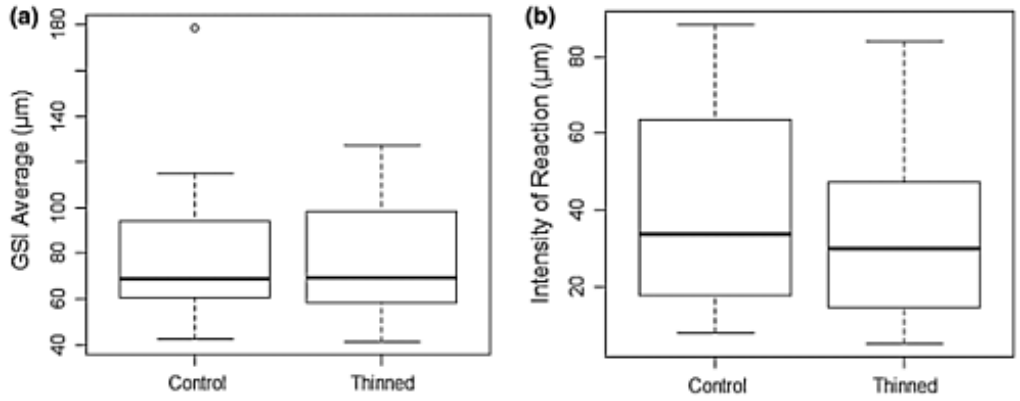

Fig. 4 **a** Average GSI between control and thinned trees, **b** intensity of reaction between control and thinned trees

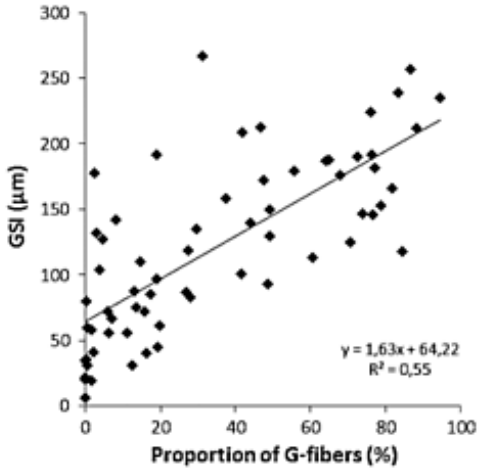

Fig. 5 Relationship between proportion of G-fibers and GSI

opening when compared with young trees. Another possible explanation is related to the social status of our trees. As suppressed trees, the poles may need to often reorient their stems in order to benefit from each light pocket compared to well establish dominant trees leading to quite high tension wood occurrence before thinning. Therefore, in our situation, thinning is not a high stimulus of reorientation leading to higher intensity of reaction nor a release of biomechanical constraints associated to GSI decreasing.

Relationship between GSI and anatomical features

Proportion of G-fibers and GSI

The proportion of G-fibers is plotted against GSI in Fig. 5. It shows a positive relationship between the two variables. Larger the G-fibers proportion, higher the GSI value is.

Such a result was expected, as maturation tensile stresses are known to reach extreme levels in pure cellulosic G-fibers (Clair et al. 2003). Similar correlations were reported for example by Fang et al. (2008). However, the R^2 value reported by Fang et al. (2008) is 0.716 which is slightly higher than the value reported in this study (0.533).This difference can be explained by the differences between the methods of GSI measurements: Fang et al. (2008) used the strain gauge method which is a more localized measure. Results show also that a high variability of GSI, (from 0 to 180), is observed when no tension wood (almost no G-fibers, proportion below 5 %) is observed. Such variations demonstrate that as previous authors emphasized (Clair et al. 2003), other features that typical G-layers, probably at the cell wall level, can lead to high intensity of reaction and tree reaction, even without typical tension wood.

Effect of GSI on vessel proportion and vessel frequency

Figure 6a shows the relationship between GSI and vessel proportion. The result indicates a negative correlation between vessel proportion and GSI. Larger the GSI values, lower the vessel proportion is. Relationship between GSI and vessels frequency is shown in Fig. 6b. It shows a slight negative relation between both variables.

Our result shows that vessel proportion decreases when GSI increase. Vessel frequency is also decreasing with the increase of GSI and the proportion of G-fibers. No relation was found between size of vessels and GSI or proportion of G-fibers. It suggests that lower vessel proportion is due to a lower vessel frequency and not to a change in size of the vessel elements. These results are consistent with research by Jourez et al. (2001) who found the vessel elements decreasing in frequency in tension wood of poplar. A decreasing in the frequency of vessel in tension wood was

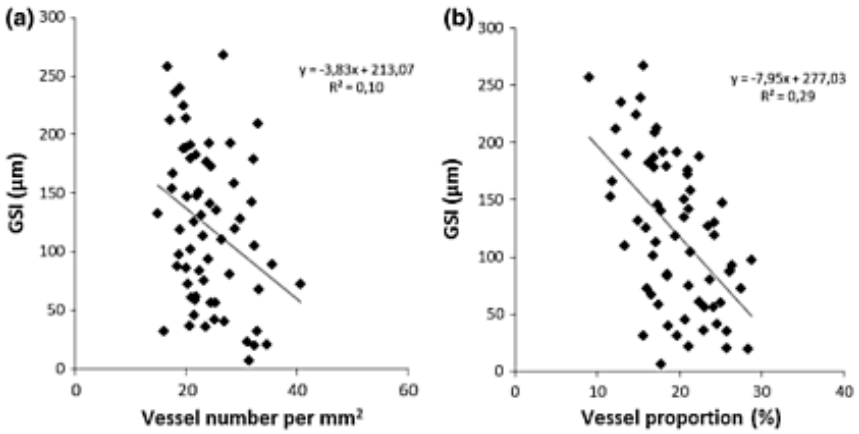

Fig. 6 **a** Relationship between vessel frequency and GSI, **b** relationship between vessel proportion and GSI

found also by Ruelle et al. (2006) in 21 tropical trees. Christensen-Dalsgaard et al. (2007) study the changes in vessel anatomy in response to mechanical loading in six species of tropical tree. She found that the smallest vessels and the smallest vessel frequency were found in the parts of the trees with the greatest stresses or strains. These changes appear to be an adaptation towards reinforcing mechanically loaded areas.

Conclusion

Thinning treatment did not affect the GSI average values and intensity of reaction in old beech poles. This rather unexpected result may be related to the high age of these trees and long growth period in suppressed condition. Considering the relationship between the proportions of G-fibers and the level of GSI, a significant positive correlation was found in agreement with previous studies on other species. Further, a negative correlation was found between vessel proportion and GSI level, mainly due to decrease in vessel frequency.

Acknowledgments We thank E. Cornu, E. Farré, C. Freyburger, P. Gelhaye, L. Dailly, F. Vast, D. Rittié, F. Bordat and A. Mercanti for field work and M. Harroué for sample preparation in the laboratory. This work was supported by the WADE project funded by the French National Research Agency (ANR) as part of the "Investissementsd'Avenir" program (ANR-11-LABX-0002-01, Lab of Excellence ARBRE) and Beasiswa Unggulan BPKLN Ministry of Education of The Republic of Indonesia. The silvicultural experiment is a collaborative work between INRA and the French National Forest Office (ONF).

References

Abasolo WP, Yoshida M, Yamamoto H, Okuyama T (2009) Stress generation in aerial roots of *Ficus elastica* (Moraceae). IAWA J 30(2):216–224

Alméras T, Yoshida M, Okuyama T (2006) The generation of longitudinal maturation stress in wood is not dependent on diurnal changes in diameter of trunk. J Wood Sci 52(5):452–455

Badia MA, Mothe F, Constant T, Nepveu G (2005) Assessment of tension wood detection based on shiny appearance for three poplar cultivars. Ann For Sci 62(1):43–49

Bonser RHC, Ennos AR (1998) Measurement of prestrain in trees: implications for the determination of safety factors. Funct Ecol 12(6):971–974

Chang SS, Clair B, Ruelle J, Beauchêne J, Renzo FD, Quignard F, Zhao G, Yamamoto H, Gril J (2009) Mesoporosity as a new parameter for understanding tension stress generation in trees. J Exp Bot 60(11):3023–3030

Christensen-Dalsgaard KK, Fournier M, Ennos AR, Barfod AS (2007) Changes in vessel anatomy in response to mechanical loading in six species of tropical trees. New Phytol 176(3):610–622

Clair B, Ruelle J, Thibaut B (2003) Relationship between growth stress, mechanical-physical properties and proportion of fibre with gelatinous layer in chestnut (*Castanea sativa* M.). Holzforschung 57(2):189–195

Clair B, Ruelle J, Beauchêne J, Prévost MF, Fournier M (2006) Tension wood and opposite wood in 21 tropical rain forest species. 1. Occurrence and efficiency of G-layer. IAWA J 27(3):329–338

Clair B, Alméras T, Pilate G, Jullien D, Sugiyama J, Riekel C (2010) Maturation stress generation in poplar tension wood studied by synchrotron radiation microdiffraction. Plant Physiol 152(3):1650–1658

Clair B, Alteyrac J, Gronvold A, Espejo J, Chanson B, Alméras T (2013) Patterns of longitudinal and tangential maturation stresses in *Eucalyptus nitens* plantation trees. Ann For Sci 70(8):801–811

Dassot M, Fournier M, Ningre F, Constant T (2012) Effect of tree size and competition on tension wood production over time in beech plantations and assessing relative gravitropic response with a biomechanical model. Am J Bot 99(9):1427–1435

Evans DJ, Jackson RJ (1972) Red beech management: implications from early growth plots. New Zeal J For 17(2):189–200

Fang CH, Clair B, Gril J, Liu SQ (2008) Growth stresses are highly controlled by the amount of G-layer in poplar tension wood. IAWA J 29(3):237–246

Ferrand JC (1982) Etude des contraintes de croissance Deuxième partie: Variabilité en forêt des contraintes de croissance du hêtre (*Fagus sylvatica* L.). Ann For Sci 39(3):187–218

Résumé

Réponses des perches de hêtre (*Fagus sylvatica* L.) à l'ouverture de la canopée : approche multidisciplinaire et multi-échelle.

L'ouverture de la canopée présente des avantages (disponibilité des ressources) mais aussi de nouvelles contraintes (vent, demande évaporative, etc.). Souvent étudié chez les semis, la dynamique de réponses est peu renseignée chez les grands arbres. Cette thèse vise à identifier les dynamiques de réponses à l'ouverture de la canopée chez des perches de hêtre dominées durant de longues périodes. L'approche adoptée est multidisciplinaire et multi-échelle, basée sur une analyse rétrospective de la croissance radiale et axiale, d'anatomie et de traits biomécaniques. Sous couvert, la compétition pour la lumière fait que les perches favorisent la croissance axiale devant la croissance radiale résultant en un élancement important. Par ailleurs, un tiers des perches s'affaisse. Après ouverture, l'élancement des perches présente un risque biomécanique : 15 sur 36 perches libérées ont été cassées par le vent deux ans après l'éclaircie. Pour se stabiliser face au vent, la croissance axiale des perches est diminuée pendant quatre ans après l'éclaircie tandis que la croissance radiale augmente et atteint un plateau après deux ans probablement à cause des limitations liées à la taille et à l'accès aux ressources. Les perches ayant une inclinaison initiale supérieure à 6° se redressent après l'éclaircie. La conductivité hydraulique potentielle du cerne augmente et se stabilise elle aussi après deux ans. Les dynamiques de réponses sont donc clairement spécifiques du trait étudié. Par ailleurs, l'approche intégrative a permis de mettre en évidence l'importance de la taille des individus dans les mécanismes de réponses : tandis que les semis modifient et la croissance et les propriétés des tissus, les perches se reposent sur l'ajustement de leur géométrie.

Mots clés : *Fagus sylvatica* L., ouverture de la canopée, croissance, biomécanique, anatomie, bois.

Abstract

Beech (*Fagus sylvatica* L.) poles responses to canopy opening: mutli-disciplinary and multi-scale approaches.

Opening of the canopy exhibits advantages (resources availability) but also new constraints (wind, higher evaporative demand). Rather well documented in saplings, response dynamics to canopy opening is less known in large trees. The thesis aims to identify the dynamics of responses to canopy opening in beech trees suppressed during long periods. Adopted approach is multi-disciplinary and multi-scale, based on a retrospective analysis of axial and radial growth, anatomy and biomechanical traits. For suppressed trees, the competition for light results in preferential allocation of biomass to axial growth in comparison with radial growth resulting in trees with high slenderness. Moreover, one third of suppressed trees are sagging. After the release, high slenderness presents a biomechanical risk: 15 from 36 trees are broken by the wind two years after the release. To increase their safety against the wind-break, trees reduce their axial growth during four years after the release and boost their radial growth reaching a stabilisation plateau after two years likely due to the size and resources limitations. Trees with lean angle higher than 6° up-right after the release. The tree ring hydraulic conductivity increases and stabilises after two years also. The dynamics of responses to canopy opening are therefore clearly trait dependent. Moreover, integrative approach highlighted the importance of size in the responses to canopy opening: while saplings adjust both wood tissue properties and tree geometry, large trees rely only on geometry adjustments.

Keywords: *Fagus sylvatica* L., canopy opening, growth, biomechanics, anatomy, wood.